UNIVERSITE CATHOLIQUE DE LOUVAIN
FACULTE DES SCIENCES

Unité de Chimie Organique et Médicinale
Laboratoire du Professeur O. Riant

Synthesis of New Zinc and Cobalt Complexes: Application to the Enantioselective Hydrosilylation of Ketones

Dissertation présentée en vue
de l'obtention du grade de
Docteur en Sciences

Par Yann Pressel

2006

PhD Thesis committee

Professor MUNIZ, Kilian
Université Louis Pasteur (F)

Doctor DELAUDE, Lionel
Université de Liège (B)

Doctor HERMANS, Sophie
Université catholique de Louvain

Professor MARCHAND-BRYNAERT, Jacqueline (President)
Université catholique de Louvain

Professor MARKO, István
Université catholique de Louvain

Professor RIANT, Olivier (Supervisor)
Université catholique de Louvain

Remerciements

Au terme de ce travail, je souhaite tout d'abord exprimer ma profonde gratitude envers le Professeur Riant pour m'avoir ouvert les portes de son laboratoire et accordé une grande confiance dans mes recherches. Je lui adresse toute ma reconnaissance pour sa disponibilité, son optimisme, sa patience ainsi que pour ses encouragements très appréciés.

Je tiens également à remercier les membres de mon jury, Professeur Muniz, Docteur Delaude, Docteur Hermans, Professeur Marchand-Brynaert, Professeur Markó, pour avoir accepté d'évaluer ce manuscrit et pour leurs remarques judicieuses.

Ma reconnaissance va à tous ceux du "Lavoisier" qui, de près ou de loin, m'ont apporté leur aide ou leur soutien et témoigné leur gentillesse : Naouël et Seb, Sabine Sirol, James, Nico, Patrick, Ana, Oli, Sabine Choppin, Borus, Basto et Aurore, David, Charlotte, Alex, Dom, Isa, Chris, Julia, Nassima, Mounia, Yves, Jérôme Hannedouche et Stéphane. Sans oublier tous les anciens de l'équipe Ghosez pour leur accueil chaleureux et leur grande disponibilité : Gaëtan, Chloé, Jérôme Hoet, Anouk, Belkacem, Patrick Schanen, Alain, Karima, Jing, Prosper et Huguette. Un grand merci à tous pour les pauses, l'enthousiasme des travailleurs du week-end, les discussions ayant trait à la chimie ou encore les études de caractère rabelaisien de produits alcooliques (parfois par screening) à l'occasion de différentes soirées ou à la Maison des Sciences.

Je tiens à remercier tout particulièrement Chantal pour sa bonne humeur, son soutien, logistique en particulier, et ses encouragements continus.

Une mention spéciale à Nicolas avec qui j'ai eu très grand plaisir à travailler au laboratoire, discuter de chimie au cours de ces années, et pour ses nombreux conseils.

Je remercie Patrick pour son aide et sa disponibilité très appréciées que ce soit dans le domaine de la chimie ou de l'informatique.

Mes remerciements vont aussi à Nico et Dom pour leur relecture, aux permanents de l'Unité : Anny, Van et Claudio pour leur aide précieuse avec les GC et HPLC chirales, à Sabrina pour les analyses élémentaires, à Benoît et David du service de RMN des Professeurs Schank et Snoussi et au laboratoire de spectrométrie de masse du Professeur Habib-Jiwan.

Enfin, ma reconnaissance s'adresse à mes parents, à ma soeur et à mon frère.

Abstract

The aim of the work carried out in this thesis is to develop new efficient catalytic systems for the synthesis of enantioenriched secondary alcohols. The access to this class of important synthetic intermediates is possible either by nucleophilic addition of organometallic reagents to aldehydes or by reduction of prochiral ketones catalysed with chiral complexes. We have thus developed two new catalytic systems for the asymmetric hydrosilylation of ketones using polymethylhydrosiloxane (PMHS) as an inexpensive reducing agent.

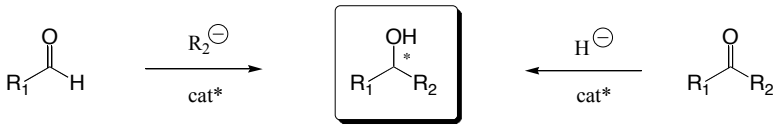

A first approach is based on the synthesis of new *N*, *S* ligands and zinc complexes bearing a ferrocenyl backbone with planar chirality. Those compounds were prepared and evaluated first in the addition of diethyl zinc to aldehydes, reaching enantiomeric excesses up to 74%.

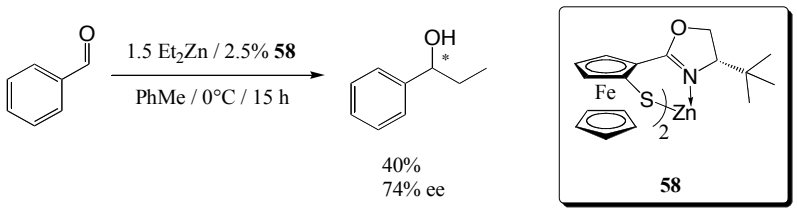

The precatalysts were also evaluated in the reduction of prochiral ketones with PMHS. In that case, a good reactivity was observed and enantioselectivities up to 61% could be reached. It is assumed that a zinc hydride complex formed by thermal ß-elimination of the corresponding ethyl complex is the active species. This catalytic system also allows the hydrosilylation of dialkyl ketones, a challenging goal in asymmetric catalysis.

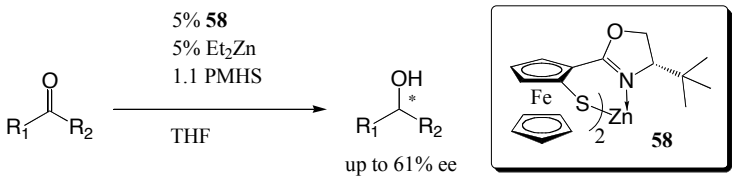

In a second part of this work, we have developed a new catalytic system for hydrosilylation of ketones based on the hypothetical formation of a chiral cobalt hydride catalyst. This intermediate is supposed to be formed by reaction of the corresponding neutral cobalt (II) complex with tetrabutyl ammonium triphenyldifluorosilicate (TBAT) as activator and a silane. Following a preliminary screening, salen type ligands were found to be the most efficient when activated with TBAT in presence of PMHS.

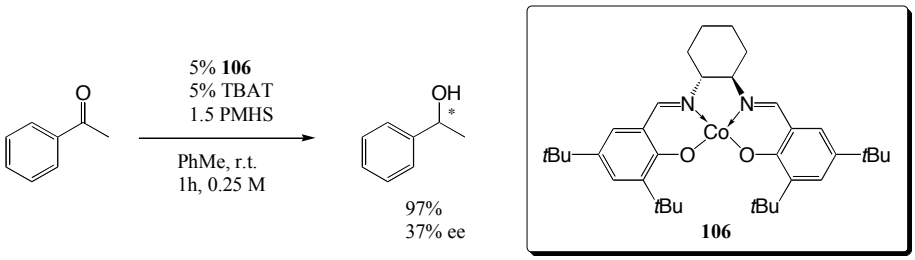

Modifications on this structure by replacing the phenol group of the ligand by various sulfonamide groups led, after optimisation of the reaction parameters, to a highly efficient catalytic system with enantioselectivities reaching 84 % for the reduction of tetralone. This work should thus open new perspective for the design of highly enantioselective and low cost catalytic systems for the hydrosilylation of prochiral ketones.

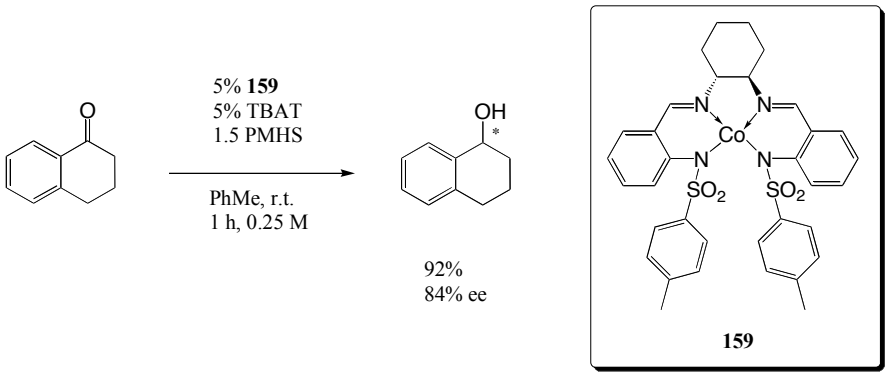

Résumé

Le but du travail effectué dans cette thèse est de développer de nouveaux systèmes catalytiques efficaces pour la synthèse d'alcohols secondaires énantiomériquement enrichis. L'accès à cette classe d'intermédiaires synthétiques importants est possible soit par addition de réactifs organométalliques soit par réduction de cétones prochirales catalysées par des complexes chiraux. Nous avons ainsi développé deux nouveaux systèmes catalyiques pour l'hydrosilylation de cétones en utilisant du polymethylhydrosiloxane (PMHS) comme agent de réduction peu onéreux.

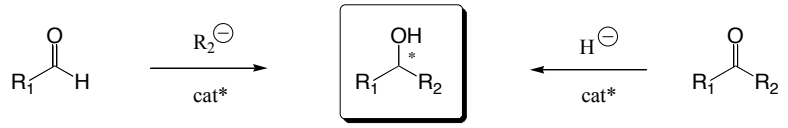

Une première approche est basée sur la synthèse de nouveaux ligands et complexes de zinc *N*, *S* présentant un squelette ferrocénique avec une chiralité plane. Ces composés ont été préparés et évalués d'abord dans la réaction d'addition de diéthylzinc sur du benzaldéhyde, atteignant des excès énantiomériques jusqu'à 74%.

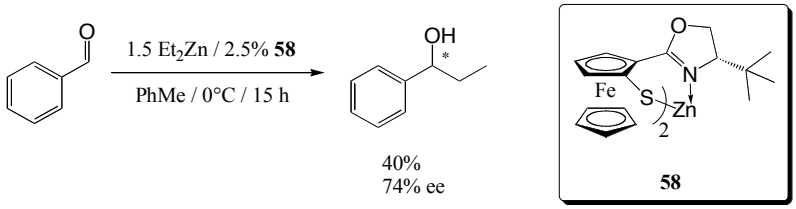

Les précatalyseurs ont également été évalués dans la réduction de cétones prochirales avec du PMHS. Dans ce cas, une bonne réactivité a été observée et des énantiosélectivités jusqu'à 61% ont pu être atteintes. Il est supposé qu'un complexe d'hydrure de zinc, formé par ß-élimination thermique du complexe éthyle correspondant, est l'espèce active. Ce système catalytique permet également l'hydrosilylation de dialkylcétones, un objectif difficile en catalyse asymétrique.

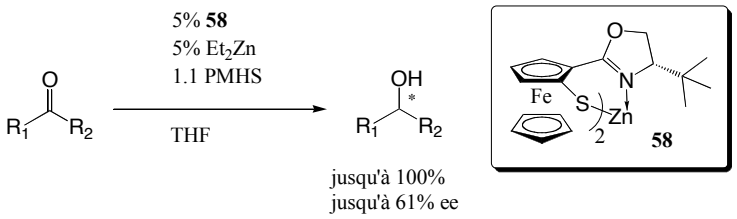

Dans une seconde partie de ce travail, nous avons développés un nouveau système pour l'hydrosilylation de cétones reposant sur l'hypothétique formation d'un catalyseur chiral d'hydrure de cobalt. Cet intermédiaire est supposé être formé par réaction du complexe de cobalt (II) neutre correspondant avec du tétrabutylammonium triphényldifluorosilicate (TBAT) comme activateur et un silane. Suite à un criblage préliminaire, les ligands de type salen se sont avérés être les plus efficaces par activation avec du TBAT en présence de PMHS.

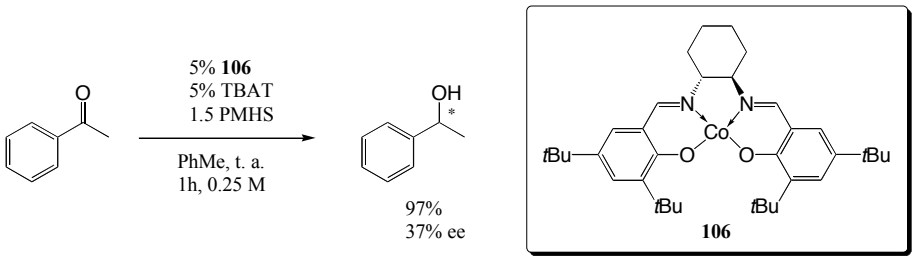

Des modifications de cette structure en remplaçant le groupe phénol par des groupes sulfonamides variés ont mené, après optimisation des paramètres de réaction, à un système hautement efficace avec des énantiosélectivités atteignant 84% pour la réduction de la tétralone. Ce travail devrait ainsi ouvrir de nouvelles perspectives pour le design de systèmes catalytiques hautement énantiosélectifs et à moindre coût pour l'hydrosilylation de cétones prochirales.

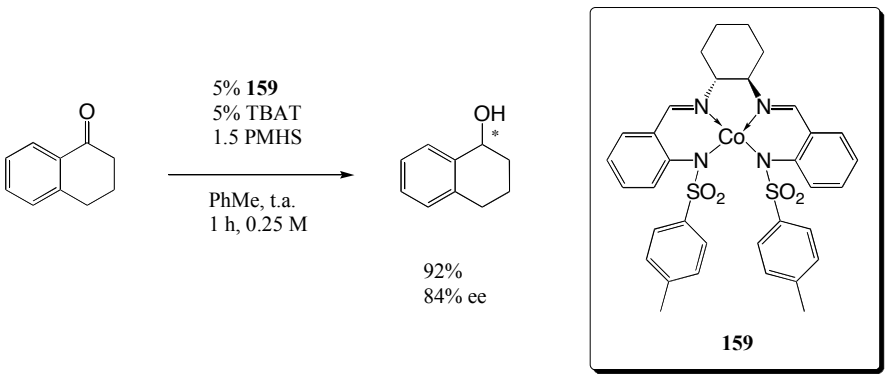

Abbreviations

δ	Chemical shift
Cp	Cyclopentadienyl
Cy	Cyclohexyl
d	Doublet
DIBAH	Di-*i*-butyl aluminium hydride
e.e.	Enantiomeric excess
eq	Equivalent
Et	Ethyl
GC	Gas Chromatography
h	Hour
Hz	Hertz
I.R.	Infrared
J	Coupling constant
m	Multiplet
M^+	Molecular ion
Me	Methyl
mol	Mole
MS	Mass spectrometry
n.d.	Not determined
NMR	Nuclear magnetic resonance
Ph	Phenyl
PMHS	polymethylhydrosiloxane
r.t.	Room temperature

Red-Al	Bis-(2-methoxyethoxy) aluminium sodium hydride
R_f	Reference front
s	singulet
salen	Salicylidene ethylene diamine
t	triplet
TBAF	Tetrabutyl ammonium fluoride
TBAT	Tetrabutylammonium triphenylsilyldifluorosilicate
THF	Tetrahydrofuran
TLC	Thin Layer Chromathography
TMS	Tetramethylsilane
TOF	Turn Over Frequency
TON	Turn Over Number

Introduction

Catalysis can be defined as a process during which compounds either enable or accelerate the reaction between reagents without being consumed or retrieved in the formed products. Its asymmetric version using chiral catalysts allows from achiral starting materials to yield enantiopure or enantiomerically enriched products.

During the last decades, there has been a considerable and continuously increasing interest in enantioselective catalysis as shown by the number of industrial processes developed. Some classical examples are the production of L-DOPA by Monsanto used to cure Parkinson's disease[1,2] or the herbicide Metolachlor produced by hydrogenation with Xyliphos-Ir.[3]

This interest is explained by different factors. In many biologically active compounds, one enantiomer presents the desired activity whereas the other one can present a fully different property ranging from inactivity to toxicity. In addition to this, synthesis of the sole active enantiomer presents an atom economy, which has environmental as well as financial impacts.

From a more chemistry oriented point of view, chiral building blocks can be obtained by other means, which present conceptually some disadvantages: use of the chiral pool (structural and absolute configuration limitation), chiral auxiliary (stoechiometric quantity of chiral fragment which requires grafting and removal), racemate resolution (unwanted product recycling and/or conditions specificity) and chromatographic separation on a chiral phase (recycling of the undesired enantiomer).

Asymmetric catalysis appears then as more interesting since substoechiometric amount of chiral information relative to the substrate is necessary and no grafting and removal of the chiral information is required. It presents however as constrain that high enantiomeric excesses should be reached to be really useful.

Asymmetric catalysis can be classified in three main categories: bio-catalysis, heterogeneous and homogeneous catalysis. Use of enzymatic and biotechnological fermentation processes presented interesting results for the industrial production of optically active intermediates. Their use allows the access to enantioenriched amino acids, carboxylic acids, amines alcohols or epoxides.[4] Lipases are an important class of enzymes that catalyse either hydrolysis reactions or esters synthesis. In addition to their stability in organic solvents, these catalysts display generally a low substrate specificity and high enantioselectivities. An interesting approach is based on the combination of them with metal catalysts in dynamic kinetic resolutions.[5]

Heterogeneous catalysis can employ chiral modifier on metal surface. From a general point of view, this approach presents a narrow scope, since it was successful in hydrogenation reactions. With tartrate modified Ni catalysts[6] or *Cinchona* modified Pt catalysts,[6,7] high enantioselectivities were reached for the reduction of keto-esters. Another approach in this category is based on the heterogenisation of homogeneous catalysts with demonstrated enantioselectivity and activity either on solid support or with a two-phase system. In the latter case, ruthenium hydrogenation was performed with cationic BINAP-type ligands with both high enantioselectivities and activities.[8]

In enantioselective homogeneous catalysis with transition metals, the chirality can be present in the catalyst (1) at the metal, (2) at the coordinating atom or (3) contained in the ligand (**Figure 1**).[9] In the early stages of this discipline, the thumb rule was that the closer the chirality center to the metal where reaction takes place, the higher will be the enantioselectivity of the formed product.

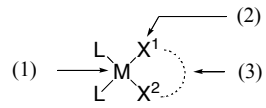

Figure 1: Possible locations of chirality centers in a complex.

When the complex is chiral-at-metal, a strong influence should be exerted on a prochiral substrate if reaction occurs within the metal coordination sphere.[9] Therefore, the chirality induction should be the best with this system because it presents the shortest distance between the chirality element and the substrate. Unfortunately, the studied complexes were either too stable or inactive in the tested catalytic system. Another difficulty encountered is the lability of the chiral metal, whose epimerisation precludes any applications in asymmetric catalysis. To circumvent this problem, a second element of chirality is added within the ligand X^1, X^2. This allows the formation of diastereoisomers differing in the chirality at the metal. Their ratio is strongly influenced by the chiral ligand and reflects the relative stability of the diastereoisomers. Some catalysts distinguished

themselves as **1** in Diels-Alder reactions[10] or **2** in transfer hydrogenation to ketones[11] (**Figure 2**).

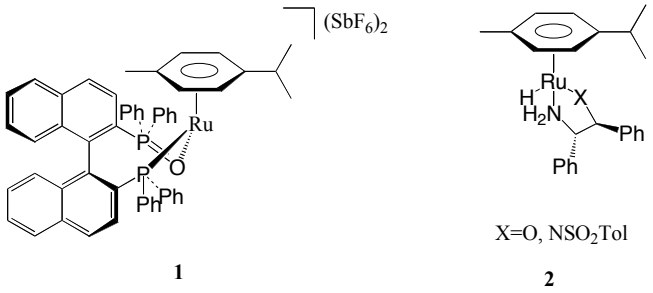

1 **2**

Figure 2: Two successful catalysts, which are chiral-at-metal and present an additional chiral center in a bischelating ligand.

Chirality at the coordinating heteroatom was expected to be highly selective because of its close proximity to the reaction center. Indeed, enantioselectivities up to 88% were obtained by Knowles for the Rh-based hydrogenation of dehydroaminoacids with ligand CAMP **3** (**Figure 3**).[12] This ligand remained for a long time one of the most successful for monophosphosphorus ligand in asymmetric catalysis as the introduction of bidentate phosphorus based ligands led for a long time to the idea that chiral bidentate ligands were necessary to reach high enantioselectivities in asymmetric catalysis. However, monodentate chiral ligands recently came back into fashion, especially since simple ligands, such as chiral phosphoroamidites, phosphonites and phosphinites were shown to be extremely efficient for some asymmetric catalysed transformations (such as

rohdium catalysed hydrogenation[13] or rohdium catalysed conjugated addition of potassium organotrifluoroborates to electrophilic double bonds[14]).

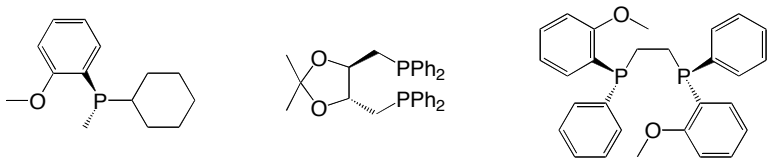

(*R*)-CAMP **3** (*R*,*R*)-DIOP **4** (*R*,*R*)-DiPAMP **5**

Figure 3: Mono- and diphosphines used in the asymmetric hydrogenation of dehydroaminoacids.

Even if successful, ligands bearing chirality at the coordinating atom were overwhelmed by diphosphines where the chiral information is located in the bridging ligand. The first ligand of this kind, DIOP **4**, [15] was described and employed successfully by Kagan in the hydrogenation of dehydroaminoacids with up to 83% enantioselectivities (**Figure 3**). This achievement is a milestone in asymmetric catalysis because it showed that chirality centers must not necessarily be located in the direct proximity of the metal center, contrarily to the early belief in a beneficial proximity effect. Furthermore, it is also the first use of a C_2-symmetric ligand, which allows reduction of the transition states number relative to C_1-symmetric ligand. Based on this concept, many developed ligands implement this key feature. Later, Knowles developed DiPAMP **5**,[1] which was applied in the synthesis of L-DOPA with 95% of enantioselectivity (**Figure 3**).

The researches of Knowles as well as those of Noyori and Sharpless in the field of hydrogenation and oxidation had an important impact on the synthesis of biologically active compounds and were rewarded by the Nobel prizes in 2001.[2,11,16]

Prior to the presentation of our results in the synthesis of new chiral precatalysts and their applications in asymmetric catalysis, a short and conceptual review of the literature will present how catalysts can affect the reagents reactivity, especially by electrophile activation, nucleophile activation and finally by both electrophile and nucleophile activation.

Chapter 1
Bibliographic introduction

Asymmetric induction in the reaction between two components can be carried out with a chiral catalyst by activation of either one reagent or both of them. The activation of the electrophile such as a carbonyl (aldehyde, ketone, …) or an electrophilic double bond can be done for instance by a chiral Lewis acids. In this class of reaction, we can include several examples such as the asymmetric catalysis of the Diels-Alder reaction by several classes of chiral Lewis acids (such as chiral copper (II) bisoxazoline complexes).[17] On the other hand, activation of the nucleophile can occur by coordination or ligand exchange on the metal. In this class of reaction, the activation of silicon based nucleophiles (silanes, silyl enol ethers, allyl silanes, …) by chiral bases have been widely developed for the enantioselective addition of nucleophiles onto aldehydes and ketones. Among this class of catalytic reactions, some of the most famous examples have been reported by Denmark who used chiral phosphoroamide based ligands in those transformations.[118,19] However, one of the most successful

[1] However, Denmark postulated at first that the activation of the silicon atom by the Lewis base gives rise to the formation of a cationic silicon which acts then as a Lewis acid which will in turn activate the carbonyl electrophile. Therefore, this case could also be considered as a dual activation of both nucleophile and electrophile.

and reliable method in catalysis lies in both the activation of the electrophile and the nucleophile by the chiral catalyst. This concept, inspired by nature was widely developed for the design of highly enantioselective chiral catalysts. One of the most efficient systems in this area has been reported by Shibasaki who have recently reviewed this area of research.[20,21] In most cases, the catalysts bear two different docking sites (usually one Lewis acid and one Lewis or Bronsted base), which allow the activation of both electrophile and nucleophile. Furthermore, as it allows to bring both partners in a close vicinity of each other, it will lead to a transition state in which the degree of liberty will be more restricted, a more favorable situation to obtain high enantioselectivities.

Selected examples of the literature will introduce some classes of reactions that might best exemplify these strategies for the successful synthesis of enantioenriched products. As it was already quoted, numerous examples from the literature could be found to illustrate those three concepts. We thus decided to exemplify each case by only one family of catalytic reaction, two of them being closely related to our research projects (**Figure 4**).

This hypothesis was recently confirmed. It shows the difficulty of a real classification of the catalysts according to their mode of activation.

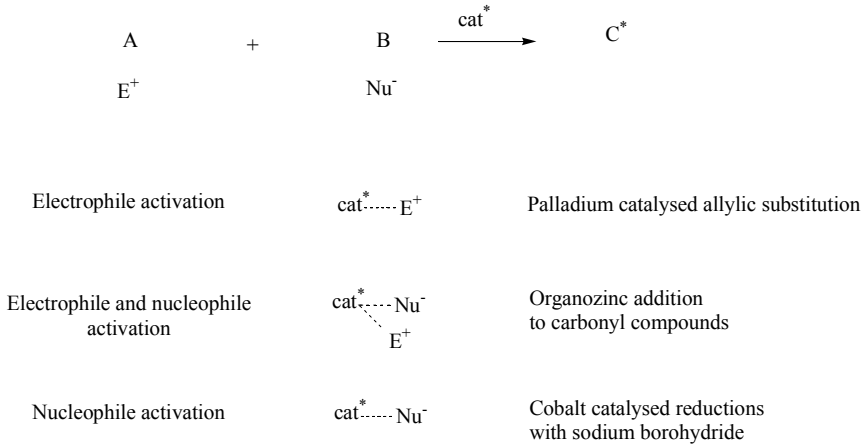

Figure 4: Activation types exerted by a chiral catalyst.

1.1. Activation of the electrophile: palladium catalysed allylic alkylation

One of the most studied catalytic asymmetric reactions for which the electrophile is activated may be the allylic alkylation. It has been mainly studied with palladium complexes[22-24] but researches focussing on other transition metals, such as copper[25], molybdenum[26], iridium[27,28] or ruthenium[29], are gaining more and more interest and present complementary selectivities. The main features of the palladium-catalysed nucleophilic allylic substitution will be presented followed by studies classified according to the type of the chiral ligand.

1.1.1. General considerations

The reagents involved are mostly stabilised nucleophiles such as dialkylmalonate and electrophiles incorporating a leaving group in allylic position such as a carbonate in presence of a transition metal (**Scheme 1**). Trost described the first example with DIOP as a chiral ligand.[30]

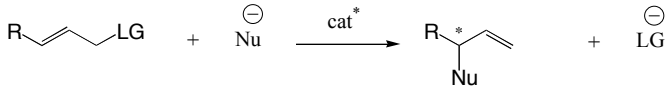

Scheme 1: General reaction of allylic alkylation.

As isolation of π-allyl palladium and some palladium π-complexes is possible, their characterisation greatly helped the understanding of the species involved in the catalytic cycle as well as the design of more efficient ligands. The first step consists in a complexation between the zero valent palladium complex and the allylic substrate (**Scheme 2**). Then ionisation takes place followed by nucleophilic addition. Finally, the decomplexation from the product regenerates the initial palladium complex. Every step in this cycle presents the possibility to induce an enantioselectivity in function of the substrate structure at the exception of the decomplexation because the chirality center is already formed.

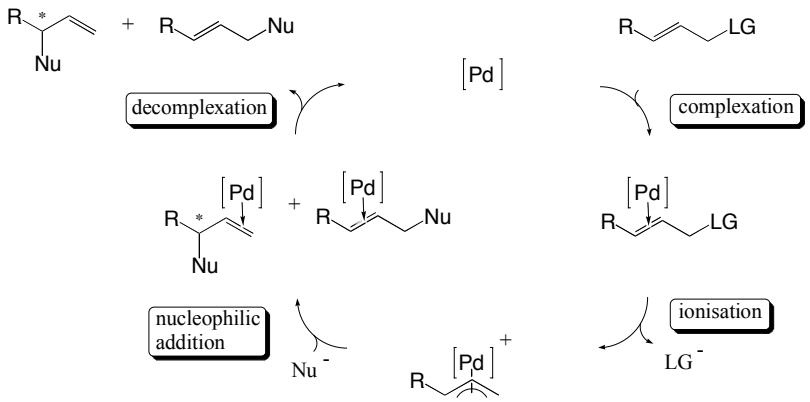

Scheme 2: Proposed catalytic cycle for the allylic alkylation.

Generally, the ionisation step proceeds with inversion of stereochemistry at the allylic moiety (**Scheme 3**). However, the nucleophilic addition can lead to two different stereochemical issues depending on the nature of the nucleophile used. Indeed, the so called "soft" nucleophiles (stabilised), derived from conjugated acid with a $pK_a < 25$ attack the electrophilic allyl ligand on the opposite face to the metal. Consequently, a global retention of stereochemistry is observed. Other nucleophiles such as phenols, alcohols or amines have also been used in this reaction and act as "soft" nucleophiles. However, "hard" nucleophiles (unstabilised, $pK_a > 25$) react first through a transmetallation reaction followed by a reductive elimination leading to a global inversion of stereochemistry. Considering that there is a direct interaction between the transition metal and this type of nucleophiles, their reactions will not be taken into account.

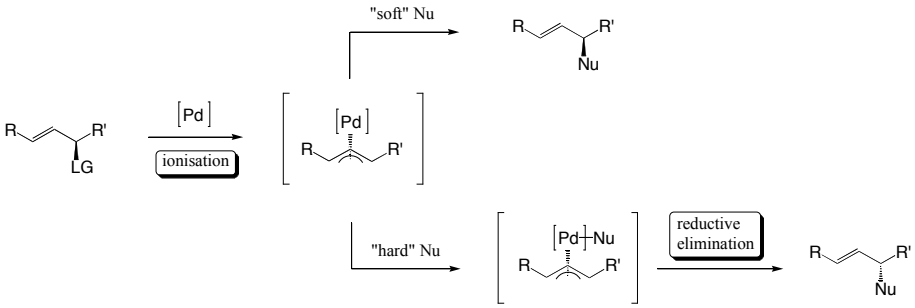

Scheme 3: Reactivity of "soft" and "hard" nucleophiles.

Different strategies were developed to induce enantioselectivity according to the structure of the substrate (**Scheme 4**).[24] Enantiotopic faces discrimination can involve either a prochiral electrophile or nucleophile. By deracemisation, a meso π-allyl complex is formed starting from a racemic and enantioselectivity is induced by favoring the nucleophilic attack on one of the enantiotopic allylic termini. Lastly, desymmetrisation can be achieved by discrimination between enantiotopic leaving groups. Prior to the presentation of successful ligands in deracemisation of 1,3-disubsituted allylic substrates, the stereodynamic of π-allyl palladium complexes will be first described in order to show the complexity of the involved catalytic cycles.

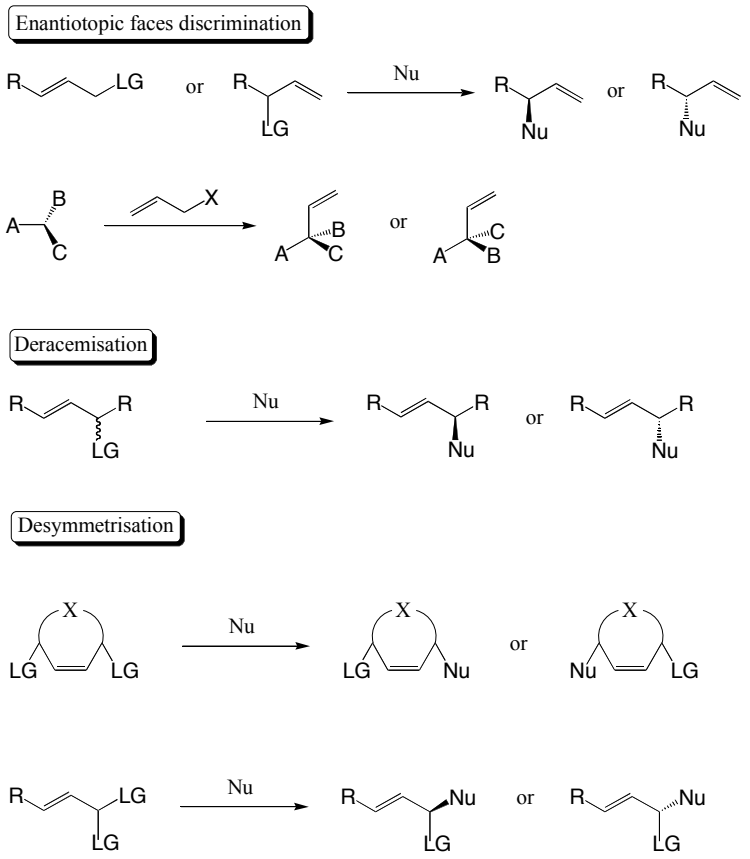

Scheme 4: Strategies for enantiodiscrimination in asymmetric palladium allylic substitution.

Stereodynamic of π-allyl palladium complexes[24]

Different mechanisms lead to changes in the conformation of π-allyl palladium complexes through intra- or intermolecular processes. These take place at rates that can be competitive or not with the nucleophilic addition.

This presents either detrimental or beneficial effects on the reaction outcome.

One of the intramolecular process is the so called "η^3-η^1-η^3 (or π-σ-π) isomerisation", in which the rotation around a C-C bond in the η^1 intermediate lead to a *syn*/*anti* interconvertion without changing their position relatively to the ligands *trans* to them (**Scheme 5**).

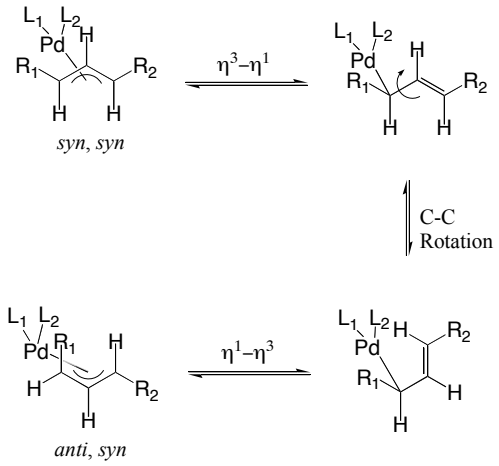

Scheme 5: η^3-η^1-η^3-isomerisation process.

Another intramolecular process is the apparent allyl rotation, where there is a switch in the position of the allylic termini. Three different possible pathways were described (**Scheme 6**). As in the η^3-η^1-η^3 process described previously, there is a change in hapticity followed by a Pd-C bond rotation and finally reassociation. Another pathway implies the dissociation of one ligand forming thus a coordinatively unsatured palladium complex. Here again, rotation around the Pd-C bond followed by reassociation

completes the apparent allyl rotation process. Finally, external ligands such as chloride or DMSO can lead to a pentacoordinated complex and then to a pseudorotation. This causes the isomerisation of the allyl complex.

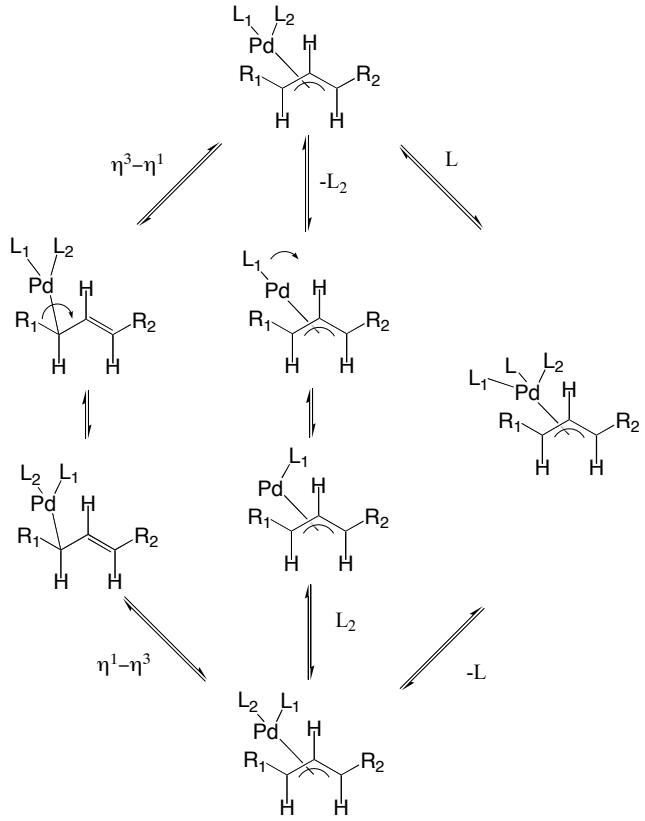

Scheme 6: Possible mechanisms for apparent allyl rotation.

Finally, isomerisation can arise intermolecularly from the attack of Pd (0) on the free face of the allyl complex through an S_N2 like mechanism (**Scheme 7**). Changes in the transition metal concentration generally support this pathway. However, as catalyst concentration is relatively low compared

to that of the nucleophile, Pd (0) allyl exchange should present minor effects on the reaction outcome.

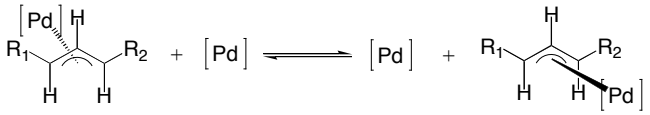

Scheme 7: Racemisation by a Pd (0) catalysed allyl exchange.

1.1.2. Developed chiral ligands for the deracemisation of 1,3-disubstituted allyl substrates

The three developed strategies (enantiotopic faces discrimination, deracemisation and desymmetrisation) were already subjected to a review.[22] Therefore, only the design of precatalyst for the deracemisation of 1,3-disubstituted allyl substrates will be introduced with emphasis on the origin of enantioselectivity.

The main difficulty for diphosphine ligands is to convey the chiral information on the other side of the allylic system. Ligands, which were successful in asymmetric hydrogenation, failed in allylic substitution reactions because they could not influence the nucleophilic attack efficiently. An effective class of diphosphines, which are able to overcome this problem, were developed by Trost (**Figure 5**).[22,24] This kind of ligand, such as **6**, presents the particularity to have a more important bite angle, creating thus a chiral cavity where the allyl moiety is located. Good levels of enantioselectivity where reached for substrates such as 1,3-dimethylallyl acetate or their related linear alkyl derivatives. However, 1,3-diaryl and

dicyclohexyl allyl derivatives presented low enantioselectivities because the chiral pocket could not envelop well these types of voluminous substrates.

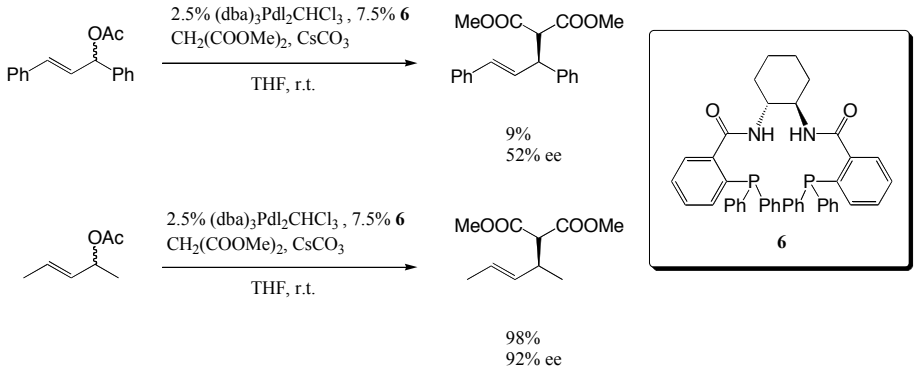

Figure 5: Application of the chiral C_2 symmetric diphosphine ligand **6** developed by Trost.

Another successful approach developed independently by Helmchen[31], Pfalz[32] and Williams[33,34] was based on an electronic effect. It takes advantage of the *trans* effect exerted by the *N*, *P* bidentate ligand such as **7** (**Scheme 8**). The combination of a hard (N) and a soft donor (P) allows differentiation of the allylic termini. Soft nucleophiles attack then the allylic position *trans* to the phosphorus ligand. In contrast to the diphosphines developed by Trost, the larger the groups of the 1,3-disubstituted allylic substrate, the higher the enantioselectivity will be. For instance, the enantioselectivity was rather modest with methyl groups (56% ee), whereas phenyl groups gave an enantioselectivity of 98%.

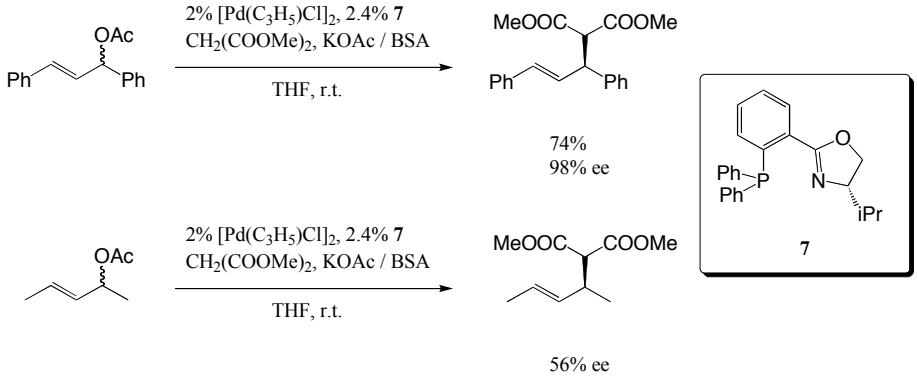

Scheme 8: Phosphino oxazoline ligand developed for the palladium catalysed allylic substitution.

As shown previously, high enantioselectivities could be reached by playing either with steric or electronic effects. A last possibility would be to influence the trajectory of the incoming nucleophile. Indeed, the introduction of a side chain in the chiral ligand that coordinates the nucleophile so as to orientate the nucleophilic attack is effective, as demonstrated by Hayashi (**Scheme 9**).[35] It was shown that the side chain length in **8** as well as the nature of the functional group strongly influences the reaction outcome.

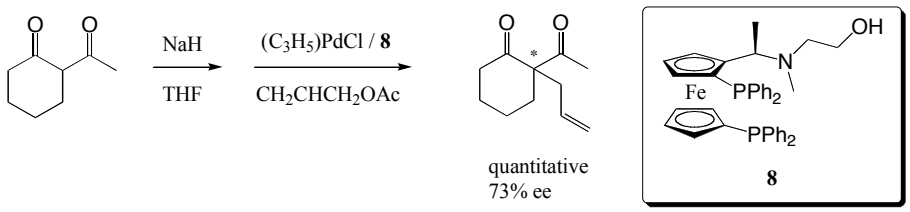

Scheme 9: Allylic alkylation catalysed by a palladium-based catalyst orienting the nucleophile approach.

In another approach, Trost has developed a two-components system, in which both electrophiles and nucleophiles are activated (**Scheme 10**).[36] This was achieved by addition of a catalytic quantity of borane, which promotes the addition of alcohols to vinyl epoxides with high enantioselectivities.

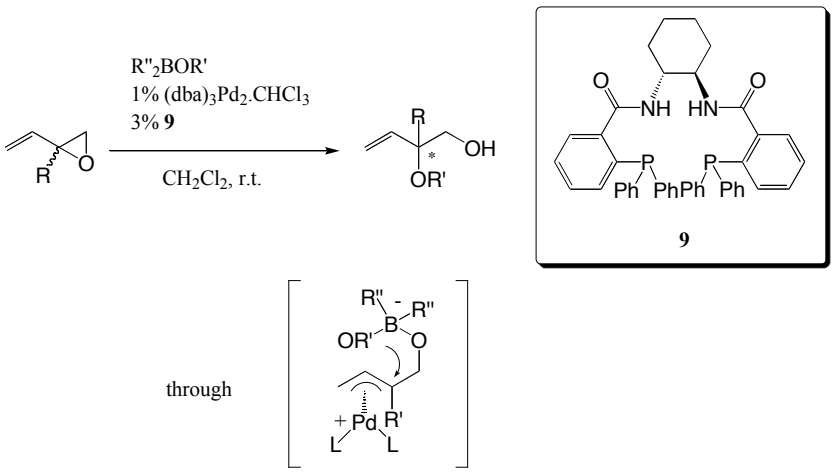

Scheme 10: Palladium catalysed allylic substitution with alcohols.

This concept of activating both the electrophile and the nucleophile, even if little used in allylic substitution, was used for the development of efficient catalysts in other fields of asymmetric synthesis. One of the most representative is the field of organozinc addition to carbonyl compounds that will be presented in the next section of this literature review.

1.2. Activation of both the nucleophile and the electrophile: organozinc addition to carbonyl compounds

Activation of both the nucleophile and the electrophile can be achieved with a transition metal acting as Lewis acid to activate the electrophile and a Lewis base activating the nucleophile. This concept was successfully applied in the enantioselective addition of organozinc reagents to carbonyl compounds.[37]

The discovery by Oguni and Omi that amino alcohols can catalyse the enantioselective addition of diethyl zinc to aldehydes is a milestone for the synthesis of enantiomerically enriched alcohols (**Scheme 11**).[38] This reaction takes advantage of the low nucleophilic nature of dialkyl zinc compounds, since they present a linear structure. For corresponding unsatured complexes such as aryl zinc compounds, an uncatalysed reaction, that forms the product by an achiral pathway, requires the use of catalyst presenting not only a high enantioselectivity but also a high reactivity.

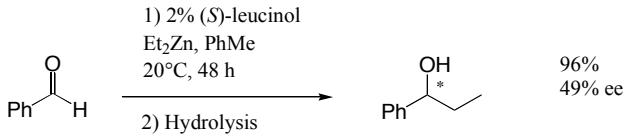

Scheme 11: First reported addition of diethylzinc to benzaldehyde.

Noyori described the use DAIB **10** as the first highly enantioselective ligand for the diethyl zinc addition to aldehydes (enantioselectivities up to 95%).[39] A catalytic cycle for this reaction was also

presented (**Scheme 12**). At first an equimolar equivalent of diethylzinc reacts with the amino alcohol to form a five-membered ring zinc complex, which is in the form of a dimer. From this intermediate, transfer from the organozinc to an aldehyde is not possible. A second equivalent of organozinc nucleophile is required. As they present vacant coordination sites, donor ligands such as oxygen or sulfur can change their hybridisation concomitant to a weakening of the Zn-C bond. This allows to increase its nucleophilic character. It is by coordination to an oxygen lone pair that activation takes place and allows thus the transfer of an alkyl group to the substrate coordinated to the zinc amino alcoholate. The catalytic cycle is closed by reaction with either a carbonyl compound or a zinc species, which releases a zinc alkoxide.

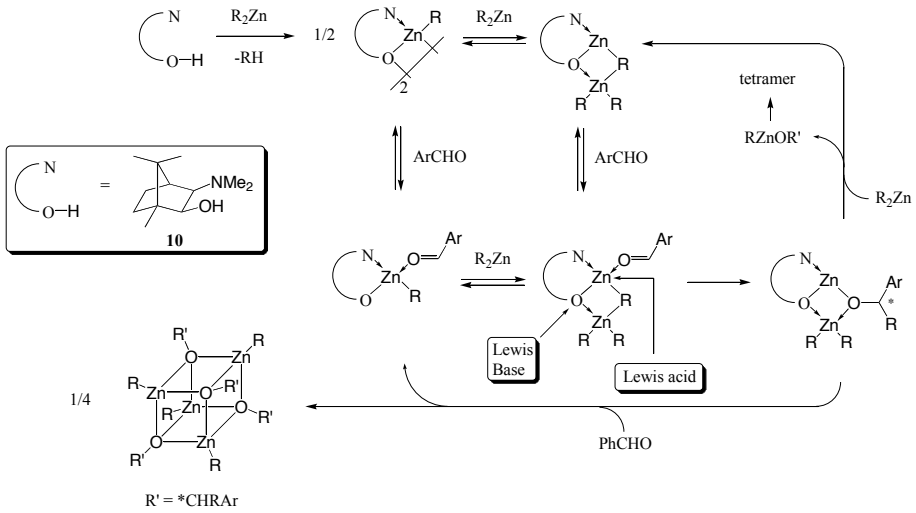

Scheme 12: Catalytic cycle for the alkyl zinc addition to aldehydes.

The two strategies developed for this purpose used the *N*, *O* motif. In this ligand, nitrogen can be sp^3 or sp^2 hybridised whereas oxygen remains in form of an alkoxide. With this system substrate activation arises by complexation to the zinc alcoholate and the nucleophile is activated with an oxygen electrons lone pair. The activity enhancement can be achieved either by increasing the Lewis acidity of the zinc coordinating the substrate or by stronger activation of the organozinc compound.

Some increase in the Lewis acidity of the catalyst can be achieved by decreasing the electron density on the ligand backbone. This approach was used in the asymmetric transfer of arylzinc to aldehydes (**Scheme 13**). Indeed, the change of a ferrocenic core in **11** to a less electron rich η^5-cyclopentadienyl rhenium (I) tricarbonyl **12** gave an increase in enantioselectivity for a variety of substrates.[40,41]

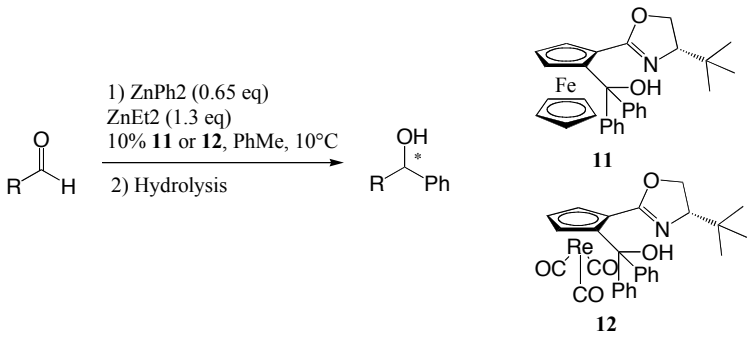

Scheme 13: Phenyl zinc transfer to aldehydes.

As depicted previously for the enantioselective addition of diethyl zinc to carbonyls, the coordination of a ligand to an organozinc species leads to an increase in its nucleophilicity. Therefore, it was expected that coordination by an additional Lewis acid would lead to an increased reactivity (**Figure 6**). [42]

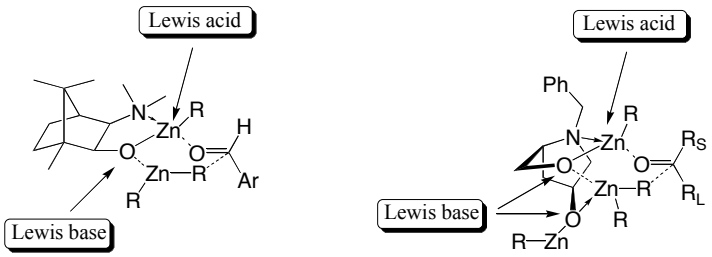

Figure 6: Dual catalyst activation of nucleophile and electrophile.

The introduction of an additional hydroxyl group on the ligand **13** (compared to **14**), gave increase in enantioselectivity as well as in reactivity for the asymmetric alkylation of α-ketoesters (**Scheme 14**). The position of this group relative to the other hydroxyl function was found to be decisive. The proximity of the two oxygen atoms in the ligand with the 2,4-*cis*-configuration led to suppose that both of them activate dimethyl zinc. This hypothesis could explain the lower enantioselectivity observed for **15**.

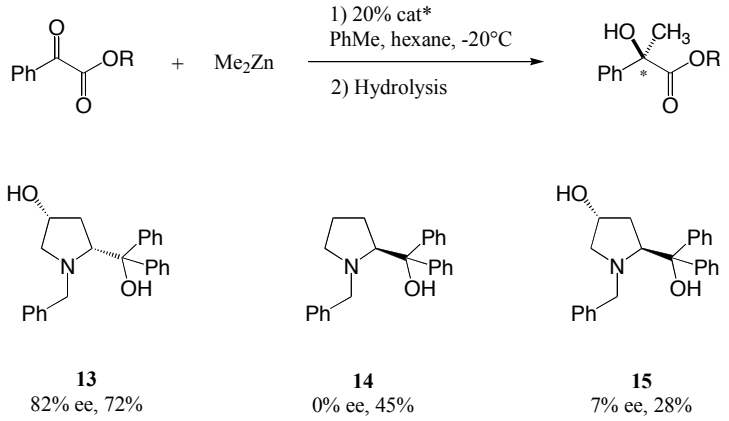

Scheme 14: Dimethyl zinc addition to α-ketoesters.

Studies on *N*, chalcogen based chiral ligands has attracted less attention compared to the usual *N*, *O* based catalyst. However, the use of such ligands associated with organozinc nucleophiles presented very good results in some catalytic reactions such as the alkylation of aldehydes. This was attributed to a better affinity of sulfur towards zinc (HSAB principle) and a lower tendency of the thiolate anion to diminish the Lewis acidity of the zinc center compared to alcoholates.[43] Examples illustrating this effect are scarce in the literature. The *N*, *S* ligand **16**, based on the *L*-proline structure, catalysed the diethylzinc addition on aromatic aldehydes with 73-98% enantioselectivities (**Figure 7**). The *N*, *O* analogue presents a lower asymmetry induction (30-64%).[44] With the pyrrolidine-based ligand **17**, a higher chirality induction was observed for the thiol than with the corresponding alcohol.[45] The use of **17** for the alkylation of aromatic as well as aliphatic aldehydes gave products with enantioselectivities between 77

and 99%, whereas in the test reaction with benzaldehyde, an enantioselectivity of only 44% was reached.

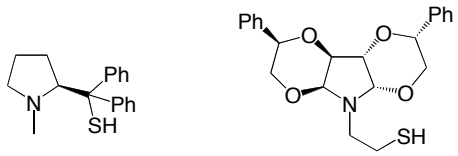

16 **17**

Figure 7: *N*, *S* ligands presenting higher enantioselectivities than their *N*, *O* analogues in the organozinc addition to aldehydes.

Interestingly, amino thioacetates such as **18** can also be employed to catalyse the diethylzinc addition to various aldehydes without affecting the enantioselectivity (**Scheme 15**).[46] The use of the corresponding amino alcohol **19** lead to an erosion of enantioselectivity. With the amino thiol **20**, a constant enantiomeric excess higher than 99% was obtained when the substrate to catalyst ratio varied from 20% to 0.02%. The same study shows that the corresponding amino alcohol presented a constant altering of the enantioselectivity as the catalytic loading was decreased.

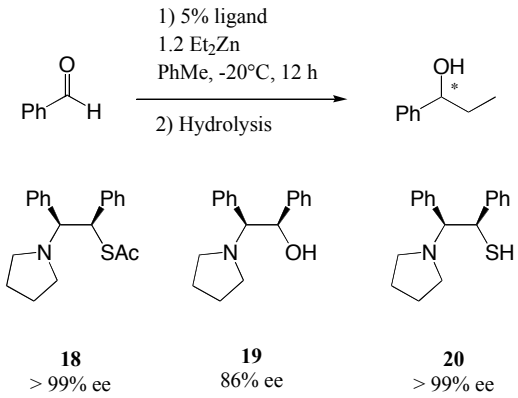

18
> 99% ee

19
86% ee

20
> 99% ee

Scheme 15: Amino thioacetate and thiol display higher efficiency in the diethyl zinc addition to benzaldehyde.

The *N*, *S* complex **21**[47] and *N*, *Se* ligand **22**[48] both catalysed the classical alkylation of benzaldehyde with high enantioselectivities (**Scheme 16**). It should be noticed that in case of the *N*, *S* complex **21**, 4% of active complex are generated, whereas for the *N*, *Se* ligand **22** only 0.5 % of effective catalyst is generated (*vide infra*). For this reason, no general trend can be withdrawn from these studies.

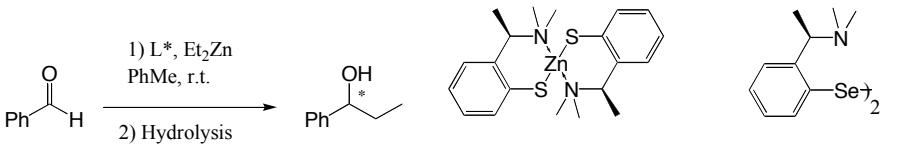

21
catalytic loading: 2%
94% ee, 99%

22
catalytic loading: 1%
91% ee, 70%

Scheme 16: *N*, *S* and *N*, *Se* precatalysts in the alkylation of benzaldehyde.

A ferrocene-based *N*, *Se* ligand **23** incorporating a planar and a central chirality was described for the diethyl and diphenyl zinc addition to aldehydes.[49] Enantioselectivities up to 44 and 85% were reached for diethyl and diphenyl zinc additions, respectively. Interestingly, the corresponding phenyloxazoline diselenide catalysed the diethylzinc addition to benzaldehyde with 1% yield and 8% ee. This showed that planar chirality is not only important for the enantioselectivity but also for the reactivity. Compared to the highly enantioselective ligand presenting a diphenylcarbinol next to the oxazoline moiety, the diselenide ligand lacks a pseudo-C_2 symmetry. This might explain the lower enantioselectivities between the two precatalysts. No studies concerning the corresponding diastereoisomer presenting the other planar chirality was described.

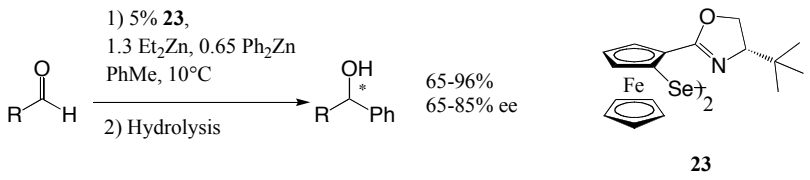

Scheme 17: Ferrocenyl oxazoline diselenide promoted diphenyl zinc addition to aldehydes.

Further increase in nucleophilicity can be achieved by the formation of an ate complex. To the best of our knowledge, this has not been reported for enantioselective zinc catalysed nucleophilic additions to carbonyl

compounds but it is described for cobalt catalysed reductions with sodium borohydride. For this reaction, only the nucleophile is activated.

1.3. Activation of the nucleophile: cobalt catalysed reductions with sodium borohydride

Pfaltz described semi-corrins such as **24** as highly enantioselective ligands for the conjugated reduction of α, β unsaturated esters and amides by sodium borohydride when used with $CoCl_2$ as a metal source (**Scheme 18**).[50-52]

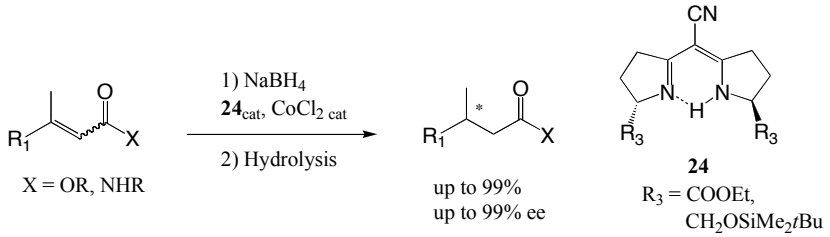

Scheme 18: Cobalt catalysed reduction of α, β unsaturated esters and amides by sodium borohydride.

Despite these impressive results, limitations were noted by other groups to explain the relatively small impact of this system such as the lack of possible structural modification of the ligands,[53] the number of steps required for their synthesis or long reaction times.[54] From a more practical

point of view, the requirement to run freeze-and-thaw cycles was perhaps the most prohibitive drawback. Regardless of the weak points, this system stimulated researches for the development of new ligands for the cobalt-catalysed reductions with sodium borohydride. It should be noted that no mechanism was proposed for the formation of the active catalyst in those publications.

Recently, the catalytic system developed by Pfaltz was found to be efficient for the cobalt catalysed reductive cyclisation of azido and cyano substituted α, β-unsaturated esters (**Scheme 19**). This highly enantioselective reaction was applied to the synthesis of (-)-Rolipram.[55]

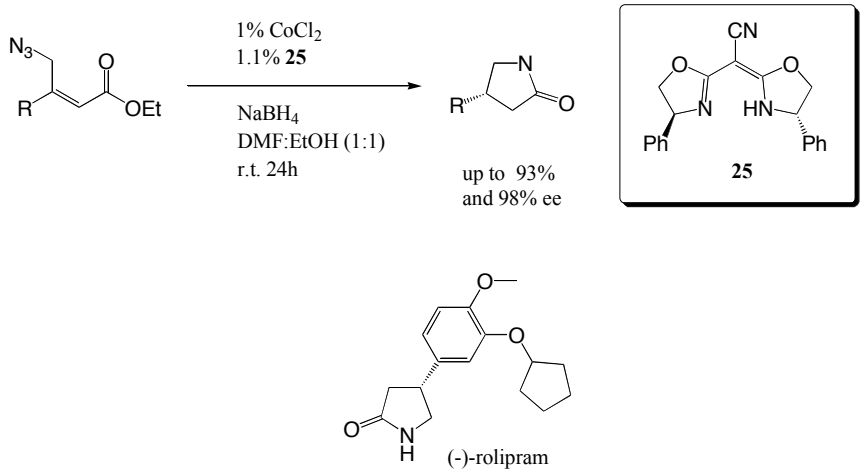

Scheme 19: Cobalt catalysed reductive cyclisation with sodium borohydride.

More recently, Reiser designed highly efficient azabis(oxazoline) **28** for the conjugated reduction of α, β unsaturated carbonyl compounds (**Scheme 20**).[53] The concept underlying the use of this class of precatalyst is the following: change from the semicorrin developed by Pfaltz to bisoxazoline for the reduction of α, β unsaturated esters lead to a total loss in reactivity. A more electron rich ligand, such as aza(bisoxazoline) was then thought to be more efficient. This is indeed the case as α,β unsaturated esters and amides are reduced in good yields with high enantioselectivities with 2.5% $CoCl_2$.

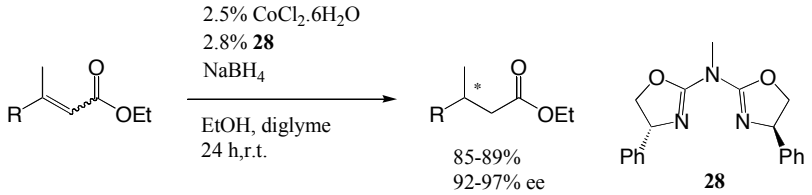

Scheme 20: Conjugated reduction of α, β unsaturated esters with $NaBH_4$ catalysed by $CoCl_2$/**28.**

Yamada and Mukaiyama used successfully new aldiminato cobalt complexes **26** (**Figure 8**) that were effective for the asymmetric reduction of ketones and imines in the presence of modified borohydride reagents. C_2-Symmetrical diols and *anti*-aldol-compounds could also be prepared with enantioselectivities higher than 90%.[56]

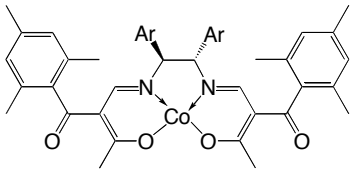

26a: Ar = Ph
26b: 3,5-dimethylphenyl
26c: 2,4,6-trimethylphenyl

Figure 8: Optically active cobalt (II) complexes.

All of these reactions require the activation of the borohydride by addition of alcohols. Usually, the alcohol system is a mixture of one alkyl alcohol, such as methanol or ethanol, and a coordinating alcohol such as tetrahydrofurfuryl alcohol (THFA) (**Scheme 21**). Any change in their nature or in their number of equivalents relative to the reducing agent affects the reactivity as well as the enantioselectivity. Addition of THFA renders the reaction mixture homogeneous and generally improves the enantioselectivity. It should be underlined that the activation procedure has an important impact on the reactivity without affecting the enantioselectivity, when using the same alcohol(s). Indeed, with a premodified borohydride, the same reaction, which is incomplete after one day, is quantitative after 20 minutes and with 5 times less of the precatalyst **26** compared to the *in situ* procedure. Increasing the temperature from -20°C to 0 °C reduced the reaction time to less than 15 minutes without affecting the enantioselectivity significantly.

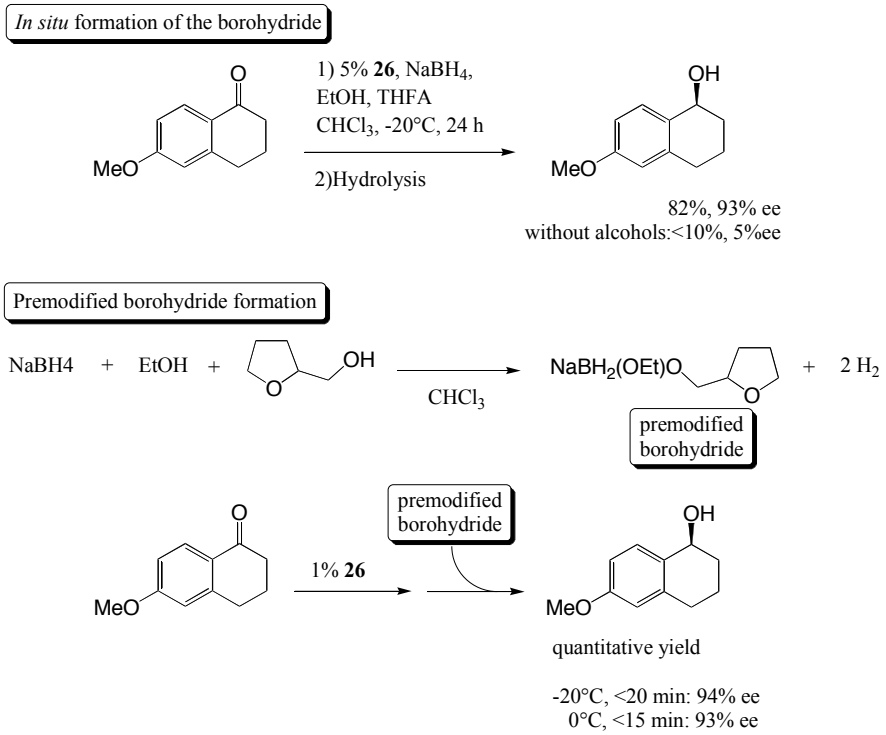

Scheme 21: Comparison between the *in situ* and the premodified borohydride formation in the enantioselective reduction catalysed by cobalt complexes.

The suitable alkyl alcohol can be chosen according to the following thumb rule. Mixtures of ethanol and THFA are generally suitable for aromatic ketones with a relatively low steric demand, such as cyclopropyl or primary alkyl groups. Concerning combination of methanol and THFA, sterically hindered ketones are most efficiently reduced by this system.

For ketones reduction, the choice of the complex is also of importance and a general trend emerged. With complex **26a** bearing a 1,2-diphenylethylenediamine backbone, sterically hindered substrates at the α-position are reduced with high enantioselectivities. Aromatic cyclic ketones required use of complex **26b** with a 1,2-bis-(3,5-dimethylphenyl)ethylenediamine. Finally, complex **26c** matches best with acyclic alkyl aryl ketones. By a proper choice of the appropriate cobalt complex and premodified borohydride, substrates are reduced quantitatively with enantioselectivities varying between 90 and 98% using 1% of precatalyst at -20°C for 12 hours (**Scheme 22**).[56]

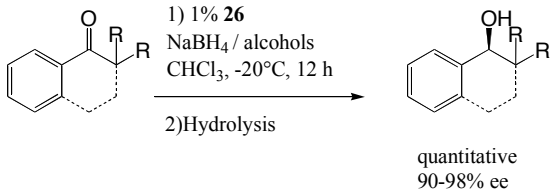

Scheme 22: Quantitative reduction of ketones in high yields with complexes of type **26**.

The extension of this catalytic system to cobalt salen complexes was performed by Xia for the sodium borohydride reduction of ketones. Up to 70% enantiomeric excess with >99% yield were reached after 24h at room temperature.[57]

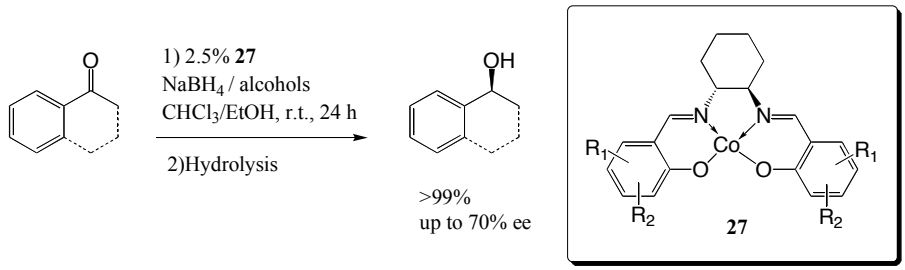

Scheme 23: Cobalt salen catalysed sodium borohydride reduction of prochiral ketones.

Imines were best reduced when substrates were of *N*-diphenylphosphinoyl type because of their inertness towards premodified borohydride. Reduction were carried out at 0°C for 4 hours with 1% cobalt complex **26** and allowed to reach 90-99% enantioselectivities with 81-98 % yields (**Scheme 24**). As for ketone, cyclic aryl imines are best reduced with complex **26b** whereas complex **26c** matches better acyclic aryl imines.[56]

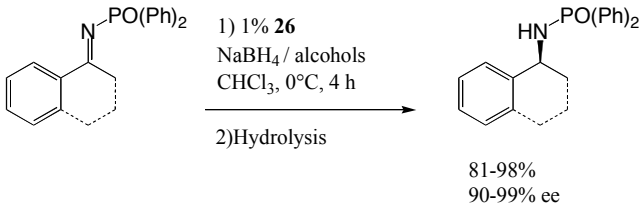

Scheme 24: Cobalt catalysed *N*-diphenylphosphinyl imines reduction by borohydride.

Synthesis of highly enantiomerically enriched C_2-symmetrical diols can be achieved with 94-100% yield with 1% of precatalyst at -20 °C for 40 to 60 hours (**Scheme 25**). A good to high *dl* selectivity was observed. The most suitable cobalt complex **26c** incorporates the 1,3-bis(2,4,6-trimethylphenyl)ethylenediamine unit.[56]

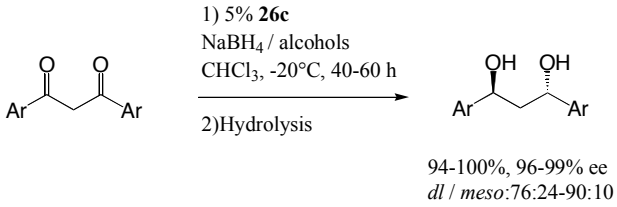

Scheme 25: Cobalt catalysed 1,3-diaryl-1,3-propanediones reduction by borohydride.

With the same type of cobalt complexes, *anti*-aldol products could be synthesised starting from 2-alkyl-1,3-diaryl-1,3-propanediones (**Scheme 26**). Very good yields and 99% of *anti* selectivity were obtained. The enantioselectivities varied between 91and 99%.[56]

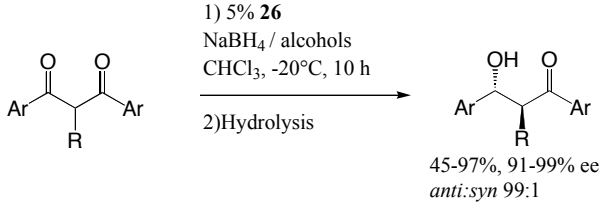

Scheme 26: Cobalt catalysed 2-alkyl-1,3-diaryl-1,3-propanediones reduction by borohydride.

As the borohydride reduction proceeds with high chemoselectivity in favor of the aromatic ketones over aliphatic ones, unsymmetrical 1-alkyl-3-aryl-1,3-diketones could be reduced not only with high enantioselectivity (**Scheme 27**), high *anti*-selectivity but also with high chemoselectivity. This catalytic system required however four times the addition of 0.1 equivalent of modified borohydride with two hours interval between each addition to avoid a decrease in selectivities.[56]

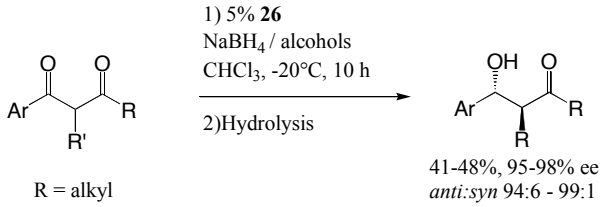

Scheme 27: Cobalt catalysed 1-alkyl-3-aryl-1,3-diketones reduction by borohydride.

In presence of a base, such as sodium methoxide, dynamic kinetic resolution of 2-alkyl-3-aryl-3-ketoesters could be performed (**Scheme 28**). Exclusively *anti*-aldol-products could be generated in 68-97% yield and 97-99% enantioselectivies.[56]

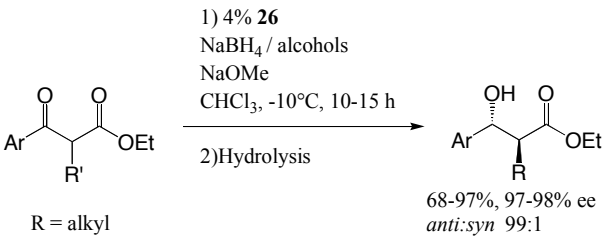

Scheme 28: Dynamic kinetic resolution of 2-alkyl-3-aryl-3-ketoesters.

Mechanistic studies by mass spectrometry showed the formation of an ionic cobalt hydride species by reaction of the cobalt (II) precatalyst with sodium borohydride. By reaction between the same cobalt complex and sodium borodeuteride generated the corresponding cobalt-deuteride complex. The aromatic ring on this catalytic active compound would then favor the approach of the substrate by π-π-interactions (**Scheme 29**).[56]

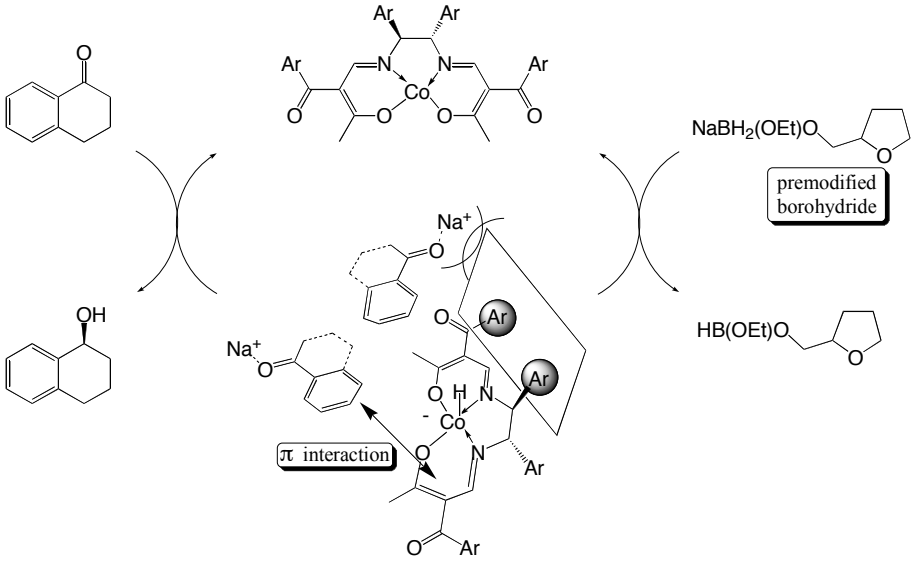

Scheme 29: Catalytic cycle and possible explanation for the observed enantioselectivity.

Chapter 2

Synthesis and applications of *N*, *S* ligands and zinc complexes

Ferrocene based catalysts present, in addition to their high stability, an easy introduction of planar chirality. It allows the introduction of two elements of chirality in the same 1, 2 disubstituted ferrocene compound if a chiral center is incorporated in a lateral group. Chiral cooperativity between these two elements was shown to be critical for the enantioselectivity as well as the activity of the catalyst. This interesting characteristic was useful in some asymmetric catalytic reactions involving different transition metals and ligand binding mode. An effective class is constituted, for example, by ligands with the ferrocenyl oxazoline structure.

2.1. Applications of ferrocenyl oxazoline ligands with planar chirality in asymmetric catalysis

The introduction of a diphenylphosphino group in the α position relative to the oxazoline leads to DIPOF ligands **29** and **30**. Their palladium and nickel complexes catalyse allylic substitution with C or N nucleophiles (**Scheme 30**).[58] In the given examples, planar chirality exerted only a minor influence with dimethylmalonate as nucleophile but significantly affected the enantioselectivity when benzylamine was used. Interestingly, the

addition of TBAF enhances the selectivity in the latter case. For the Ni catalysed cross coupling of allylic compounds with Grignard reagents, the enantioselectivities varied from 15 to 95%.[59] The main problem is the side reaction forming biphenyl in non-negligible quantities.

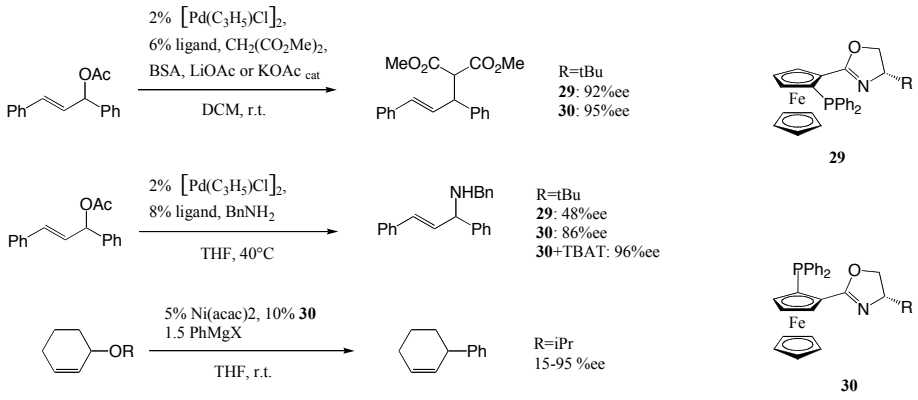

Scheme 30: Pd and Ni catalysed allylic substitution by DIPOF ligands.

The application of DIPOF ligands, such as **31** and **32**, in Rh and Ir catalysed hydrosilylation of ketones[60,61] and imines[62] were also investigated (**Scheme 31**). Generally, long reaction times are required for both substrates classes. An interesting aspect for ketones reduction is that with the same ligand **31**, access to both enantiomers is possible simply by switching the metal from Rh to Ir. Concerning cyclic imines reduction, such an effect is not observed and enantioselectivities up to 88% were reached with **32**. The Ir based catalytic system of ketones and imines hydrosilylation reached up to 97 and 88% ee, respectively, but the selectivities varied largely.[63]

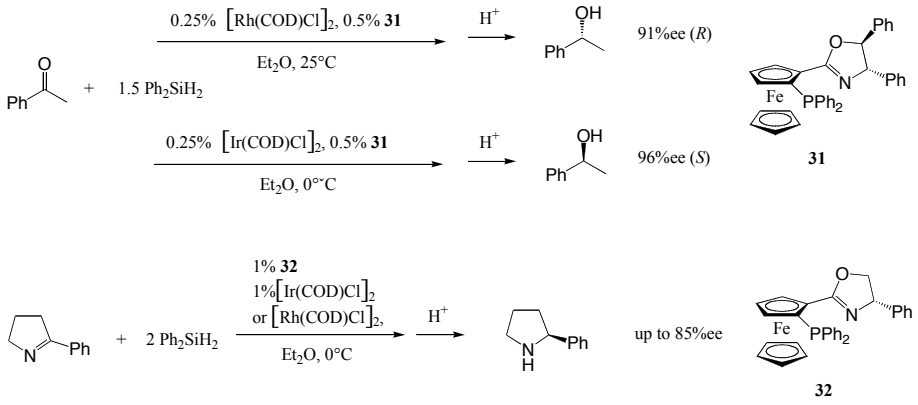

Scheme 31: Ir and Rh catalysed hydrosilylation of ketones and imines.

Transfer hydrogenation uses *iso*propanol as a hydrogen source. The reaction is driven by mass action so that high dilutions are necessary to generate useful product yields. However, high yields and enantioselectivities were reached for a large variety of ketones with **33** as precatalyst.[64] The choice of the metallic precursor is of importance because without triphenylphosphine the reduction of acetophenone proceeded with 9% enantioselectivity.[65] Addition of the phosphine to the reaction mixture followed by *p*-methylacetophenone lead to the corresponding reduction product with 80% enantioselectivity. This strongly suggests that triphenylphosphine is bound to the Ru in the enantiodetermining step.

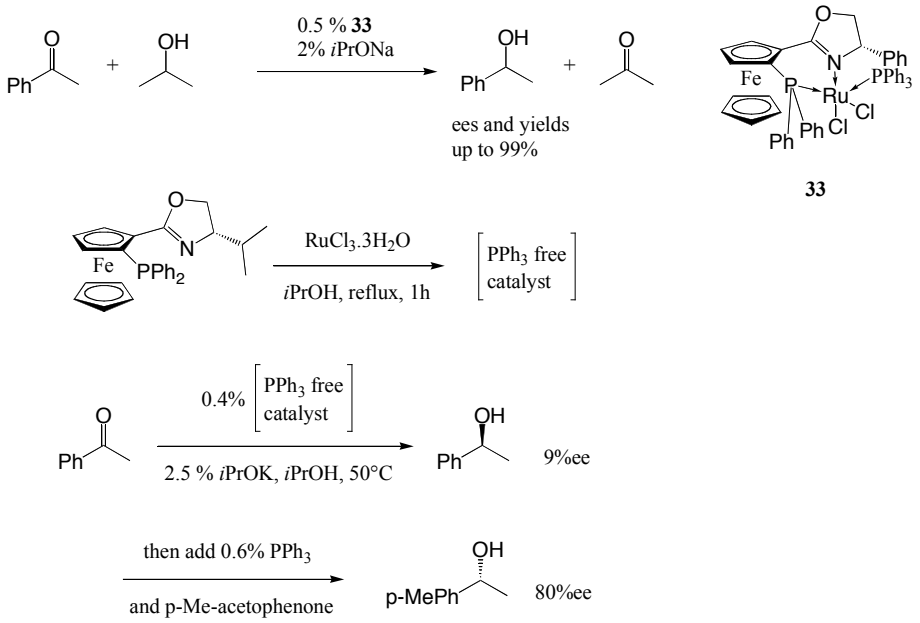

Scheme 32: Transfer hydrogenation with Ru complexes of phosphinoferrocenyloxazolines.

Chiral ferrocenylphosphine-Ru complexes, such as **33**, catalysed the oxidative kinetic resolution of racemic alcohols where acetone is working as an hydrogen acceptor.[66] With this system, impressive results were obtained. For example, the oxidative kinetic resolution of 1-indanol with 0.0025% of **33** furnished the enantioenriched 1-indanol (94% ee) with a TOF of 40,000 (h^{-1}) (**Scheme 33**).

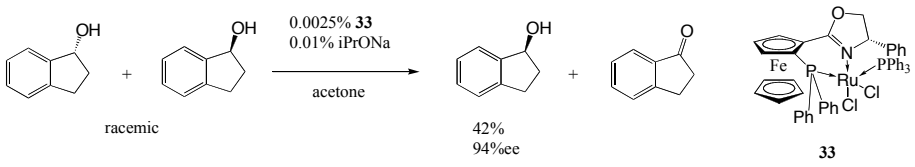

Scheme 33: Kinetic resolution of racemic 1-indanol.

Another interesting catalysed reaction using 1,2 disubstituted ferrocene ligands is the addition of alkyl[67] and aryl[68] zinc reagents to aldehydes with high enantioselectivities using *N*, *O* ligands (**Scheme 34**). The planar chirality in **34** and **35** influences not only the enantioselectivity but also the reactivity. For the aryl zinc addition, it was shown that a mixture of Et_2Zn and Ar_2Zn can be used to synthesise arylphenylmethanol in high enantioselectivities.[40] Heterogenisation of the catalyst **34** allowed catalyst recovery and recyclability with enantioselectivities between 97 and 95%.[69] Extension to other aryl sources, namely boronic esters, gave also high enantioselectivites and yields.[70]

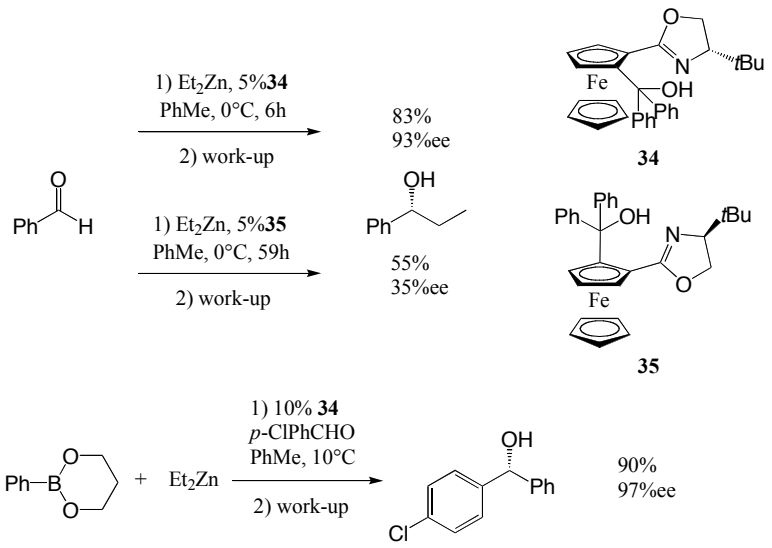

Scheme 34: Diethyl and diphenyl zinc addition to aldehydes.

2.2. Objective

The objective of this work consists in the development of catalysts that would allow a practical and efficient synthesis of secondary enantioenriched alcohols. This can be achieved either by addition of organometallic species to aldehydes or by reduction of prochiral ketones (**Scheme 35**).

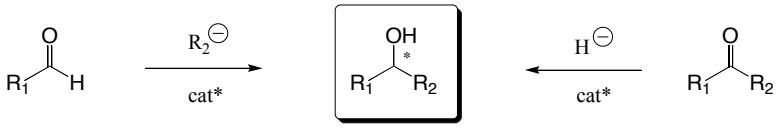

Scheme 35: Catalytic enantioselective access to secondary alcohols.

Based on the literature results exposed previously, a bifunctional catalyst was supposed to be the most appropriate to reach high selectivities, since it controls both the electrophile and the nucleophile. The search for high activities led us to synthesise precatalysts with a nitrogen and a heavier chalcogen coordinating atoms. Another additional feature of the catalyst to be developed is the presence of two elements of chirality. The study of the possible diastereoisomers would determine the "matched" pair giving the best selectivity and / or activity. Therefore the researches will be oriented towards the synthesis of precatalysts presenting the previously described characteristics and evaluated in catalytic reactions

2.3. Synthesis of new *N*, *S* based ligands and complexes

Our own researches in the field of catalysis with ferrocene based catalysts intended to take advantage of the cooperativity between two chirality elements. We were interested in the synthesis of ferrocene based ligand of *N*, *S* type incorporating a planar chirality (**Figure 9**). The sulfur coordinated to zinc can be in form of a thiolate (**36**) or a thioether (**37**). The initial aim was to study the influence of these parameters in catalytic asymmetric organozinc addition to aldehydes and hydrosilylation of prochiral ketones.

R = H, Et

36 **37**

Figure 9: General structure of the studied 1, 2 disubstituted ferrocenes.

2.3.1. Synthetic strategy

The synthetic strategy leading to optically active 1, 2 disubstituted ferrocenes, such as **36** and **37**, is based on the use of chiral oxazolines as *ortho*directing groups to undertake a diastereoselective deprotonation in the α position with a strong base. Richards[71], Sammakia[72] and Uemura[61] reported first the use of this *ortho*directing group independently in 1995 for the introduction of planar chirality on ferrocenyl oxazolines. This method was used to synthesise ligands for asymmetric catalysis, as *N*, *P* catalysts described previously.

The diastereoselectivity depends greatly on experimental conditions (solvent, base, additive). This reaction was subjected to further studies to understand the selectivity induction.[73] It was shown that (1) metallation of ferrocenyl oxazoline proceeds by coordination of lithium to nitrogen and (2) the transition state implies the rotamer **38**, where the alkyl group of the oxazoline is oriented towards the unsubstituted cyclopentadienyl, rather than the rotamer **39** (**Figure 10**). This conformation allows minimisation of steric

interactions between the alkyl lithium, the oxazoline alkyl group and ferrocene.[74] Therefore, diastereoselective *ortho*lithiation presents different selectivities, when the size of the base changes. The steric crowding of the used organolithiated bases can be increased by the binding of a chelating ligand such as TMEDA. For a given chiral ferrocenyl oxazoline, it is generally observed that an increase of the steric hindrance leads to a higher selectivity but with too important steric crowding, poor selectivities are then observed.[75]

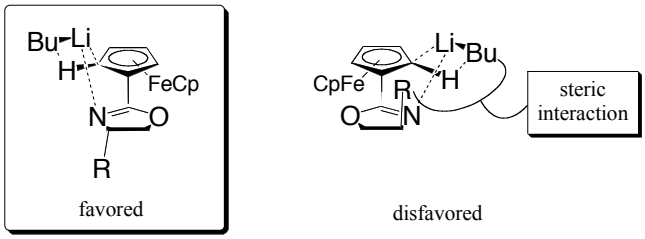

Figure 10: Explanation of the diastereoselective *ortho*lithiation.

The general strategy for the synthesis of our catalyst is based on the use of an *ortho*directing group to introduce planar chirality in ferrocene. Following a diastereoselective *ortho*lithiation of **40**, elemental sulfur was added to the ferrocenyl lithium **41**. The generated lithiothiolate **42** was then oxidised to its corresponding disulfide **43** or reacted with zinc chloride to form the corresponding zinc complexes **44**.

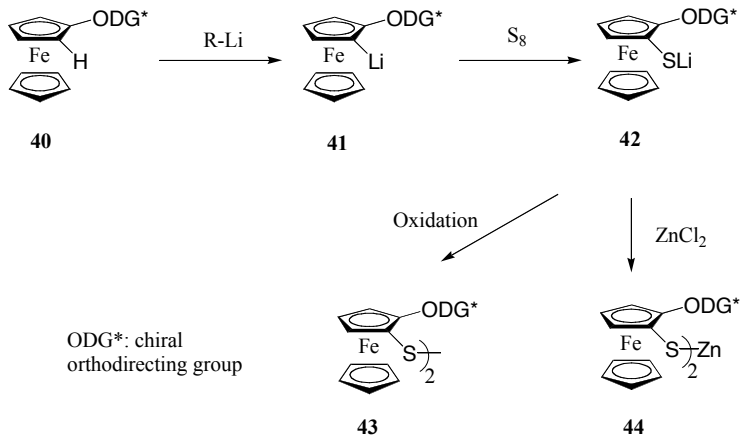

Scheme 36: General strategy leading to 1, 2-disubstituted ferrocenes **43** and **44**.

2.3.2. Synthesis of the ferrocene oxazolines 53 and 54

The synthesis of the ferrocene oxazoline **53** and **54** (**Scheme 41**) was undertaken from easily available ferrocene carboxylic acid **46**. The desired product can be synthesised in very good yields by oxidation of ferrocene carboxaldehyde **45** or by electrophilic trapping of ferrocenyl lithium with carbon dioxide to afford an amide, which was then cyclised.

Oxidation of the commercially available ferrocenyl carboxaldehyde **45** was achieved by reaction with a mixture of $KOH/AgNO_3$ at room temperature. After acidification, the acid **46** was obtained in 90% yield on a 80 mmol scale (Lit: 90%)[76,77] (**Scheme 37**).

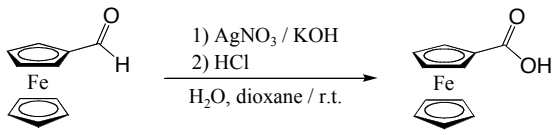

45 **46**

Scheme 37: Ferrocene carboxaldehyde **45** oxidation to the corresponding acid **46**.

An alternative was also studied for a direct access to ferrocene carboxylic acid from ferrocene **47**. Ferrocenyl lithium could be generated under the condition developed by Mueller-Westerhoff[78] and CO_2 was then bubbled into the solution. Once a yellow precipitate of FcCOOLi was formed, the mixture was allowed to reach room temperature and acidified (**Scheme 38**). The yield of ferrocene carboxylic acid **46** was quantitative but this procedure was found less convenient for scale-up to larger quantities of ferrocene.

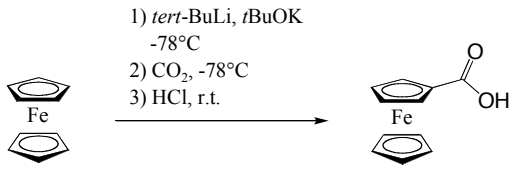

47 **46**

Scheme 38: Ferrocene carboxylic acid **46** synthesis from ferrocene **47**.

The amino alcohols required for the preparation of the oxazolines were commercially available such as (*S*)-(+)-valinol or synthesised by reduction of the corresponding acid with $NaBH_4/I_2$ as for the preparation (*S*)-(+)-*tert*-leucinol **49**[79] (**Scheme 39**).

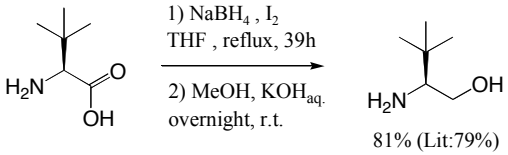

81% (Lit:79%)

49

Scheme 39: Reduction of the (*S*)-*tert*-leucine **49** with $NaBH_4$ / I_2.

We propose a mechanism involving first the reaction of iodine with sodium borohydride to form *in situ* BH_3. Its reaction with the amino acid leads to a cyclic borate **50**, which is hydrolysed with potassium hydroxide.

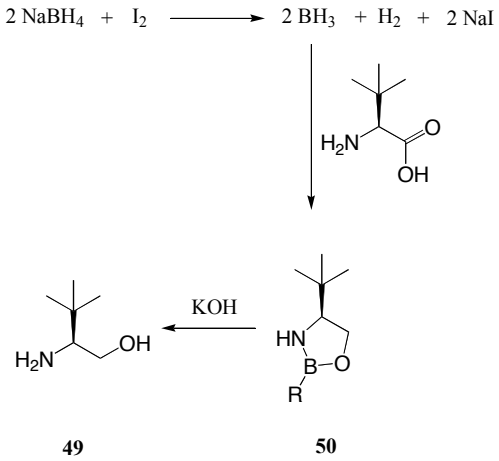

Scheme 40: Proposed mechanism for the reduction with $NaBH_4$ / I_2.

Amide formation was achieved first by activation of the acid **46** with oxalyl chloride. Removal of the solvent as well as the excess of oxalyl chloride was done by evaporation to dryness under reduced pressure. Dissolution of the acid chloride was followed by addition of the amino alcohol in presence of TEA and gave the corresponding amides in 96% yield for **51** and **52** (Lit: 84%).[71] Cyclisation occurred by reaction with TsCl, a catalytic amount of DMAP and a base yielding the ferrocene oxazoline **53** in 94% yield (Lit: 80%) and **54** in quantitative yield (Lit: 96%).[72]

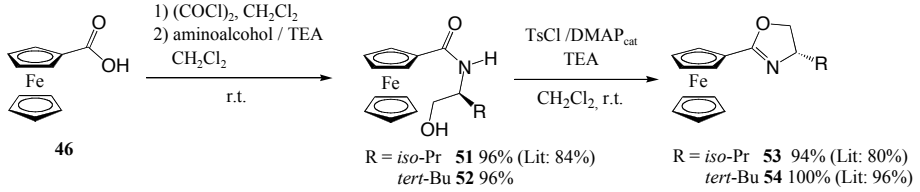

Scheme 41: Synthesis of ferrocene oxazolines **53** and **54** from ferrocene carboxylic acid **46**.

Disposing of an appreciable quantity of the ferrocenyloxazolines **53** and **54**, they were used for the synthesis of *N*, *S* bidentate ligands using a diastereoselective *ortho*lithiation in a key step to introduce the second coordinating heteroatom.

2.3.3. Synthesis of the disulfide 55

The major problem which is often encountered during the synthesis of thiols is the formation of the corresponding disulfide by air oxidation. However, this side reaction depends on the steric and electronic properties of the considered thiol. In case of a ferrocene, the corresponding thiols are extremely delicate to isolate. This problem is due to their high instability. As they are extremely sensitive to oxygen, the corresponding disulfides are usually formed during work-up. Thus we decided to synthesise their disulfides as a starting point for evaluation in catalysis.

The ferrocenyldisulfide **55** was synthesised by diastereoselective *ortho*lithiation of the ferrocenyl oxazoline **54** with *sec*-BuLi, addition of elemental sulfur followed by hydrolysis and air oxidation of the thiol (**Scheme 42**). Analysis of the crude product revealed the formation of many by-products. Their separation from the desired disulfide required two to three purifications by flash chromatography to get an acceptable degree of purity in ^{1}H NMR and the yield was very low.[76]

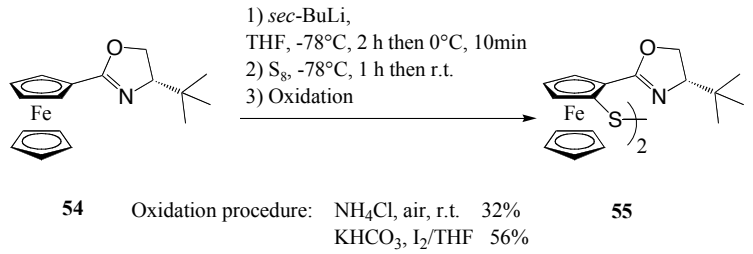

Scheme 42: Synthesis of a ferrocenyl disulfide **55**.

*Ortho*lithiation of the ferrocenyl oxazoline **54** is well documented and gives high yields and diastereoselectivities for various electrophiles. Concerning the formation of the thiolate, the reaction proceeds well as it will be shown later in section 3.2.5. Optimisation of the reaction was then oriented towards another oxidation procedure. Using a modified protocol, a solution of $KHCO_3$ and a solution of iodine in THF were subsequently added to the ferrocenic thiolate solution (**Scheme 42**).[80] A proposed mechanism is presented in **Scheme 43**. The thiolate anion reacts with the electrophilic iodine to generate a ferrocenyl sulfinyl iodine. This electrophile reacts then

with a second equivalent of thiolate anion to generate the disulfide with elimination of the iodide anion. Analysis of the crude product revealed the formation of the desired product and traces of ferrocenyloxazoline. During the purification by flash chromatography, some degradation of the product was observed as it eluted through silica gel. Nevertheless, the product was obtained in 56% yield on a 1 mmol scale. The reaction protocol was not further optimised but seems to constitute an effective way leading to the disulfide once optimal purification conditions could be found.

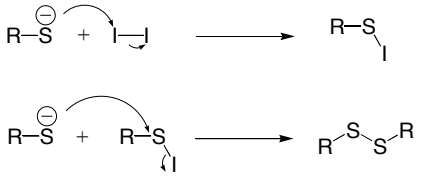

Scheme 43: Oxidation of thiolate to disulfide with iodine.

2.3.4. Synthesis of the thioether 56

The thioether **56** was synthesised by addition of Et_2Zn to disulfide **55** followed by hydrolysis of the reaction mixture (**Scheme 44**). After purification, the sole product that could be isolated was the thioether in 40% yield. It could be only characterised by ^1H NMR as it proved to be fairly instable and evaluated in a catalytic test reaction prior to its degradation. As explained later, the aim of this reaction was the isolation and identification

of the product generated by addition of Et_2Zn to disulfide. Thus no other methods were tried for the synthesis of this thioether **56**. Another reason to synthesise this product is that the thioether might catalyse alkylzinc addition to aldehydes (**Scheme 45**).

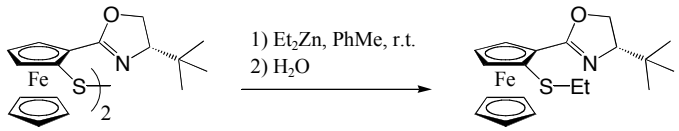

55 **56**

Scheme 44: Synthesis of ferrocenyl ethyl thioether **56**.

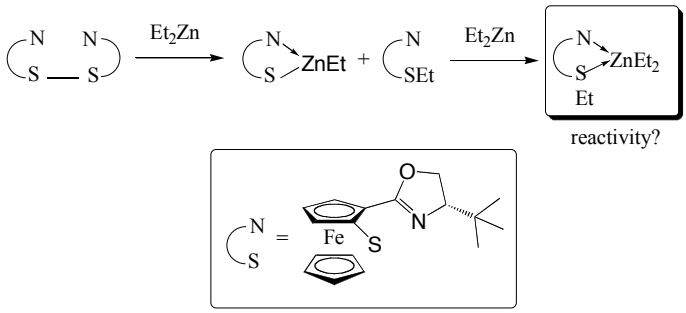

Scheme 45: Formation of thioether by reaction of diethylzinc with a disulfide.

2.3.5. Synthesis of the complex of Zn 58 with a *tert*-Bu on the oxazoline

Van Koten described the synthesis and characterisation of zinc complexes, which were bischelated with aromatic aminothiolate. Their stability depends on the nature of the *N*-alkyl groups (**Scheme 46**). Indeed, with the *N*, *N*-dimethyl aromatic thiol, the corresponding complex **57a** is formed in quantitative yield by reaction between silylated aminothiol and zinc chloride. However, the pyrrolidine **57b** and piperidinyl **57c** derivatives could not be isolated.

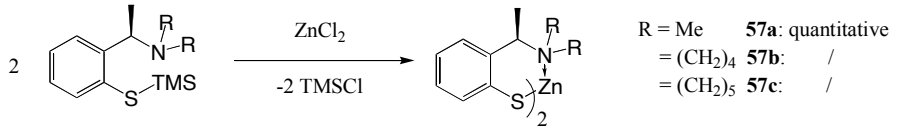

Scheme 46: Van Koten's approach to *N*, *S* zinc complex **57**.

This prompted us to synthesise the zinc complex **58**. For this purpose, the same procedure as described earlier was used to generate the lithium thiolate. To this intermediate a suspension of zinc chloride in THF was added allowing thus the formation of the desired product (**Scheme 47**). An interesting feature is its stability towards water. The highly lipophilic ligands protect the Zn-S bond against hydrolysis in a probably tetrahedral coordinated complex. Therefore, salt removal was simply done with an aqueous work-up. In addition to this, it proved to be stable during its

purification by flash chromatography over silica gel. Using this procedure, the complex **58** is obtained in 81% on a 1 mmol scale. Various attempts of crystallisation unfortunately afforded only chaffs.

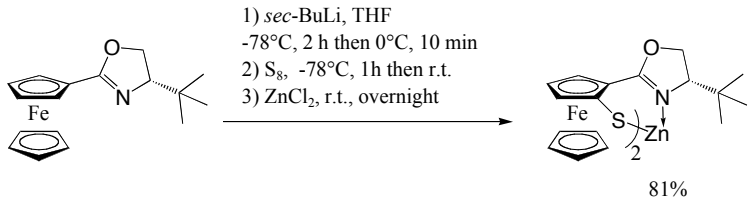

54 **58**

Scheme 47: Synthesis of a *N*, *S* zinc complex **58** with a *tert*-Bu group.

In the ^{1}H NMR spectrum of the ferrocenyl oxazoline with a *tert*-Bu **54**, the protons in α of the oxazoline ring are degenerated and their signals appear in form of two broad singulets at 4.72 and 4.79 ppm. Concerning the protons in β, a broad singulet is observed at 4.33 ppm.

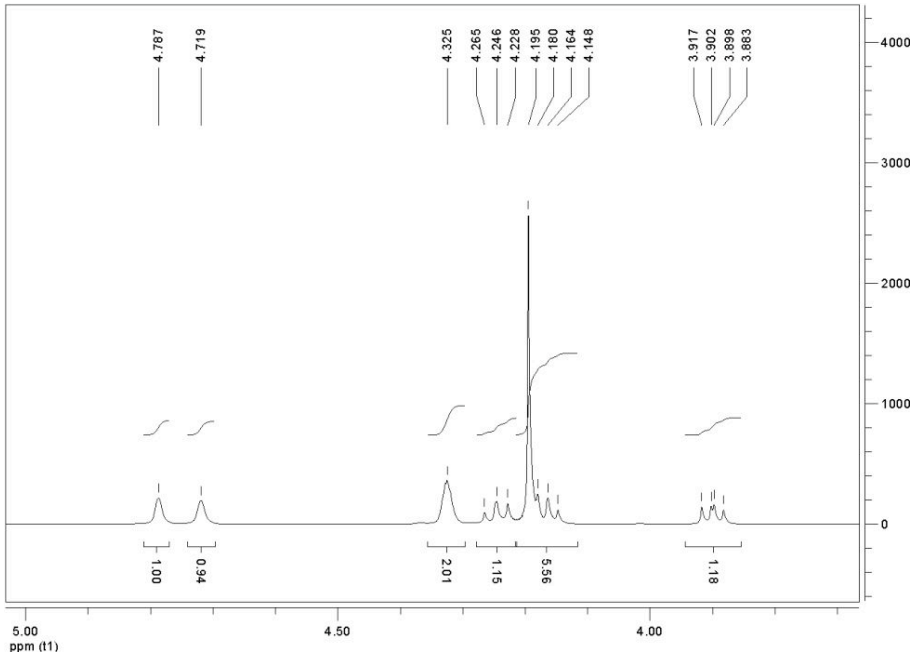

Spectrum 1: Ferrocenyl oxazoline with *tert*-Bu group **54**.

In the spectrum of the corresponding zinc ferrocenyl oxazoline thiolate **58**, the protons signal of the substituted cyclopentadienyl are clearly separated from each other in the ranges 4.27-4.28, 4.52-4.53 and 4.69-4.70 ppm.

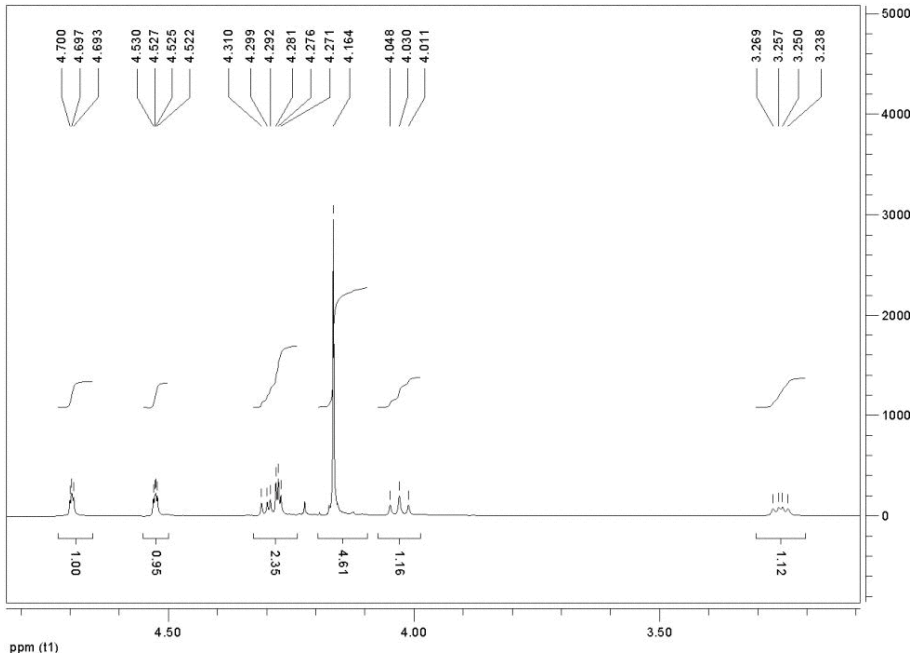

Spectrum 2: Zinc ferrocenyl oxazoline thiolate **58**.

Variation of the chalcogene was then undertaken using the same reaction scheme (**Scheme 48**). Both *N*, *Se* complex **59** and *N*, *Te* complex **60** syntheses gave lower yield than the *N*, *S* analogue probably because of the lower stability of the Se-Zn and Te-Zn bonds compared to a S-Zn one. The complexes could be characterised by mass spectrometry and ^{1}H NMR. In the analysed samples, traces of dichalcogenide could be observed. Recrystallisation to improve the purity led unfortunately to degradation.

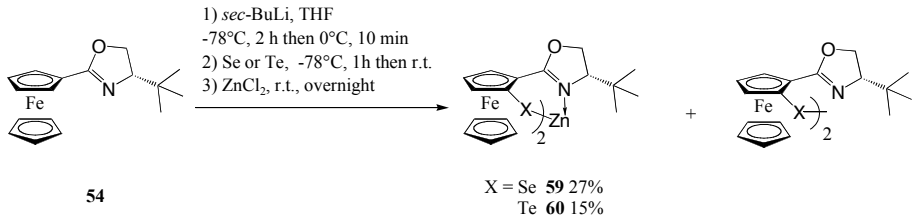

Scheme 48: Synthesis of *N*, *Se* and *N*, *Te* zinc complexes **59** and **60**.

2.3.6. Synthesis of the complex of Zn 61 with a *iso*-Pr on the oxazoline

Synthesis of the complex derived from (*S*)-(+)-valinol required the use of *n*-BuLi and TMEDA to afford high diastereoselective *ortho*lithiation (**Scheme 49**). Addition of elemental sulfur followed by zinc chloride furnished the desired product **61** in poor yield. This surprising result might be explained by the side reaction between sulfur and TMEDA.[81] In this secondary reaction, sulfur would be attacked by TMEDA.

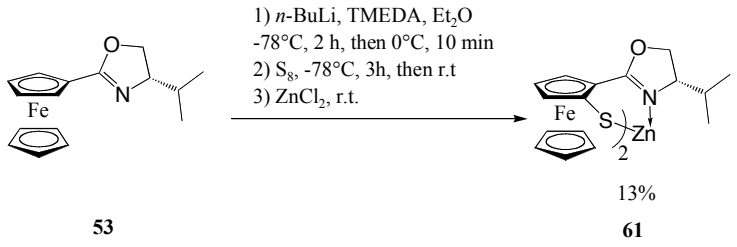

Scheme 49: Synthesis of the *N*, *S* zinc complex **61**.

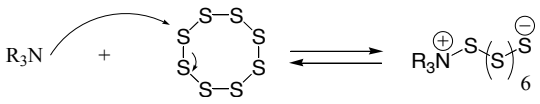

Scheme 50: Nucleophilic attack of sulfur by an amine.

Attempt to suppress this side reaction by reversal addition of zinc chloride (in excess) and elemental sulfur did not improve the results (**Scheme 51**). The aim of the last reaction was at first to trap the TMEDA with the excess of zinc chloride and secondly to form a zinc ate complex. No increase in the yield was observed.

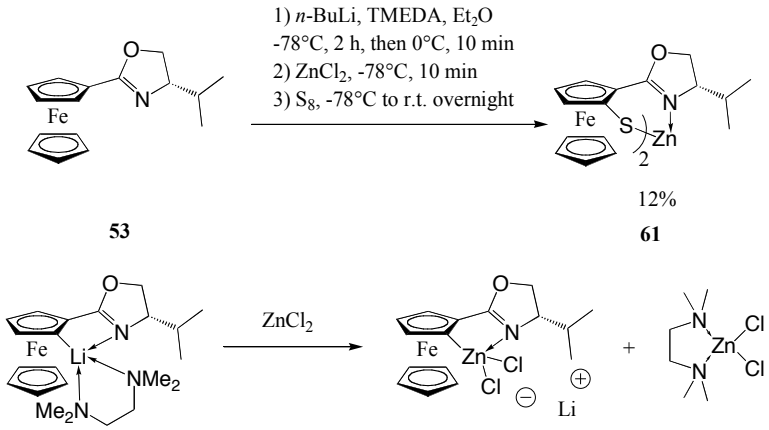

Scheme 51: Addition of zinc chloride in excess to form a zinc ate complex and to trap the TMEDA.

Following this drawback, tributyltin chloride was used as electrophile and furnished the stannylated ferrocene in 97% yield (**Scheme 52**). Attempt to generate the ferrocenyl lithium reagent by Sn / Li exchange followed by the usual addition of sulfur and zinc chloride furnished the crude product still containing the stannylated reagent. An attempt of purification by flash chromatography did not allow the separation of the product from the reactant. The stannylated ferrocene degradated when kept at room temperature.

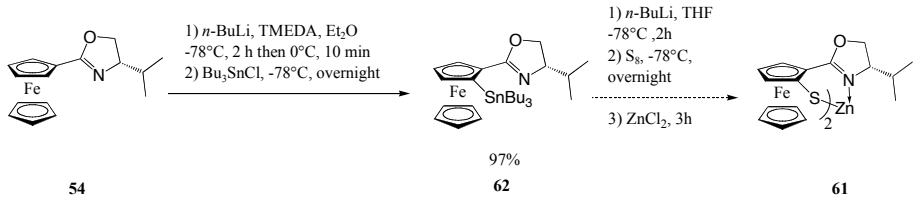

54 97% 62 61

Scheme 52: Attempt of synthesis of the *N*, *S* complex *via* a stannylated precursor **62**.

Halide introduction after *ortho*lithiation was not tried because the separation of the monohalogenated ferrocene from the reactant seems to be case dependant. For the iodinated ferrocenyl dioxane **63** developed by Riant, separation from the reactant was not possible. However, in the case of the Ugi's amine **64** bromination with $(BrCCl_2)_2$ separation proceeds well.[82] We therefore preferred to introduce an electrophilic protected thiol equivalent such as a thioacetate.

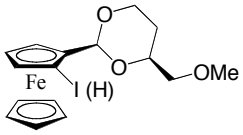

unseparable

63

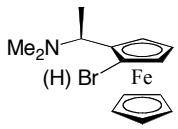

separable

64

Figure 11: Case dependent separation of monohalogenated disubstituted ferrocene from the corresponding unhalogenated starting material**.**

2.3.7. Attempt of synthesis of diacetyl-disulfane 65

An indirect introduction of electrophilic sulfur onto ferrocene was then considered with diacetyl-disulfane **65** (**Scheme 53**). To the best of our knowledge, this reagent was never used as electrophilic sulfur equivalent. Its synthesis implied oxidation of freshly distilled thiolacetic acid with iodine under basic conditions using the same modified protocol we used for the ferrocenic disulfide **55**.[80] Attempts of purification by distillation or flash chromatography were unfortunately unsuccessful.

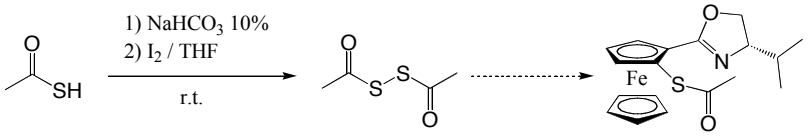

65

Scheme 53: Attempt of synthesis of diacetyl disulfane **65**.

Knochel recently described another approach for the introduction of another electrophilic sulfur equivalent by reaction of a Grignard reagent complexed with LiCl on tetramethylthiuram disulfide $(Me_2NCS_2)_2$ **66**. This electrophile led to the corresponding dithiocarbamate **67** in excellent yields (**Scheme 54**). It can be then converted into the corresponding thiol, thiolate or thioether in subsequent transformations.[83] Even if this approach seems very promising in our case, we preferred to turn our attention to another class of ligands as explained later.

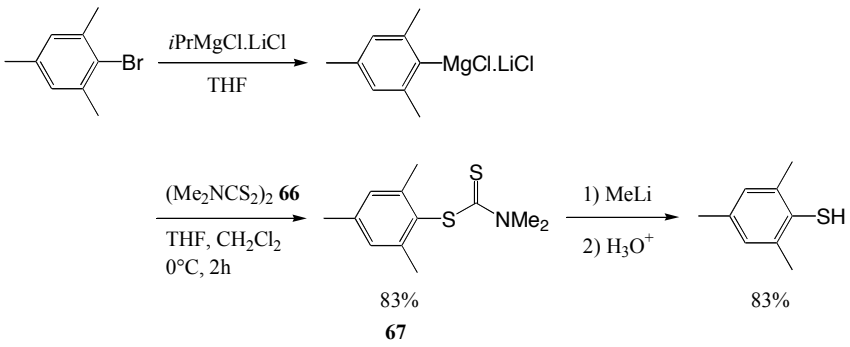

Scheme 54: Knochel's method for the synthesis of an aromatic thiol from the corresponding dithiocarbamate.

2.3.8. Synthesis of the diastereoisomeric zinc complex 69 with an *i*Pr group

Since TMEDA is problematic for the introduction of the sulfur on the ferrocene, the synthesis of the diastereoisomeric complex **69** with the opposite planar chirality was attempted. The ferrocene moiety and the *iso*-propyl group occupy quadrants that are next to each other in the diastereoisomer 1 (**Scheme 55**). But in diastereoisomer 2, the occupied quadrants are opposite each other. In this case, the structure of this ligand presents a pseudo C_2 symmetry.

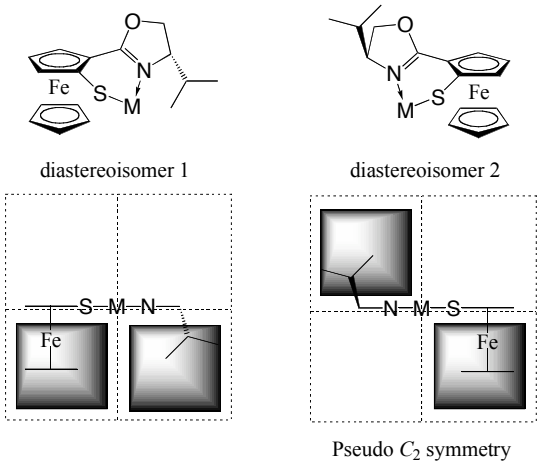

Scheme 55: Steric interactions of the ferrocenyl and oxazoline moieties in two diastereoisomeric ligands with respect to planar chirality.

The synthesis involved first a diastereoselective monolithiation with *n*-BuLi / TMEDA and electrophilic trapping with TMSCl (**Scheme 56**). The *ortho* substituted product **68** was isolated in 97% yield. A second lithiation, which required *n*-BuLi without TMEDA, was carried out and then sulfur and zinc chloride were successively added. Unfortunately, the crude product (identified by mass spectrometry) was obtained in low yield (23%, by ^{1}H NMR). This could be rationalised considering the product stability. Indeed, the TMS group might prevent the oxazoline moiety from being in the substituted cyclopentadienyl plane. Therefore, the zinc coordination by the nitrogen atom would be weakened, explaining thus the low yield. For this reason the synthesis of this precatalyst was put aside without performing any purification.

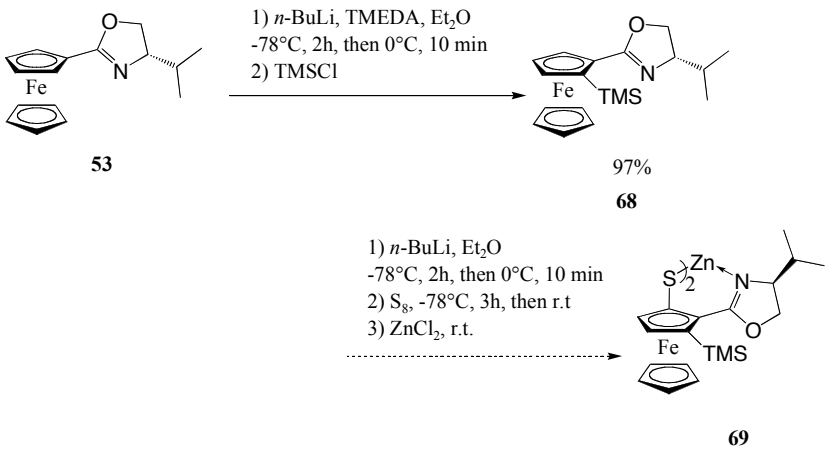

Scheme 56: Attempt of synthesis of the zinc complex **69**.

2.3.9. Synthesis of van Koten's aromatic aminothiol

The synthesis of the desired thiol **76** (**Scheme 60**) was already described by the groups of van Koten and Perrio[84]. However, the thiol proved to be fairly sensitive in our hand and was isolated in a poor yield. At first, dimethylation of (*R*)-α-phenylethylamine was carried out by an Eschweiler-Clarke methylation according to a described procedure (**Scheme 57**). A modest yield of 44% was obtained on a 83 mmol scale (Lit: 73%).[84]

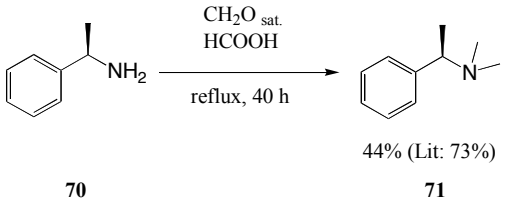

Scheme 57: Eschweiler-Clarke methylation.

Different attempts were then carried out for the formation of the thiol. Van Koten's methodology reposes on the formation of a silylated thiol which was isolated prior engaging it in the synthesis of the zinc complex (**Scheme 58**). This presents the advantage of avoiding thiol formation, and thus its air oxidation. The formed salts were removed by filtration under argon over celite, which was previously dried in the oven. The product could not be isolated in our hands due to its high moisture sensitivity.

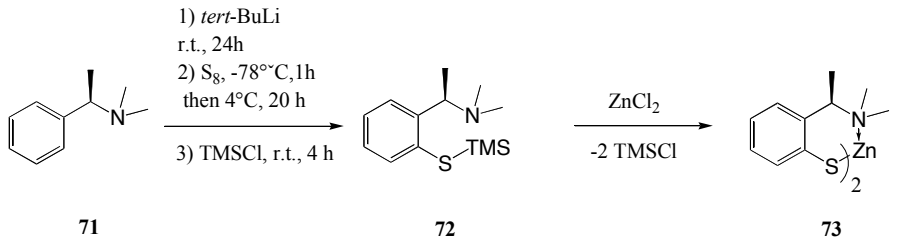

71 **72** **73**

Scheme 58: Attempt to van Koten's synthesis of *N*, *S* zinc complex **73**.

Another attempt consisted in applying the same approach as for our new zinc complex, i.e. by adding zinc chloride to the corresponding lithium thiolate (**Scheme 59**). Unfortunately, the desired complex was hydrolysed during the aqueous work-up, proving its sensitivity to moisture.

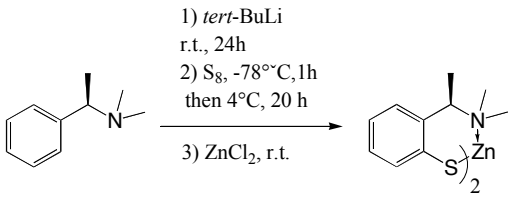

71 **73**

Scheme 59: Attempt of direct synthesis of van Koten's zinc complex **73**.

Following the silylated thiol **72** and zinc complex **73** synthesis attempts, we turned our attention towards the synthesis of the aromatic thiol. For this, the amine **71** was deprotonated in *ortho* position with *tert*-BuLi in hexane and elemental sulfur was then added to the solution of the lithiated

compound (**Scheme 60**). The lithiation procedure is described by van Koten[85] and Perrio[84] without being subject to discussion. Prior to the addition of elemental sulfur, van Koten isolated the *ortho*metallated species **74** in 76% yield. This is not necessary according to Perrio, who added directly elemental sulfur to this intermediate. Another divergent point is the hydrolysis procedure: van Koten performed it with the addition of 1 equivalent of aqueous HCl to the thiolate **75** yielding thus the aromatic thiol **76** in 65% yield whereas the yield was lower than 19% when it was reproduced by Perrio. However, when hydrolysis was done with 1 equivalent of CH_3COOH in THF, Perrio obtained the desired product in 65%. In collaboration with Stéphane Gerard, the product was obtained in 6% yield following Perrio's procedure. The latter procedure is quite reproducible for the synthesis of the thiol but extensive degradation was observed during the purification by bulb to bulb distillation. As there was enough ligand to evaluate it in asymmetric catalysis, no other attempt of optimisation was carried out.

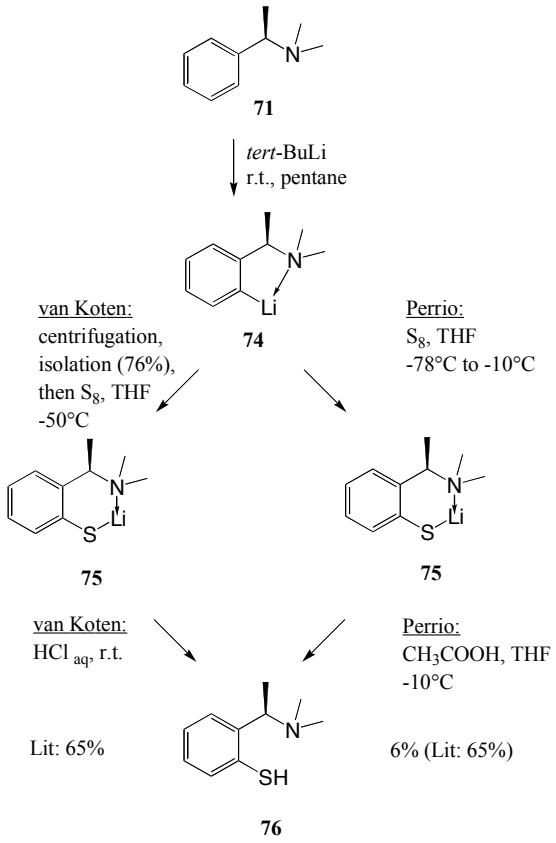

Scheme 60: Synthesis of the aromatic amino thiol according to Perrio.

2.3.10. Attempt of synthesis of the zinc complex 78 from the Ugi's amine

Similarly to the synthesis of **58**, the same reaction scheme was undertaken with the Ugi's amine **77** but without aqueous work-up to avoid

the hydrolysis of the zinc bisthiolate complex (**Scheme 61**).[86] For this purpose, the solvents were removed under reduced pressure on the vacuum line after reaction between the lithium thiolate and zinc chloride. Purification of the crude product was hampered by salt elimination problem. Many attempts of salt removal under inert atmosphere were carried out with a filtration cannula, using dichloromethane as solvent. Other filtrations over celite, silica gel or Millipore filter were in vain, as well. Due the relatively high price of the starting amine other methods for the synthesis of the complex **78** were not undertaken. In addition to this, it should be noted that the flexibility of the *ortho*directing group is higher compared to that of the oxazoline and may account for the complex lack of robustness.[87]

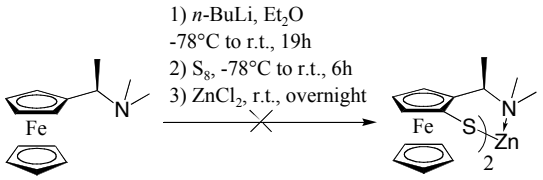

77 **78**

Scheme 61: Attempt of synthesis of a *N*, *S* zinc complex **78** derived from Ugi's amine **77**.

2.3.11. Attempt of synthesis of a ferrocenic *N*, *S* complex 82

In collaboration with David Leclercq, the synthesis of a new zinc complex was tried starting from the available ferrocenyl tertiary alcohol **79**. The introduction of a sulfur equivalent in form of a thioacetate was achieved by initial formation of a tertiary insoluble carbocation **80** with tetrafluoroboric acid (**Scheme 62**). This solid was washed with Et_2O, which was removed by filtration with a cannula under argon. Distilled thiolacetic acid was then added to a solution of the carbocation in dichloromethane followed by an excess of triethylamine. The corresponding thioacetate **81** was isolated in 56% yield after chromatographic purification.

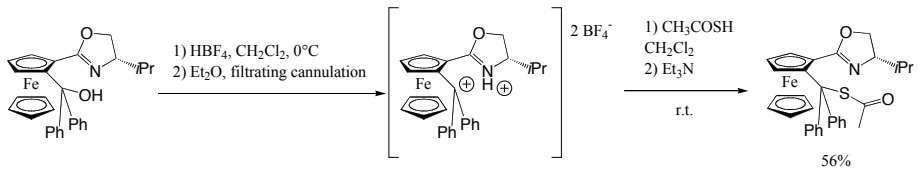

79 **80** **81**

Scheme 62: Synthesis of a ferrocenic thioacetate.

Attempt to synthesise a *N*, *S* zinc complex by addition of two equivalents of *n*-butyl lithium to release the lithium thiolate anion followed by addition of zinc chloride did not allow to isolate the desired product **82** (**Scheme 63**). This drawback might be due to the strong steric hindrance around the sulfur atom.

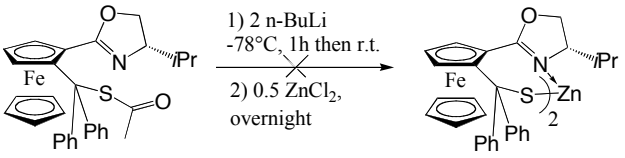

81 **82**

Scheme 63: Attempt of synthesis of the *N*, *S* zinc complex **82**.

2.4. Evaluation of the new ligands and complexes in catalytic tests

2.4.1. Organozinc addition to aldehyde

Diethylzinc addition to aldehydes is an intensive field of study. However, its application in synthesis is extremely limited compared to functionalised or unsatured organozinc reagents. Among this last class, vinylzinc reagents are interesting because of the possible functionalisation of the formed enantioenriched allylic alcohols. Two synthetic strategies have been elaborated: (1) internal or terminal hydrozirconation followed by Zr/Zn exchange to form the vinylzinc that will react with the aldehyde[88] and (2) hydroboration of terminal alkynes followed by B/Zn exchange leading to the reactive organozinc[89] (**Scheme 64**). Even if both approaches can be used with chiral *N*, *S* ligands, the Oppolzer methodology was considered more

interesting mainly for cost reasons. It is noteworthy that only the unsatured group is transferred and organometallic addition proceeds with stereochemistry retention at the double bond, as only *Z*-adducts are produced.

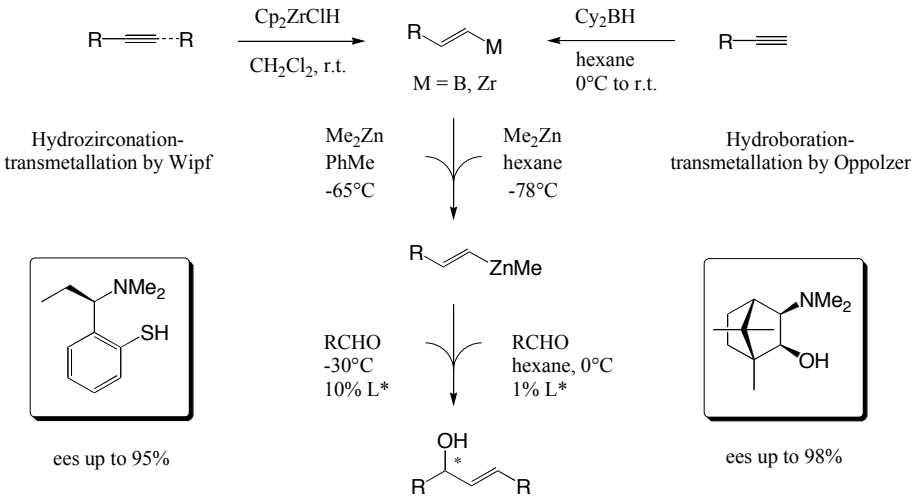

Scheme 64: Synthesis of enantioenriched secondary vinylic alcohols according to Oppolzer or Wipf.

2.4.2. Disulfide 55 evaluation in the addition of diethylzinc to benzaldehyde

To evaluate the efficiency of our new ligands and complexes, the benchwork test reaction of diethylzinc addition to benzaldehyde was initially carried out because it is more rapid and easy to perform compared to

vinylzinc addition. Beside this practical aspect, it additionally allows to compare the potential of our catalysts with those already reported in the literature. Ligands and complexes were engaged in the standard reaction on a 1 mmol scale of substrate in toluene at 0°C with 1.5 equivalent of diethylzinc (**Scheme 65**). With our disulfide **55** as catalyst, an ee of 71% and a conversion of 88% were obtained.

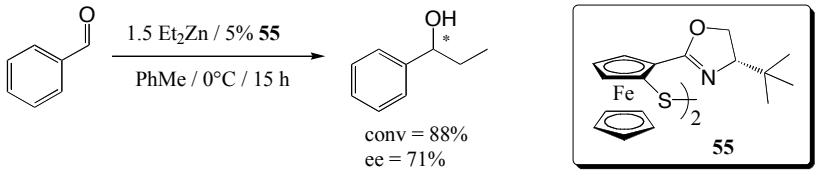

Scheme 65: Diethyl zinc addition to benzaldehyde catalysed by the disulfide **55**.

In order to understand the relatively weak chirality induction compared to other *N*, *S* catalysts, studies focussed on the role played by diethylzinc in the formation of the catalytically active species by reaction with disulfide **55**. According to Kellog,[90] diethylzinc can react with the disulfide partly as reducing agent leading to the formation of a zinc thiolate. Wirth[48] studied diselenides whose reaction with diethylzinc generates two catalytic species. The ethylselenoether formed presented a very low activity and modified thus only slightly the global enantioselectivity.

As quoted earlier, (**Scheme 44**) the reaction of diethylzinc on our disulfide **55** gives the ferrocenylthioether **56** which comes from the

alkylation of the disulfide along with some recovered disulfide after work up. Therefore, it is expected that the chiral information will be present as both a thioether **56** complexed to diethylzinc and a zinc thiolate (**Scheme 66**) (see 3.2.4). As both species can catalyse the condensation with different reactivities and/or enantioselectivities, we decided then to evaluate the thioether **56** in the standard experiment. This shows that this ligand, while retaining a good reactivity in the reaction time fixed for the experiment, gave a much lower asymmetric induction (24 % ee). This might account for the modest performances observed for the disulfide **55** although the relative reactivity of both catalytic species has not been precisely compared. However, those observation suggested that the formation of a single zinc thiolate catalyst might lead to improved enantioselectivities and we decided thus to investigate alternative methods for a better control of the catalyst formation.

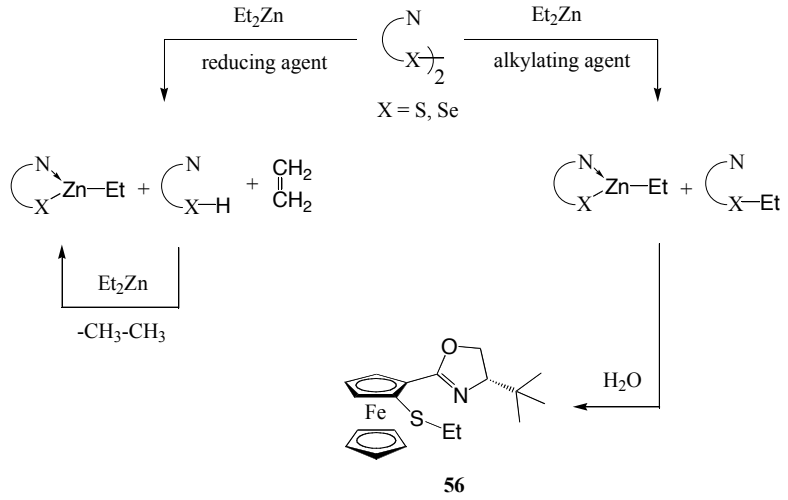

Scheme 66: Evidence of the alkylating role of diethylzinc towards disulfide **55**.

The evaluation of **56** showed that the reaction is catalysed with 24% ee and a conversion of 80% under the same reaction conditions (**Scheme 67**). This would explain why the disulfide **55** presented low enantioselectivity as half of the chiral information is in form of a thioether **56** and the remaining half would form the most enantioselective species.

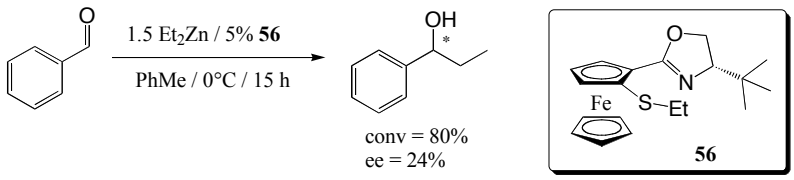

Scheme 67: Diethyl zinc addition to benzaldehyde catalysed by the thioether **56**.

To avoid the loss of the chiral thiolate ligand, a prereduction of the disulfide **55** was done *in situ* with DIBAH or Red-Al to generate the species **83** and **84** which could react with diethylzinc to form the mixed organozinc complex **85** (**Scheme 68**). However, with both reducing agents, a lower enantioselectivity was observed (**Table 1**).

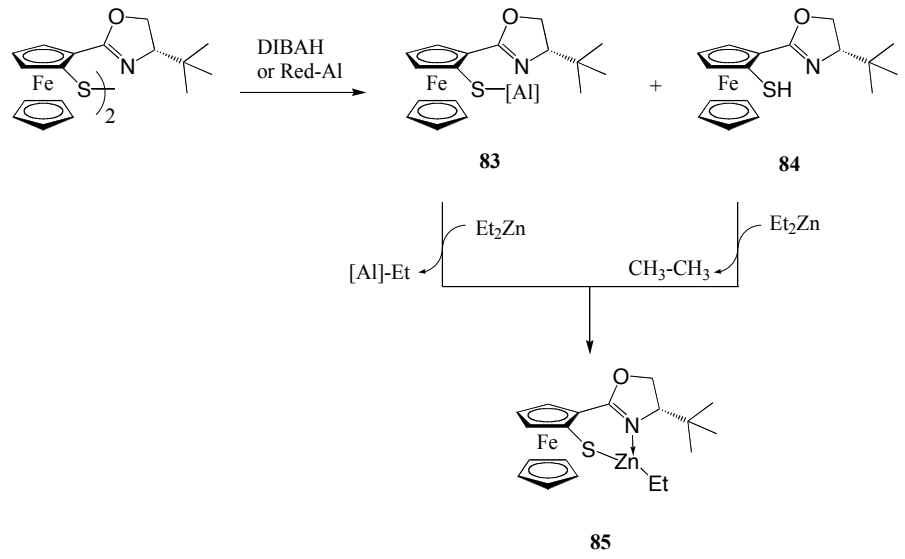

Scheme 68: Approach by prereduction of the disulfide 55 with aluminium hydride.

Table 1: Influence of the reducing agent with the disulfide **55** catalysed addition of diethylzinc to benzaldehyde.

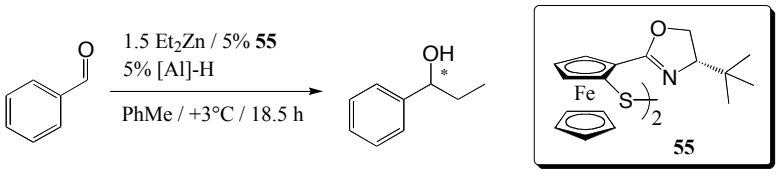

Reductant	Conversion (%)[a]	e. e. (%)[a]
DIBAH	79	69
Red-Al	91	62

a) Conversions and enantiomeric excesses were determined by chiral GC.

As the approach by disulfide prereduction led to a decrease in enantioselectivity, we chose to control the formation of the catalyst by using the bischelating zinc complex. By addition of diethylzinc to **58**, the catalytically active mixed organozinc complex **85** could be generated without loss of chiral information (**Scheme 69**). The equilibrium leading to the mixed complex was postulated on the basis of van Koten studies with the chiral complex **73**.

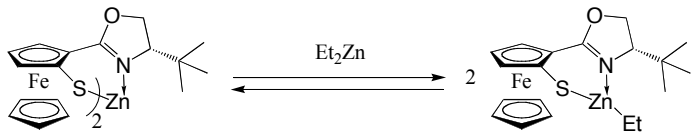

58 **85**

Scheme 69: Formation a mixed zinc complex starting from **58**.

Two tests run with a catalyst loading of 5 and 2.5% of **58** gave very similar results with 73 and 74% ee, respectively. Compared with the disulfide **55** the most significant change is the conversion, which drops to 48 and 40% for a catalytic charge of 5 and 2.5%, respectively.

Rationalisation of these results was attempted (**Figure 12**). Assuming that **85** is the catalytically active one is consistent with the fact that the disulfide **55** is more reactive than the thioether **56**. However, this hypothesis does not fit with the higher reactivity of the disulfide **55** compared to the zinc complex **58**. Another possibility, based on an activation

effect[91,92] due to the thioether **56**, would involve **86**, where the catalyst efficiency would be improved, corresponds to the observed increased conversion. However, the disulfide **55** and the complex **58** present the same enantioselectivity. It results that the coordination of the thioether **56** to the metallic center in the enantiodiscriminating step is rather unlikely. Therefore, the hypothesis of activation through the formation of intermediate 86 can be discarded.

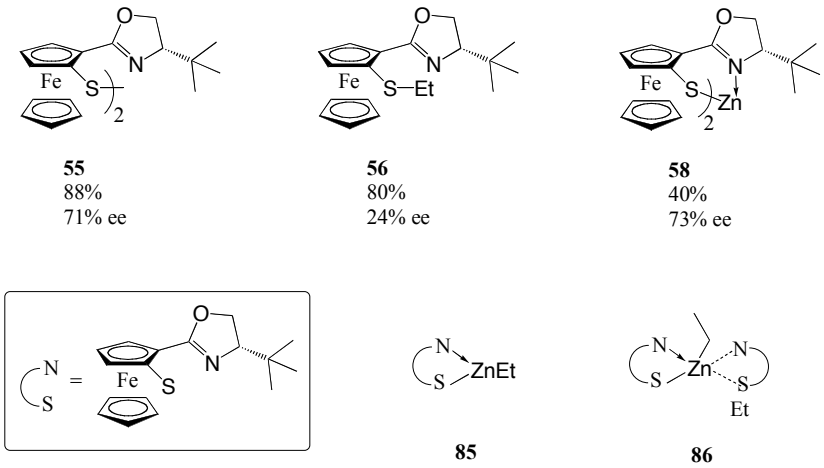

Figure 12: Precatalysts evaluated in the diethyl zinc addition to benzaldehyde and possible involved species.

With those informations at hand, we decided to check the vinylzinc transfer on aldehydes. This required at first the preparation of the racemate to determine the analytical conditions for the separation of the two allylic alcohol enantiomers. The method described by Oppolzer seemed the most

appropriate.[89] Furthermore, the use of a reaction based on the same principle but optimized by Dahmen and Bräse[93] rendered the procedure easier to perform. The studied alcohol chosen was 1-phenyl-hept-2-enol **90**. The dicyclohexylborane reagent was generated by reaction of freshly distilled cyclohexene and BH_3/Me_2S (**Scheme 70**). The vinylborane **88** is then prepared by addition of 1-hexyne **87** to the preformed borane solution. Transmetallation with 1.05 eq of diethylzinc generates the vinyl zinc reagent **89**, which is then reacted with benzaldehyde in the presence of a catalytic amount of 2-amino-2-methyl-1-propanol **90**. A TLC of the crude product revealed numerous products. After three purification attempts by flash chromatography, the desired product still contained by-products and the isolated yield was then 20%. The difficulty to reproduce this procedure from the literature was also noted by other students from the laboratory. We decided then not to focus on the optimisation of this reaction, but rather to check our complexes and ligands in different catalytic reactions.

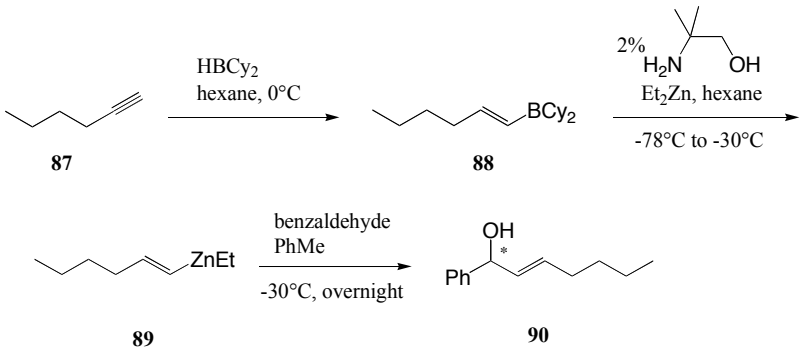

Scheme 70: Hexenylzinc addition to benzaldehyde.

2.4.3. Asymmetric reduction of prochiral ketones

2.4.3.1. The system of Mimoun

Hydrosilylation of prochiral ketones and more precisely the test reduction of acetophenone by the system of Mimoun was found very interesting to our project[94,95] (**Scheme 71**). The procedure involves the use of 2% of zinc complex and a stoechiometric quantity of PMHS to form the reduced silyl ether after 18 hours with enantiomeric excesses and conversions up to 88 and 99%, respectively. The reaction mixture requires a high substrate concentration (10M), which is necessary to obtain a good reactivity. Chiral amino alcohols, such as DAIB, were not effective as ligands. It is also possible to work with other metals such as cobalt or cadmium although the performances of the corresponding catalysts proved to be less efficient.

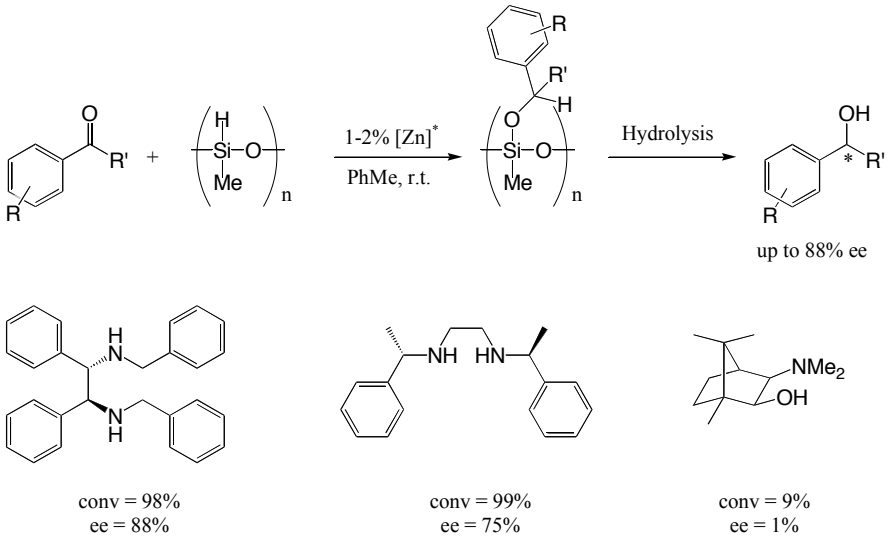

Scheme 71: Mimoun's asymmetric catalytic reduction of ketones using chiral zinc hydride catalysts and PMHS.

It was shown that an achiral zinc aminoalcoholate reacted with $(EtO)_3SiH$ via a rapid anionic exchange between silicium and zinc (**Scheme 72**).[95] It resulted that the chiral ligand was no more associated to zinc but to silicium, leading to a loss of chiral induction.

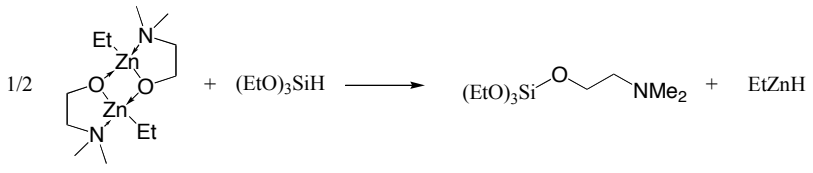

Scheme 72: Transfer of zinc amino alcoholate to triethoxysilane.

Mortreux[96] and Walsh[97] undertook further studies on this system but structural variations of the diamine/diimine core allowed rarely to reach higher selectivities than the initial system. It is noteworthy that methanol addition on the one hand accelerates the reaction but on the other hand leads to dehydrogenation of PMHS by the alcohol, requiring thus higher amounts of the silylating agent.

The system described by Mimoun is supposed to involve a hydride as a catalytic active species (**Scheme 73**). The zinc hydride reacts with PMHS to form a pentavalent dihydrosilicate in which the Si-H bond of the silane is activated. Following coordination of a carbonyl compound to the zinc atom, which acts as a Lewis acid, a six-membered ring transition state would allow the hydride transfer. This leads to an alkoxide included in a cyclic intermediate in which the silicium atom is pentavalent allowing the transfer of the alkoxide from zinc to silicium and generating thus the polysiloxane and the initial zinc hydride.

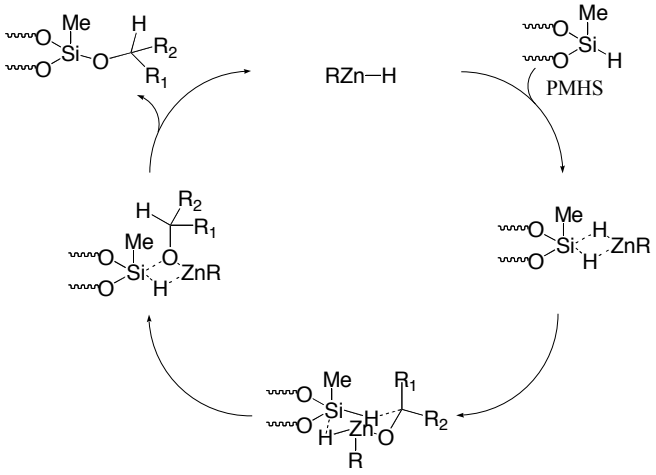

Scheme 73: Proposed mechanism for the zinc hydride catalysed hydrosilylation of prochiral ketone according to Mimoun.

2.4.3.2. Work hypothesis

Our zinc complex seemed appropriate in this system for two reasons. The first one in favor of *N*, *S* ligands, compared to amino alcohols or diamine, is the expected inertness of zinc aminothiolate towards the silylating agent. For diamines, this process is slower than for amino alcohols and for aminothiolate it should not occur.

The second reason was the possible formation of a zinc hydride from the zinc complex **58** by addition of one equivalent of benzaldehyde to form the mixed species **85**. Then, a thermal β-elimination would allow the formation of a chiral zinc hydride **85'** which would act as a catalyst for the

asymmetric hydrosilylation of prochiral ketones. This work hypothesis is also supported by the fact that a similar mechanism to the one proposed by Mimoun could be expected (**Scheme 74**).

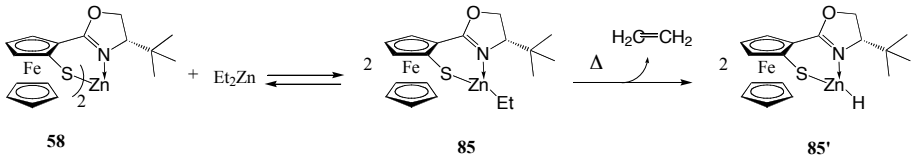

58 **85** **85'**

Scheme 74: Formation of a zinc hydride starting from **58**.

2.4.3.3. Influence of the solvents

Our studies of this system started with influence of the solvent by performing the tests with a concentration in substrate of 0.25 M and a catalytic loading of 5% in **58** (**Table 2**). THF seemed the most appropriate for our catalyst as a total conversion and an enantiomeric excess of 51% were obtained in two hours. The results for ether and dichloromethane could be explained by partial solubility of the complex with those solvents even after addition of one equivalent of diethylzinc. Generally, diethylzinc addition improves complex solubility. In toluene, a temperature of 80°C allowed complete solubility, probably through the equilibrium yielding the mixed zinc complex. However, the reaction temperature might be detrimental for the enantioselectivity. The use of 5% of complex **58** and 5%

of diethylzinc should allow the formation of a maximum of 10% of catalytic active species, which is quite important.

Table 2: Influence of the solvents under standard conditions.

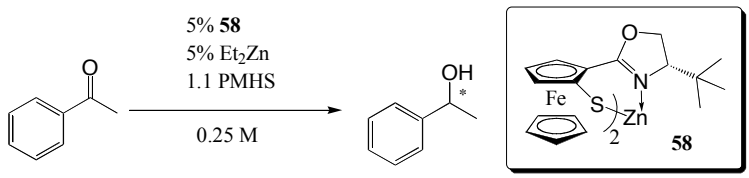

Solvent	Temperature (°C)	Time (h)	Conversion (%)[a]	ee (%)[a]
CH_2Cl_2	35	18	46	18
PhMe	80	1.5	100	42
Et_2O	35	18	57	43
THF	60	2	100	51

a) Conversions and enantiomeric excesses were determined by chiral GC.

A blank test with THF as solvent was performed (**Scheme 75**). No reaction between PMHS and acetophenone could be detected showing that there is no uncatalysed reaction.

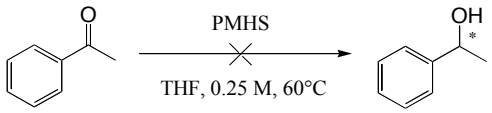

Scheme 75: Blank test showing PMHS inertness towards acetophenone.

2.4.3.4. Influence of the concentration and catalyst loading

Following these encouraging results, the effects of the substrate concentration as well as the catalyst loading were studied in view of improving the system efficiency (**Table 3**). This revealed that our initial conditions were unfortunately already optimal. As enantioselectivity could be influenced by the concentration, a catalysed reaction through an achiral pathway might not be precluded.

For the test at 6.25 M the complex was not completely soluble under these concentrated conditions. It could then be possible to obtain a similar result by decreasing the catalytic loading. Increasing the substrate concentration from 0.25 M to 6.25 M affected the enantioselectivity, which dropped from 51 to 40%.

Table 3: Concentration and catalytic loading studies in THF.

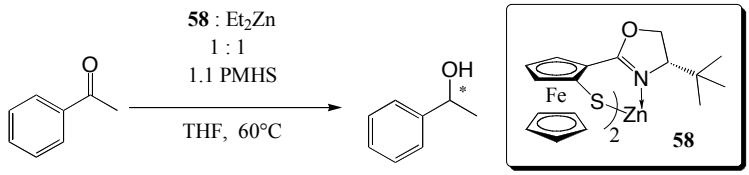

Cat. load (mol %)	Concentration (M)	Time (h)	Conversion (%)[a]	ee (%)[a]
5	0.25	2	100	51
2.5	0.25	2	100	43
2.5	0.125	5	85	43
2	6.25	3	100	40
1	0.05	5	46	42

a) Conversions and enantiomeric excesses were determined by chiral GC.

2.4.3.5. Temperature effect

The last parameter that could be varied was the temperature at which hydrosilylation took place. In a test experiment, the β-elimination was at first carried out by heating the catalyst solution and PMHS at 60°C for 30 minutes. The solution containing the zinc hydride catalyst was then cooled at 25°C and acetophenone was added. In this case, an increase in ee up to 61%

was observed at the detrimental of the conversion, which reacted with 85% after 17 h.

In another experiment, 84% conversion and an enantiomeric excess of 57% were observed after 24 h of reaction at room temperature. Further heating of the reaction mixture at 60°C for 3 h did not bring significant changes (86%, 57% ee). This showed that catalyst deactivation occurred with prolonged reaction time.

2.4.3.6. Evaluation of other catalysts

Variation of the chalcogene to selenium and tellurium decreased both conversion and enantioselectivity (**Scheme 76**) and indicated that sulfur was the optimal coordinating chalcogene.

Change of the *tert*-butyl for an *iso*-propyl in the oxazoline moiety led under the standard reaction conditions to 98% conversion albeit without enantioselectivity. This suggests that the steric hindrance generated by the group on the asymmetric carbon is important for the selectivity. Confirmation of this hypothesis could be validated using a valinol derivative with two phenyl rings next to the chiral center.[98]

The aromatic aminothiol developed by van Koten was engaged in the best reaction conditions. With a catalyst loading of 5%, acetophenone was reduced without any enantioselectivity.

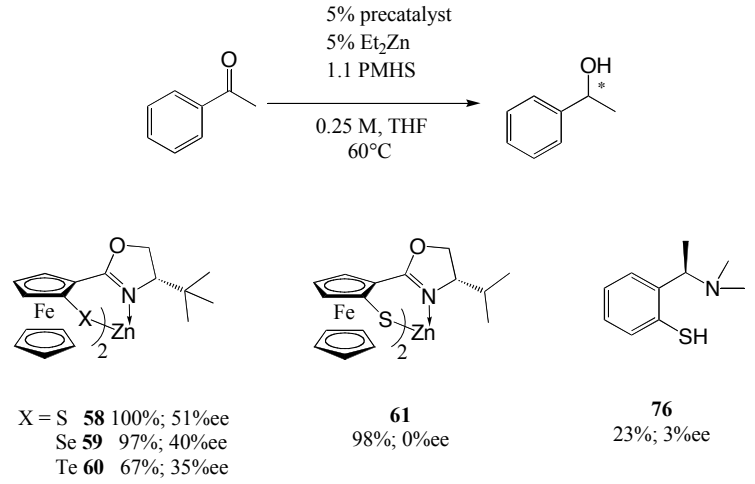

Scheme 76: Evaluation of new and described precatalysts.

2.4.3.7. Influence of the ratio **58** *: Et_2Zn*

As ZnH_2 can be formed from the mixed zinc complex, the catalytic activity of 5% diethylzinc after heating at 60°C was tested and showed that reduction was observed with 82% conversion (**Table 4**). Therefore, variations in the ratio **58** : Et_2Zn were studied. Performing the catalytic test with 5% of diethylzinc without the chiral catalyst lead to 82% of conversion. Surprisingly, a threefold excess of diethylzinc did not affect the enantioselectivity. Those results cannot allow us to conclude on the effect of the acceleration of the ligand on the catalytic reaction. Problems might as well be encountered for the reproducibility, as the solution of diethylzinc has

to be freshly prepared from neat diethylzinc for the preparation of the catalytic solution.

Table 4: Influence of the ratio **58** : Et_2Zn under standard conditions in THF

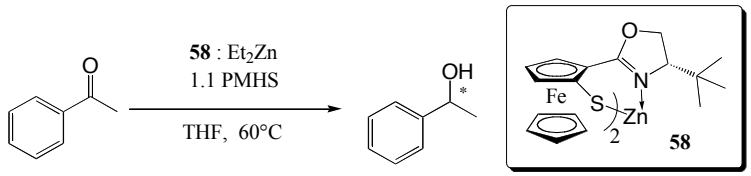

Cat. load (mol %)	Ratio 58 : Et_2Zn	Time (h)	Conversion (%)[a]	ee (%)[a]
5	0 : 1	2	82	/
5	1 : 1	2	100	51
5	1 : 2	2	88	39
5	1 : 3	2	91	52

a) Conversions and enantiomeric excesses were determined by chiral GC.

*2.4.3.8. Evaluation of the ferrocenyl thioacetate **81***

Even if the desired complex **82** could not be isolated, the thioacetate **81** is a direct precursor of a metallic thiolate. Therefore it could be generated

in situ by addition of a nucleophilic organometallic. By addition of diethylzinc the desired zinc thiolate might be formed. Performing the catalytic test of acetophenone reduction (**Table 5**), only a low activity and enantioselectivity were obtained. This might be explained by reaction of diethylzinc as base with the thioether rather than as nucleophile.

Table 5: Evaluation of the ferrocenic thioacetate under standard conditions.

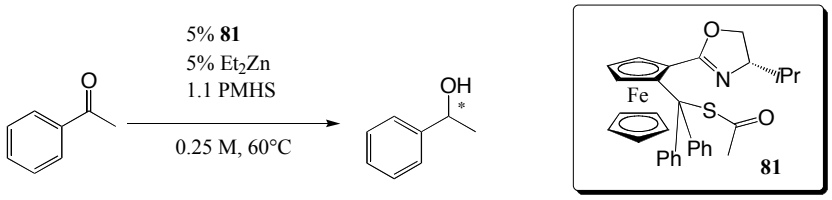

Solvent	Conv (%)[a]	ee (%)[a]
THF	/	/
PhMe	62	21

a) Conversions and enantiomeric excesses were determined by chiral GC.

2.4.3.9. Study of different prochiral ketone substrates

As presented in **Table 6** complete reduction of aromatic ketones was achieved within a few hours (2-5 h) with enantioselectivities reaching up to 55%.

Although the enantioselectivity for cyclohexylmethylketone remained modest (42%), it is quite close to acetophenone and the reactivity was very satisfactory. This modest result is however quite important as asymmetric reduction of dialkylketones occurs most often with both low conversions and enantioselectivities. Therefore, this result suggests that optimisation of the structure of the *N*, *S* ligand might lead to an efficient system for the asymmetric reduction of dialkylketones, a most challenging task in asymmetric catalysis.

Change in the α position with different groups (*n*-propyl, cyclohexyl, trifluoromethyl, cyclic chain) was considered. A decrease in enantioselectivity could be noticed except for the bulkier α-tetralone. Introduction of electron–withdrawing group at the *para*-position sensibly modified the reaction rate and slightly reduced the enantioselectivity, while donor groups in the same position did not affect the reactivity but decreased the enantioselectivities. α-Ketoester was cleanly reduced, albeit with a very low enantioselectivity.

Table 6: Substrate study.

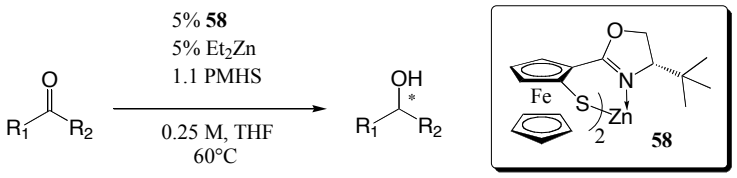

R_1	R_2	Time (h)	Conv. (%)[a]	ee (%)[a]
Ph	Me	2	100	51
Cy	Me	5	100	42
Ph	*n*-Pr	5	100	13
Ph	Cy	2	100	24
Ph	CF_3	2	100	14
α-Indanone		2	100	9
α-Tetralone		2	100	55
p-ClPh	Me	5	100	45
p-MeOPh	Me	2	100	41
Me	CH_2COOEt	2	100	15
Fc	Me	3	89	44

a) Conversions and enantiomeric excesses were determined by chiral GC.

2.5. Conclusions

The synthesis of new *N*, *S* ligands and *N*, chalcogenide zinc complexes was performed. Best results were obtained with complex **55** in the enantioselective addition to benzaldehyde with 71% enantiomeric excess but compared to the described *N*, *S* ligands our results are rather modest. Switch to the more interesting vinylzinc addition was hampered by product purification problems using Oppolzer's methodology modified by Bräse. Synthesis of secondary chiral alcohols was then considered by reduction of prochiral ketones.

The same complex **58** catalysed the hydrosilylation of acetophenone with up to 61% enantiomeric excess. This type of complex can be optimised by changes in the chiral *ortho*directing group as well as in the planar chirality. However, from a global point of view, there is a lack of flexibility since it is necessary to isolate the precatalyst in form of a zinc thiolate and its stability towards water was structure dependant. In addition to this, the other diastereoisomer, with opposite planar chirality, may be the most active and enantioselective one because it presents a kind of C_2-symmetry (**Scheme 55**). Its access would lengthen the synthesis with additional silylation, zinc thiolate formation and desilylation reactions. For these reasons, we preferred to change from *N*, *S* ligands to more modular and easily accessible precatalysts.

Chapter 3

Synthesis and application of cobalt complexes

Prior to the presentation of our results in the field of cobalt-catalysed hydrosilylation, a brief overview of metal salen complexes syntheses as well as their applications will be briefly presented.

3.1. Synthesis of salen-based ligands and their derivatives: general considerations[99]

Preparation of chiral Schiff base metal complexes involves first synthesis of the diimine ligand and then complexation of a transition metal by reaction with the appropriate metal precursor. The so formed complexes can be then employed directly in catalytic reactions or isolated prior to their use.

Salen ligands **93** are usually prepared by double condensation of a diamine **91**, which is generally chiral, with salicylaldehydes or their derivatives **92** (**Scheme 77**). Solvents for this reaction are for example dichloromethane with $MgSO_4$ to trap the generated water, refluxing methanol or ethanol in presence of a catalytic amount of acetic acid, or toluene with a Dean-Stark apparatus. The salen ligands are generally formed in quantitative yield avoiding their purification by recrystallisation.

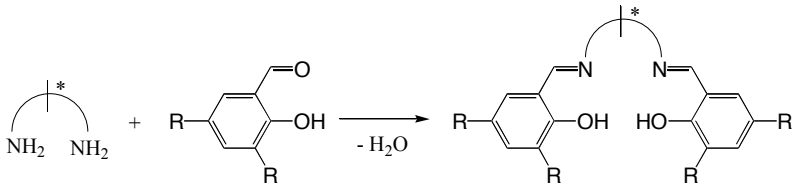

Scheme 77: Salen synthesis from diamines and salicylaldehydes derivatives

Salen complexes **94** can be prepared by different ways (**Scheme 78**). The choice of the employed metallic precursor is generally dictated by its stability and the ease with which complexes are isolated or, when used *in situ*, the side-products tolerance towards the studied catalytic system.

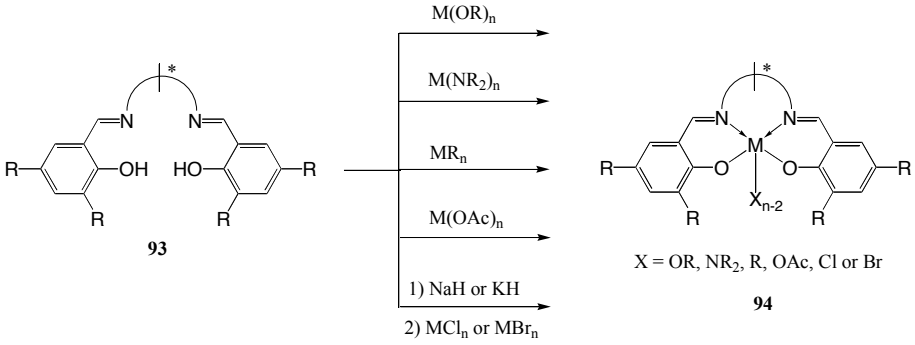

Scheme 78: Metal salen complexes synthesis from salen ligand and various metal precursor.

Metal alkoxides of titanium and zirconium are easy to handle but for other transition metals their moisture sensitivity can be problematic. It should be noticed that this reaction is an equilibrium, which can however be shifted towards the formation of the product, when bulky substituents are incorporated on the salen.[99]

Metal amides $M(NMe_2)_4$ (Ti, Zr) are effective for early transition metals since the generated $NHMe_2$ is volatile. Reaction of TMSCl with the bis-amido complex affords the corresponding dichloro complex.

For main group metals, as aluminum and indium, alkyl metals are suitable precursors. Concerning transition metals such as iron, manganese or copper, the corresponding mesityl reagents are used. They are formed by reaction between metal halide and mesityl Grignard compound. This approach presents the disadvantage that the employed reagents are moisture sensitive.

Metal acetates (Co, Ni, Cu) are effective precursors and their corresponding complexes are generally formed under reflux conditions.

Reaction with metal halide implies first deprotonation with sodium or potassium hydride leading to the phenolate intermediates, which are then allowed to react with the metal precursor. Removal of sodium or potassium salt can sometimes be problematic in the purification.

3.2. Metal salen complex conformations and their applications[100]

By reaction between the salen ligand and the metal precursor, the formed complex can be generated in three different configurations: *trans* in

which two ancillary ligands X and Y occupy the apical positions, *cis*-α and *cis*-β where these ligands are coordinated in one equatorial as well as one apical position and in two equatorial positions, respectively (**Scheme 79**).

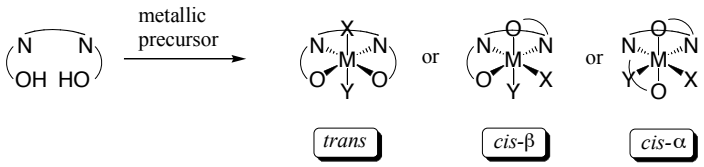

Scheme 79: Configuration forms of metal salen complexes.

Complexes with the *trans* configuration have mainly been studied in asymmetric catalysis. Those with *cis*-β configuration show also interesting results in catalysis. Lastly, complexes with *cis*-α have only been reported in the field of asymmetric synthesis with salen ligands.

3.2.1. Salen complexes with *trans* configuration

Applications of salen complexes with *trans* configuration may be best illustrated with the manganese salen **95** catalysed asymmetric epoxidation of *cis* unfunctionalised alkenes, even if the mechanism remains a field of research[101] (**Scheme 80**). Catalyst design requires knowledge of the catalytically active species as well as the substrate trajectory to the reactive center. It was generally assumed that salen O=Mn (V) **96** was the active complex responsible for epoxidation and researches focused on the design of salen ligand coordinating a manganese oxide center. It should be noticed that

some axial ligands enhanced the reactivity and enantioselectivity. Influences exerted by the salen ligand and additives will be presented. Studies of oxidants, substrate types and formed catalytic species are out of scope.

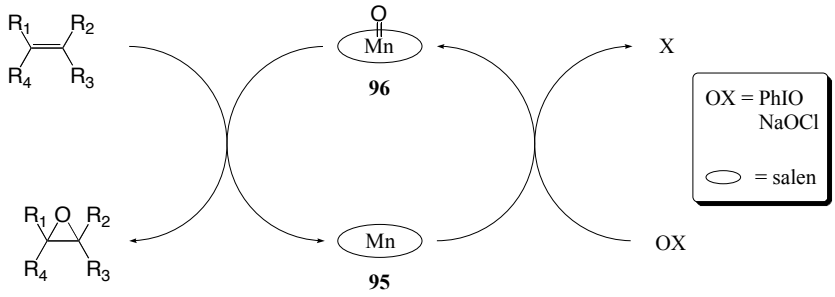

Scheme 80: Asymmetric epoxidation of alkene catalysed by manganese salen **95**.

The design of salen ligands to reach high selectivities intended to influence the orientation of the incoming *cis* olefin to the manganese oxide **96**. This goal was mainly achieved by introduction of substituents with different steric and electronic properties on the aromatic or the diimine bridge (**Scheme 81**). The influence of each part of the ligand will be presented. It is well accepted that for the *cis* olefin, the approach to the M=O bond arises in a side-on way, in which the substrate approaches the metallic center parallel to the plane of the salen complex (**Scheme 81**).

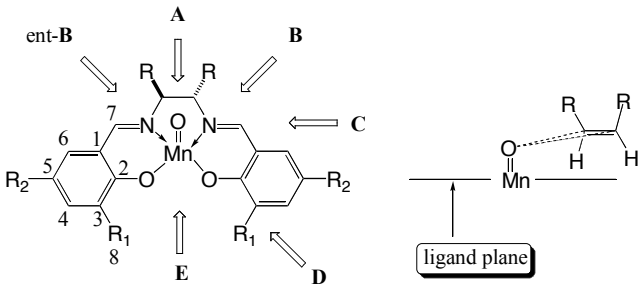

Scheme 81: Possible approaches of an olefinic substrate to the metallic center (left) and side-on approach (right).

It was shown that the structure of the *N*, *N* bridge is responsible for the enantioinduction, when it is the unique source of chirality in the salen, as in the Jacobsen type ligands **97**. With inverted stereochemistry at the diimine, products of opposite configuration are obtained. Independently of its substituents R (R≠H), the approaches A and ent-B are disfavored. However, it presents not only an impact on the selectivity but also on the catalyst activity. For example, changing from *trans*-1,2-diphenylethylendiimine to *trans*-1,2-dimesitylethylendiimine decreased both the reactivity and enantioselectivity.[102] It results that substituents size should be neither too small nor too large. With salen bearing additional axial chirality at the C3 and C3' position (Katsuki type **98**), it was observed that these catalysts were also effective.[103,104] Interestingly, Jacobsen (**97**) and Katsuki (**98**) type catalysts with the same configuration at the diimine backbone present the same sense of asymmetric induction for the epoxidation of chromene.[105] With the precatalyst **99**, the other enantiomeric product was generated (**Scheme 82**). This was explained by the fact that

phenyl groups and cyclohexyl chain are positioned in equatorial, whereas the $ROCH_2$- group is located in axial position (**Figure 13**).

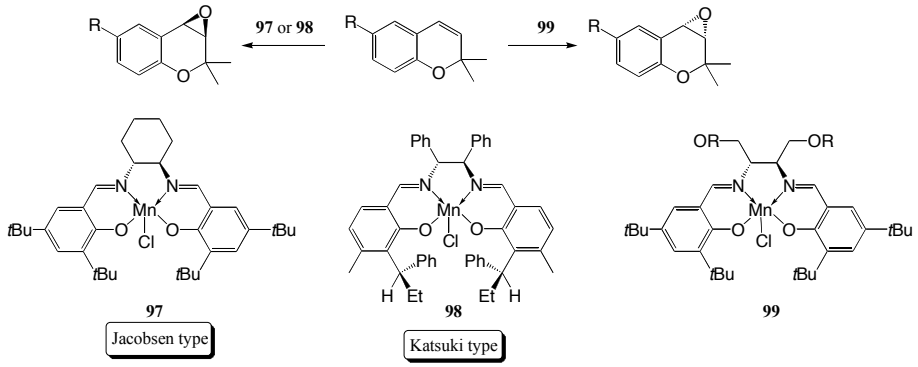

Scheme 82: Influence of the catalyst over the asymmetric induction.

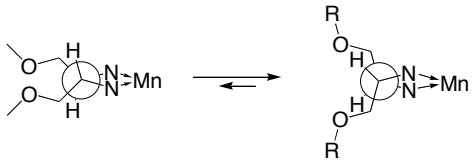

Figure 13: Newman projection of the equatorial/axial conformer of C along the *CH-CH*-bond in the complex **99**.

Substituents R_1 in position C3 and C3' strongly influence the selectivity. Jacobsen noticed that changing from R_1=H to *t*Bu raised the enantiomeric excess from <10 to 84%.[102] This can be explained by preventing the approaches D and E in addition to the steric hindrance caused by the diphenylethyldiimine backbone, which precludes approach A. More bulky groups than *t*Bu generally afforded a slight improvement or furnished

decreased results.[106] Use of R_3Si- groups led to a significant drop in enantioselectivity.[107]

Change in the pattern in position C5 and C5' afford better results when the substituent is bulky as a *t*Bu, blocking thus the approach C[102] but further increase in steric hindrance presented only little improvement.[108,109]

Introduction of a chiral center at the C3 and C3' positions exerted a strong influence over the reaction outcome. This complex class presented however lower results compared to Jacobsen type catalysts for the epoxidation of *cis* alkenes.[103,104] Catalyst design was oriented so as to favor approach B exclusively. Introduction of axial chirality as in Katsuki type precatalyst **99** allowed to reach enantioselectivities higher than 99%. Even if excellent results were achieved, the availability of this kind of complexes, compared to Jacobsen type ones, might account for their limited use.

Electronic effects were recognised to exert important influences on the reactivity as well as the enantioselectivity for Jacobsen type precatalysts. Catalyst tuning with this parameter was achieved by modifying the C5 and C5' substituents. It was observed that electron-withdrawing groups increased the reactivity.[110,111] The enantioselectivity was shown to increase with electron releasing groups and to decrease with electron donating groups.[112] As a linear relationship between enantioselectivities and σ values was observed, no steric influence should be exerted by these substituents. This trend could be explained by the Hammond postulate. More reactive catalysts present a more reactant like transition state with lower interactions between substrate and catalyst. At the opposite, electron deficient catalysts react

through a more product like transition state presenting more specific non-bonded interactions. However, for Katsuki type catalyst, electron donating groups in C5 and C5' position were shown to diminish the enantioselectivity.[113] It results that conclusions withdrawn for a given catalyst cannot be transposed to other types of catalysts.

Beside steric and electronic influence exerted by the salen moiety, addition of axial ligands could have dramatic effects on the reaction outcome. Structural studies of salen chromium oxide **100** revealed that without donor ligand, the metallic center is located 0.53 Å over the plane defined by the four coordinating atoms of the salen complex. In presence of a pyridine-*N*-oxide, the distance is shortened to 0.27 Å (**Figure 14**). In addition to this, the O=M bond is weakened, explaining thus rate enhancement. [110]

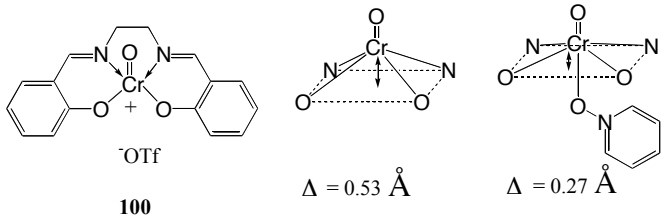

Figure 14: Effect of axial ligand on oxo chromium salen complex.

Beneficial effects on enantioselectivity of *cis* olefines epoxidation were also observed for nitrogen heterocyclic additives such as pyridine or

imidazoles.[101] Combination of chiral donor ligand with salen manganese complex devoided of any chirality element allowed enantioselectivity induction. This could be rationalised, as achiral salens exist in form of enantiomeric conformers. Coordination of a chiral ligand to the metal center shifts the equilibrium towards the formation of the most stable diastereoisomeric entity.[114-116] Other effects are possible as Lewis acidity lowering, which might suppress uncatalysed epoxidation pathways.[111,113,117,118] In addition to this, axial ligand coordination can prevent the formation of inactive μ-oxo dimers from salen Mn (III) **95** and a salen O=Mn (V) **96** complexes or favor their dissociation.[119]

3.2.2. Salen complexes with *cis*-β configuration

Two different factors favor the formation of cis-ß salen complexes: either by further addition of bidentate ligands on a *trans* salen complex or by the influence of configurational stability relative to other conformations due to the nature of the diimine bridge.[120]

Addition of a bidentate ligand was shown to alter the *trans* conformation of an achiral cobalt salen to the *cis*-ß configuration by coordination of acetylacetonate (**Scheme 83**).[121] In the case of titanium-based complexes, *trans* conformation is usually favored. However, addition to salen Ti (IV) Cl_2 complex of one equivalent of water and two equivalents of triethylamine lead to the corresponding dimeric di-μ-oxo-complex in a

cis-ß configuration. In this complex, the di-μ-oxo bridge acts as a bidentate ligand. [122,123]

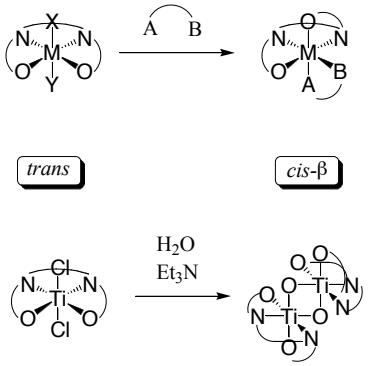

Scheme 83: Formation of *cis*-ß salen complexes from complexes of *trans* configuration ligand by addition of bidentate ligand.

The diimine backbone can also favor the formation of the *cis*-ß configuration provided it incorporates axial chirality as in the following complexes (**Figure 15** and **Figure 16**). In the first case, the metallic center is not part of a five membered heterochelate ring, as in the Jacobsen complex. Instead, it is included in a seven membered ring, which adopts the form of a twist-boat conformation because of the large dihedral angle between the naphthalene groups.[124]

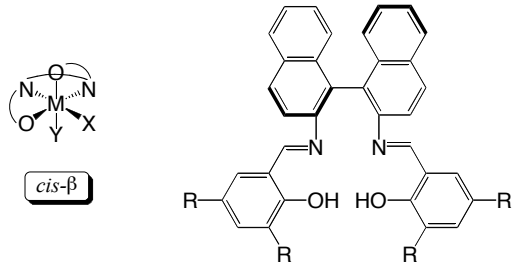

Figure 15: Salen ligand derived from an axially chiral diimine adopting the cis-ß configuration.

When substituents are present in the C7, C7' and C8, C8', the steric hindrance between these two groups favors also formation of the *cis*-ß configuration (**Figure 16**). If only the C7, C7' substituents are present in the salen complex, then *trans* configuration is observed.[125]

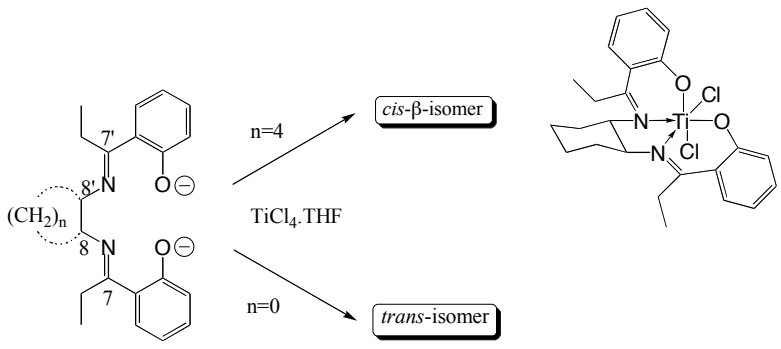

Figure 16: Adopted cis-ß configuration due to steric repulsion.

An interesting application in asymmetric catalysis that takes advantage of the *cis*-ß configuration in salen titanium complexes was reported by Belokon for the cyanosilylation of aldehydes (**Scheme 84**).[122,123] Indeed, with a catalytic load of 0.1%, enantioselectivities between 75 and 92% were reached for aromatic aldehydes. Concerning aliphatic aldehydes, enantioselectivites varied in a 52-66% range.

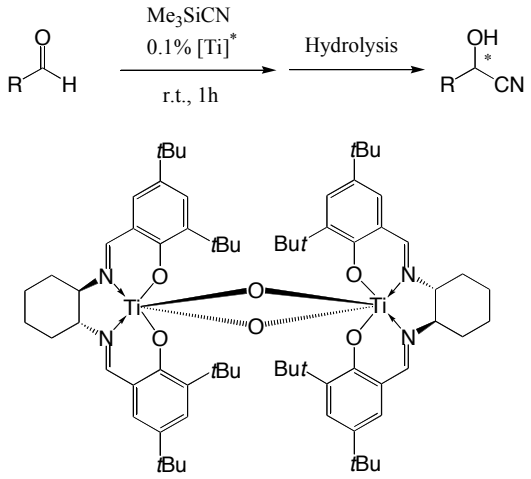

Scheme 84: Titanium catalysed cyanosilylation of aldehydes.

Catalyst preparation is of importance since a di-μ-oxo-complex **101** has to be generated according to the procedure described previously in **Scheme 83**, namely by addition of water and triethylamine. In the mechanism proposed, reaction of this dimeric structure with trimethylsilyl cyanide generates a *trans*-μ-oxo titanium cyanide complex **102**, which upon displacement of a cyanide ligand by an aldehydic substrate forms then a *cis*-

β-μ-oxo titanium species **103**, allowing then substrate cyanation (**Scheme 85**). Subsequent reaction of **104** with TMSCN liberates the cyanosilylated product and regenerates **102**, closing thus the catalytic cycle.

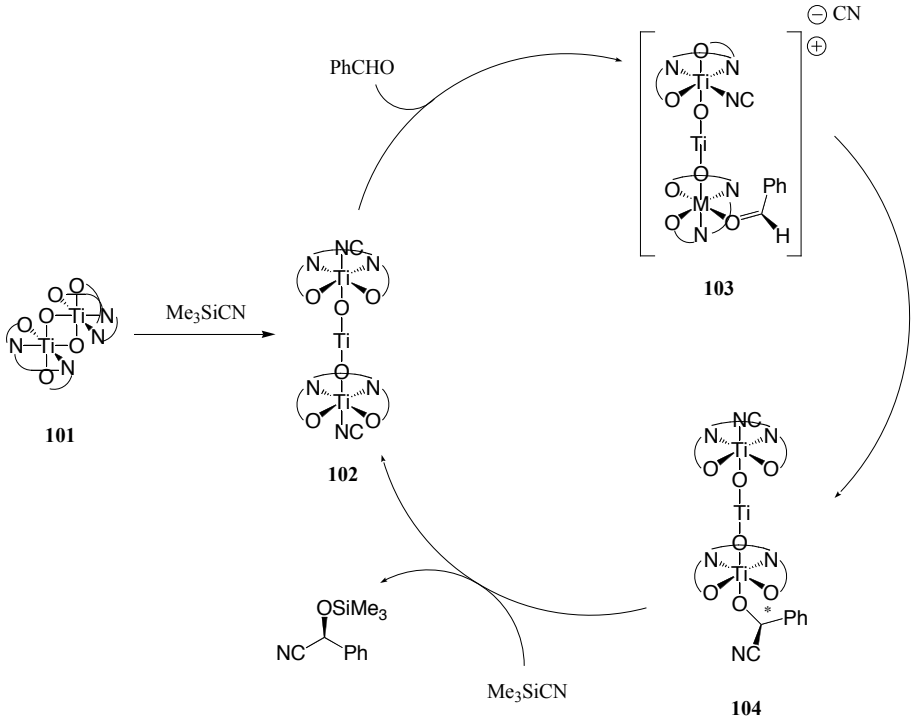

Scheme 85: Mechanism proposed by Belokon for the cyanosilylation of aldehydes catalysed by salen titanium complexes.[123]

3.3. Cobalt catalysed asymmetric hydrosilylation

There is only one report by Brunner concerning the use of cobalt-based catalysts in the asymmetric hydrosilylation of acetophenone with diphenylsilane (**Scheme 86**).[126] The employed metallic precursor, $[Co(Py)_6][BPh_4]$, was used in a ratio of 1 : 200 relative to the substrate. The used ligands were of pyridinyloxazoline type such as **105**. The enantiomeric excesses reached up to 56%. For the most enantioselective ligand, the yield was 35%. No investigation of this catalytic system with different substrates was reported.

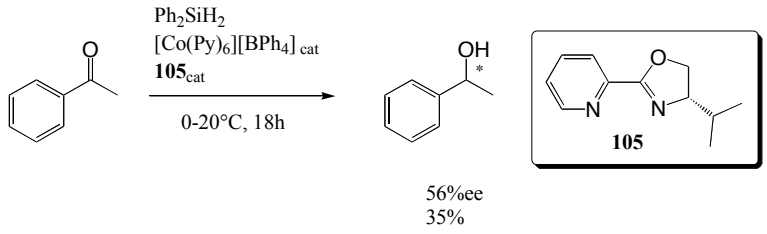

56%ee
35%

Scheme 86: Hydrosilylation of acetophenone with a pyridinyloxazoline cobalt complex.

3.4. Reorientation of the objectives

Salen and salenol type ligands are easy to synthesise and allow thus a rapid access to a variety of complexes. At first a procedure generating a cobalt hydride has to be developed with this kind of precatalysts. Then, various complexes will be prepared and evaluated in the established procedure forming the active species. Steric and electronic variations will only be performed with the type of precatalysts that are the most active and enantioselective. Following this, the scope and limitation of the system will be investigated.

3.5. Preliminary results

During the course of our group research in the discovery of new hydrosilylation catalysts, some experiments carried out in the laboratory that showed the efficiency of simple cobalt salen catalysts such as **106** for the hydrosilylation of acetophenone with PMHS, when the precatalyst was activated by TBAT (tetrabutyl ammonium triphenyldifluorosilicate), an anhydrous fluoride source (**Scheme 87**). This led to put aside our researches concerning the use of *N*, *S* ligands in the zinc catalysed hydrosilylation and to focus our attention to this new catalytic system. Reasons explaining this are especially the high structural modularity of the salen ligand and the observed activity.

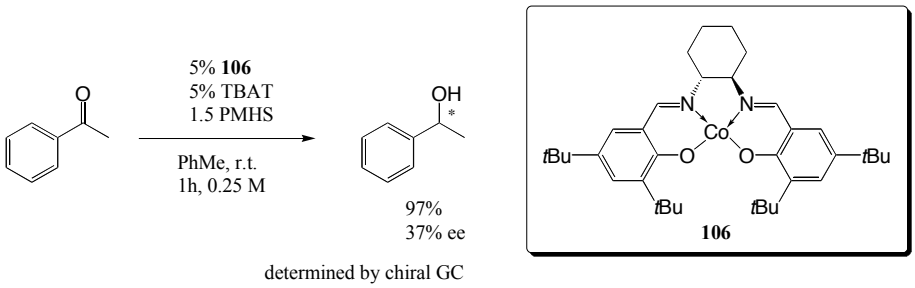

Scheme 87: Preliminary results in the cobalt catalysed hydrosilylation.

It was first expected that a cobalt hydride Co(III)-H was generated by oxidation of the cobalt (II) precursor (via an unknown process) followed by ligand exchange.

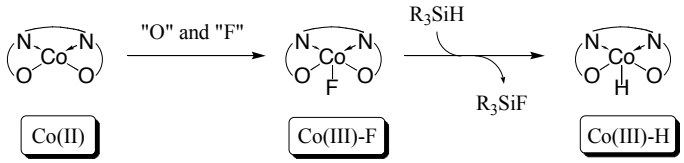

Scheme 88: First hypothesis explaining the formation of a Co(III)-H hydride species.

However, it was shown that the salen cobalt fluoride complex prepared by oxidation of the salen cobalt (II) by AgF in methanol gave some catalytic activity, albeit without any enantioselectivity.

This led us to consider a second hypothesis, namely the possibility of the generation of an anionic cobalt intermediate, Co (II)-H^-, a species also involved in the catalysed sodium borohydride reduction of prochiral ketone by cobalt complexes described by Yamada and Mukaiyama in part 2.3. Based on this assumption, the aim of our project was to modify the structure of the salen cobalt (II) precatalyst **106** in order to further improve the enantioselectivity. In addition to this, mechanistic investigations would provide further insight concerning the mechanism involved in this catalytic cycle.

In a screening of complexes, several transition metals and ligands were evaluated in the hydrosilylation of acetophenone with TBAT as activator in toluene at room temperature for 1 hour. Some complexes were readily available in the laboratory and others were prepared as described below.

3.5.1. Synthesis of salenol (derivatives) cobalt complexes

Salenol cobalt complexes as well as some aminosulfonyl derivatives were synthesised from aromatic aldehydes by condensation with a chiral aminoalcohol or an amine-sulfonamide followed by complex formation (**Scheme 89**). When the complexes were synthesised by the *in situ* procedure, yields were rather low (**107** and **108**). However, cobalt complexes were isolated in high yields (**109** and **110**), when isolated ligands were used.

In these products, the sulfonamide moieties were "introduced" in place of the hydroxy group of the salenol pattern. Only four complexes bearing different patterns (electronic and steric) were chosen for a preliminary evaluation of this family of ligands.

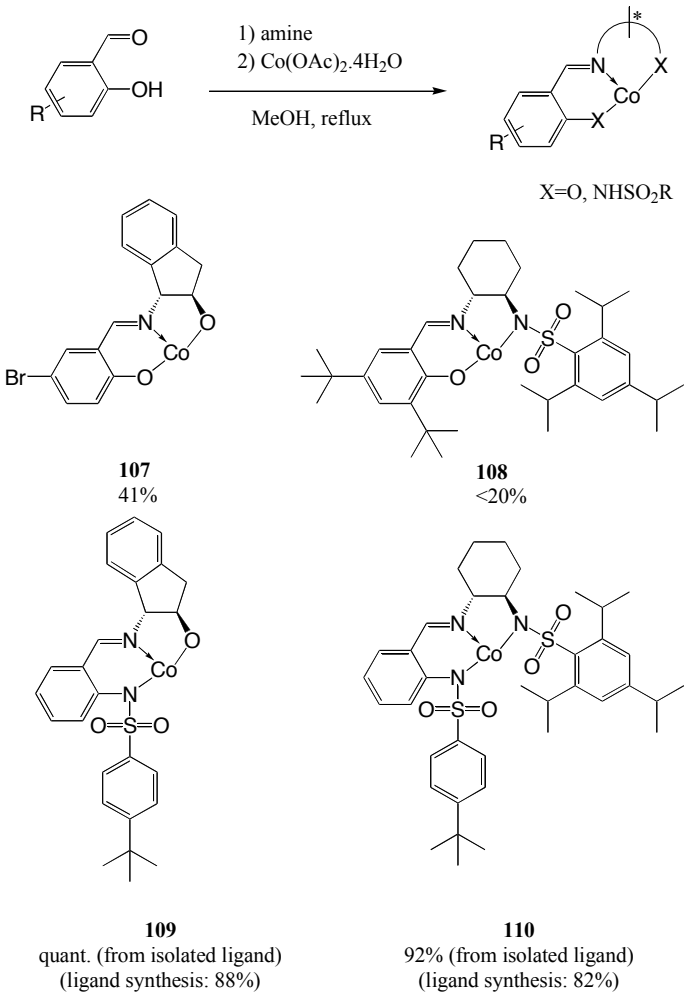

Scheme 89: Synthesis of salenol (derivatives) cobalt complexes.

3.5.2. Synthesis of a bis (oxazoline phenolate) cobalt complex

The oxazoline phenol ligand **111** was generously provided by Doctor Jerôme Hoet and Professor Ghosez (UCL). Its reaction with cobalt acetate furnished quantitatively the desired complex **112** by precipitation in the reaction medium. [127]

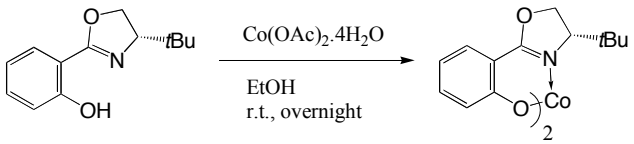

111 **112** quant.

Scheme 90: Synthesis of a bis (oxazoline phenolate) cobalt complex.

3.5.3. Complexes screening

The reduction of acetophenone was used to evaluate the potential of the precatalyst with a catalytic loading of 5%, when activated with TBAT (**Scheme 91**). For all series of catalytic tests, the Jacobsen cobalt complex **106** was used as standard to validate the data obtained for the other precatalysts and check the reproducibility of the catalytic system. In this way, it was shown that if toluene is not freshly distilled, the catalytic reactions did not work.

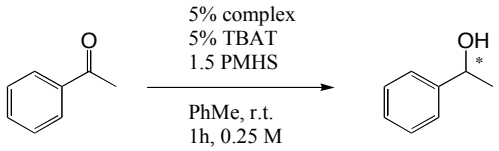

Scheme 91: Acetophenone reduction for the screening of precatalysts

As quoted earlier, a series of metal complexes (Cu, Ni, Al, Zn, Cr) was already available in the laboratory. The catalytic activity in our reaction was first checked for comparison with the cobalt complexes bearing various patterns of complexation.

With the copper (II) complexes, no enantioselectivity was observed (**Figure 17**). Only a modest conversion of 66% was noticed for the salen based complex **113**, whereas for the salenol derivatives **114** and **115**, the conversion was lower than 10%.

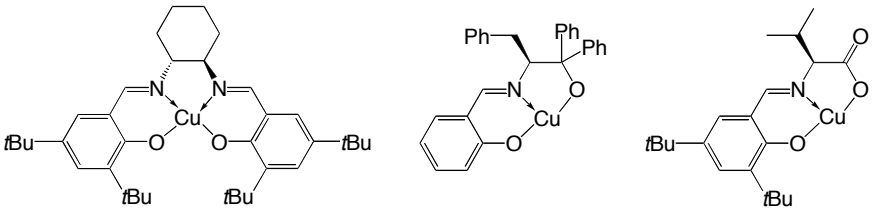

113

Conv: 66%
ee: 0%

114

Conv: 7%
ee: 0%

115

Conv: 8%
ee: 0%

Figure 17: Cu based complexes and their evaluation in the hydrosilylation of acetophenone.

The salen aluminum (III) chloride complex **116**, presented no conversion when one equimolar quantity of TBAT was added (**Figure 18**). With a second equivalent of activator, 22% conversion was observed. The salen chromium (III) chloride complex **117** showed almost no conversion. The salenol zinc (II) complex **118** reduced the substrate quantitatively, albeit as a racemate.

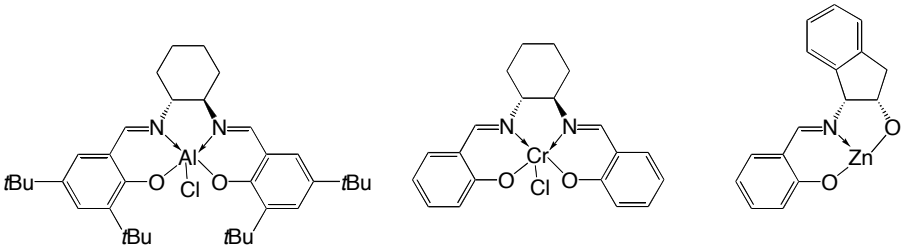

Figure 18: Al, Cr and Zn based complexes and their evaluation in the hydrosilylation of acetophenone.

The last transition metal evaluated was nickel. Complexed to a salen and salenol ligand, it gave 92 and 68% conversion, albeit without enantioselectivity (**Figure 19**).

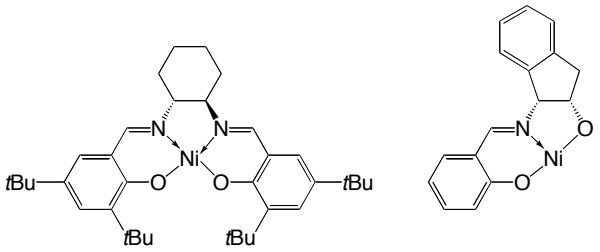

119 **120**

Conv:	92%
ee:	0%

Conv:	68%
ee:	0%

Figure 19: Ni based complexes and their evaluation in the hydrosilylation of acetophenone.

Following these results, which did not present any enantioselectivity when the catalyst was active, our attention turned back to cobalt based complexes. With salenol type (**107-110**) or oxazoline phenolate (**112**) ligands, the complexes were active and only in the latter case an enantiomeric excess of 11% was reached (**Figure 20**). Another structure without chiral diamine (**121**) was catalytically active but only the racemic product was obtained. Changes of the alkoxide with a sulfonamide moiety in the salenol pattern presented an interesting result. Indeed, 98% conversion with 34% enantioselectivity could be reached with **108**.

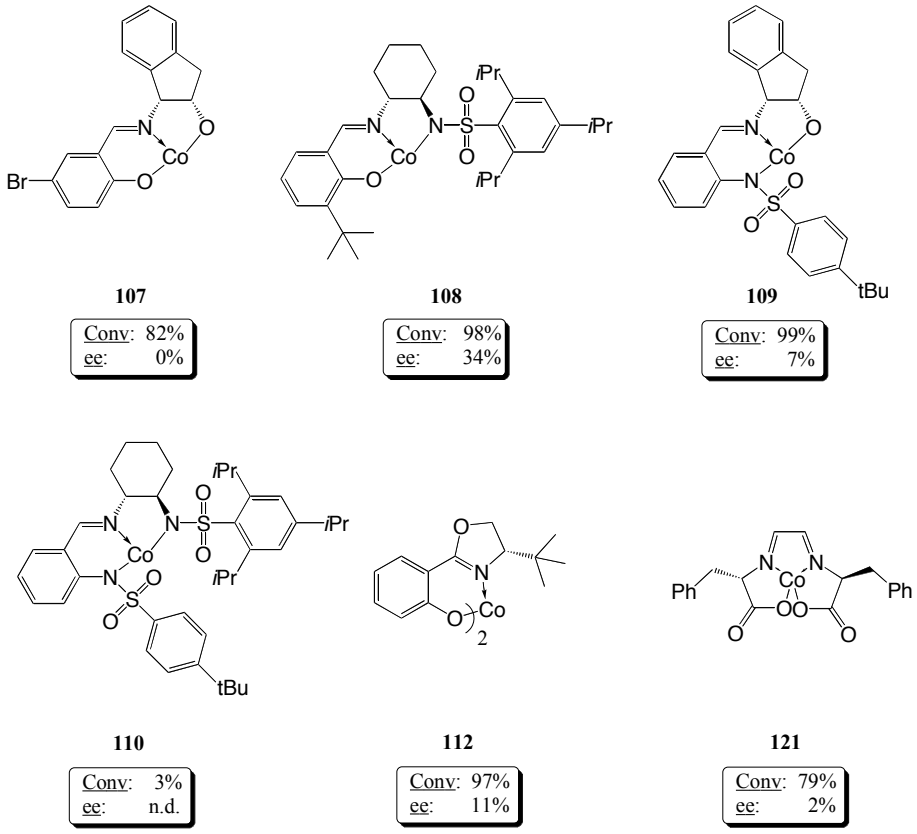

107

Conv: 82%
ee: 0%

108

Conv: 98%
ee: 34%

109

Conv: 99%
ee: 7%

110

Conv: 3%
ee: n.d.

112

Conv: 97%
ee: 11%

121

Conv: 79%
ee: 2%

Figure 20: Co based complexes and their evaluation in the hydrosilylation of acetophenone.

Since the Jacobsen complex **106** presented the most interesting result, researches focussing on derivatives of this precatalyst and optimisation of the reaction parameters for the catalytic test were carried out.

3.6. Synthesis of the chiral cobalt complexes

3.6.1. Synthesis of salen based cobalt complexes

Using the same synthetic procedure described for salenol derivatives, cobalt complexes were obtained by condensation of various aldehydic precursors with diamine and subsequent reaction with cobalt acetate (**Scheme 92**, **Figure 21**).

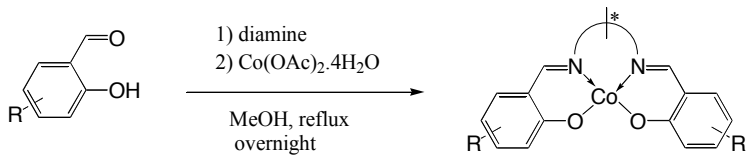

Scheme 92: General synthetic scheme for the synthesis of cobalt complexes.

Due to the sensitivity of the cobalt (II) complexes towards oxidation, the reactions were carried out under inert atmosphere. The complexes usually precipitated from the reaction mixture and can be isolated by simple filtration.

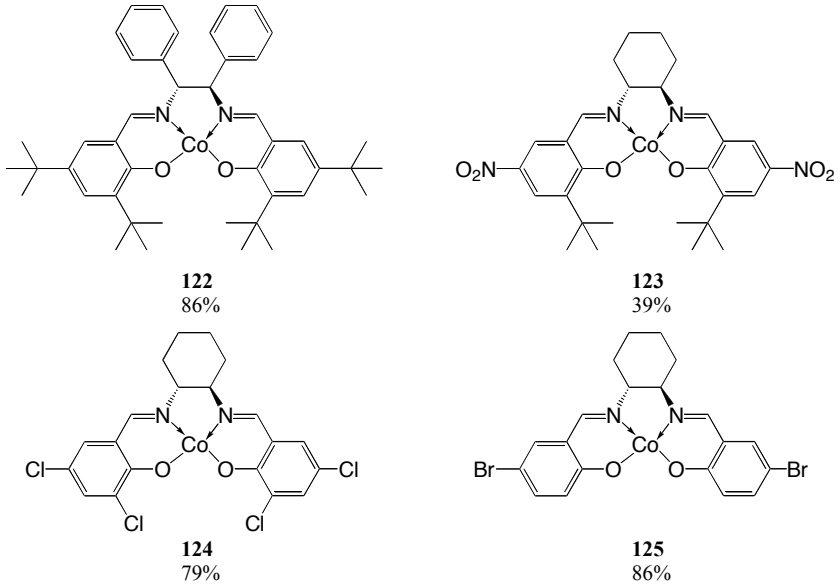

122
86%

123
39%

124
79%

125
86%

Figure 21: Cobalt complexes synthesised according to the previous synthetic scheme

The cobalt (II) complexes were obtained as an orange to red powder. The cobalt (II) being paramagnetic, a direct analysis by NMR proved impossible. Therefore, the complexes were analysed by IR, microanalysis as well as mass spectrometry. With the latter analysis, the formation of the complex can be put into evidence by its molecular peak. This method proved also very useful to check the purity of the complexes, as it was possible to notice the signal of ligand in the mass spectrum. Although this method is not quantitative, it was used to check the formation of the complex and to have a first evaluation of its purity.

3.7. Evaluation of Jacobsen type salen cobalt complexes in hydrosilylation

3.7.1. Evaluation of salen cobalt complex or PMHS activating agents

The previous results made evident that a highly efficient catalytic system can be generated with a reagent activating the salen cobalt complex, namely TBAT. Further researches were then carried out to check other system activators (**Table 7**). With an equimolar amount of $NaBH(OAc)_3$ relative to the cobalt complex, in order to generate a cobalt hydride species, no conversion was observed, unfortunately. PMHS activators acting as fluoride source, such as $LiBF_4$ and TBAF, gave unsatisfactory results. Indeed, $LiBF_4$ was unable to activate the silylating agent and TBAT catalysed the reaction with 95% conversion, albeit with poor enantioinduction. The use of alkaline *tert*-butoxides presented poor conversion. Optimisation of the new catalytic system was then performed by changing the reaction parameters with TBAT as activating agent.

Table 7: Influence of the activating agents.

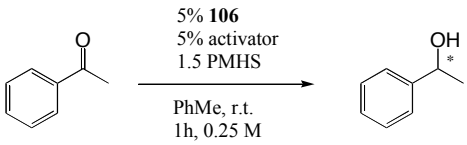

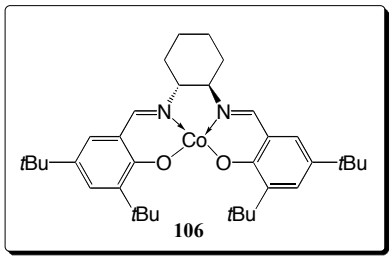

Activator	Conv (%) [(a)]	e.e. (%) [(a)]
TBAT	97	37
$NaBH(OAc)_3$	<1	n.d.
$LiBF_4$	<1	n.d.
TBAF	95	7
*t*BuOLi	17	19
*t*BuONa	0	n.d.
*t*BuOK	8	n.d.

(a) conversions and enantiomeric excesses determined by chiral GC.

3.7.2. Influence of the cobalt complex to activator ratio

Variation of the ratio between the chiral complex and the activating agent was investigated (**Table 8**). In the test reactions, it should be noticed that acetophenone was added prior to PMHS. It was noticed that with half an equimolar equivalent of activator with regard to the complex, a drop in conversion was observed and the enantiomeric excess decreased to 30%. However, the use of 1.5 equivalent of TBAT did no lead to any changes. Inversion in the addition order of acetophenone and PMHS did not lead to significant changes. Following these results, an equimolar ratio between the salen cobalt complex and the activating agent was kept for the next catalytic tests. It should be noticed that the concentration relatively to the substrate was arbitrary kept constant at 0.25 M for our investigations.

Table 8: Influence of the ratio [Co]* / TBAT.

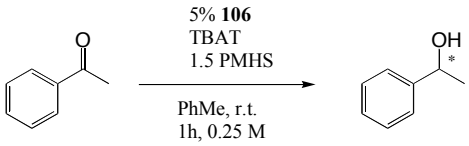

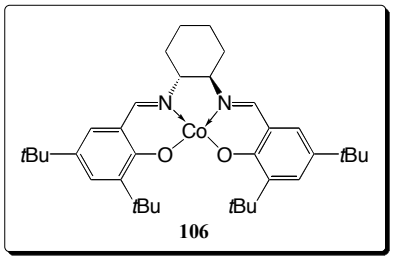

[Co]* / TBAT	Conv (%) [a]	e.e. (%) [a]
1 :0.5	45	30
1 : 1	97 (93)[b]	37 (34) [b]
1 : 1.5	99	36

(a) conversions and enantiomeric excesses determined by chiral GC. (b) test run with reagents addition in reverse order (PMHS then acetophenone)

3.7.3. Influence of the solvents

After establishment of the optimal conditions to activate the precatalyst, a solvent study was undertaken (**Table 9**). Toluene and diethyl ether present the best results concerning both the conversion, with 97 and 99%, and the enantioselectivity, with 37 and 35% respectively. Use of more polar solvents such as THF or acetonitrile gave lower enantioselectivities.

Chlorinated solvents such as dichloromethane or 1,2-dichloroethane presented very poor enantioselectivities. As toluene presented the best results, it was used as solvent for the next studies.

Table 9: Influence of the solvents.

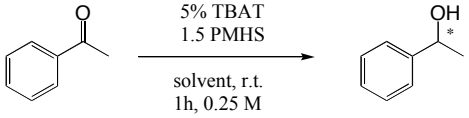

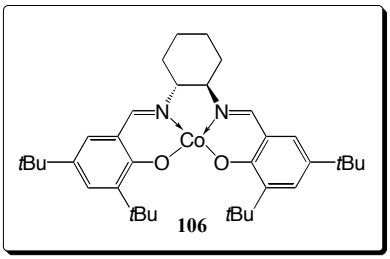

[Co]* / TBAT	Conv (%) [a]	e.e. (%) [a]
PhMe	97	37
Et_2O	99	35
THF	92	24
CH_3CN	91	5
CH_2Cl_2	86	7
$ClCH_2$-CH_2Cl	5	n.d.

(a) conversions and enantiomeric excesses determined by chiral GC

3.7.4. Influence of additives

As explained in the bibliographic introduction, dealing with salen complexes catalysed reactions, additives can influence the reaction outcome in a non-negligible way. Study of their influence showed that triphenyl phosphine or its oxide did not lead to any changes. *N*-coordinating ligands such as DMAP or *N*-methylimidazole did not affect the conversion but gave a decrease in enantioselectivity to 29 and 25%, respectively (**Table 10**). It was deduced from these results that the studied additives did not present any beneficial effect in our catalytic system.

Table 10: Influence of additives.

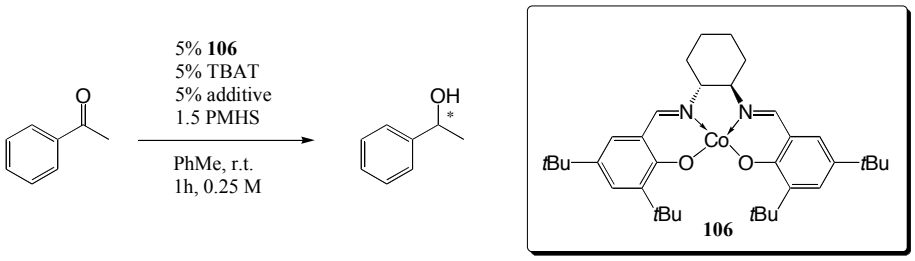

Additive	Conv (%) [a]	e.e. (%) [a]
none	97	37
$P(Ph)_3$	99	35
$O=P(Ph)_3$	100	36
DMAP	96	29
N-methylimidazole	95	25

(a) conversions and enantiomeric excesses determined by chiral GC.

3.7.5. Influence of the reaction temperature

Prior to undertake some variations of the salen structure, the temperature influence over our catalytic system was studied (**Table 11**). Performing the reaction at 0°C decreased the conversion from 97 to 60% in

parallel to a marginal increase in enantiomeric excess from 37 to 39%. With a reaction temperature of -20°C, the reaction was sluggish with a conversion of 12% after 1h. Extension of the reaction time to 24 h led to only 53% of conversion and 18% of enantioselectivity. The best results were thus obtained when the reaction was performed at room temperature.

Table 11: Influence of the temperature.

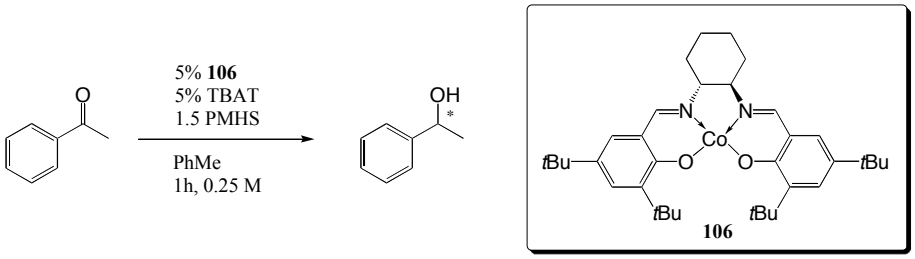

Temperature (°C)	Conv (%) [a]	e.e. (%) [a]
r.t.	97	37
0	69	39
-20	12	n.d.
-20[b]	53	18

(a) conversions and enantiomeric excesses determined by chiral GC. (b): reaction time: 24h.

3.7.6. Catalytic loading and concentration influence

Different reaction pathways may be involved if the concentration influences the enantioselectivity. However, at a concentration in substrate of 1M rather than the usual 0.25 M, neither decrease in conversion nor in enantioselectivity was noticed after 1 hour of reaction and this with only 1% of catalyst. To our delight, the enantiomeric excess remained unchanged (conv: 87%; ee: 37%) after 45 minutes of reaction when lowering the catalytic loading to 0.2%. It should be noticed that in the last case a TON of 580 was reached.

A first trial of kinetic study was performed with the salen cobalt complex. Samples were regularly taken by syringe and quenched in a KOH / MeOH solution. After filtration on a small plug of silica, the solution was analysed by chiral GC. It revealed at first that no change in the product enantiomeric excess was observed after 15 min reaction (**Chart 1**). Before 15 min the enantiomeric excess presents a constant increase. This could be attributed to a low precision of the determined excesses when there is little conversion. There was only 75% of conversion after 1 h and 72% after 1 h 30. This showed that by taking samples, the catalytic system was perturbed. For time reasons, the catalytic reaction could not be kinetically studied with an IR probe.

Chart 1: Kinetic study of the cobalt catalysed hydrosilylation of acetophenone by a salen cobalt complex.

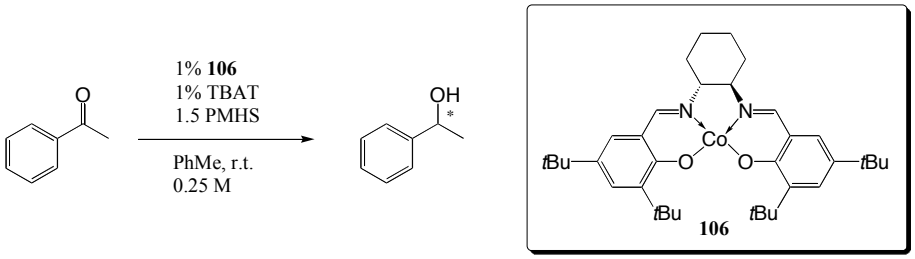

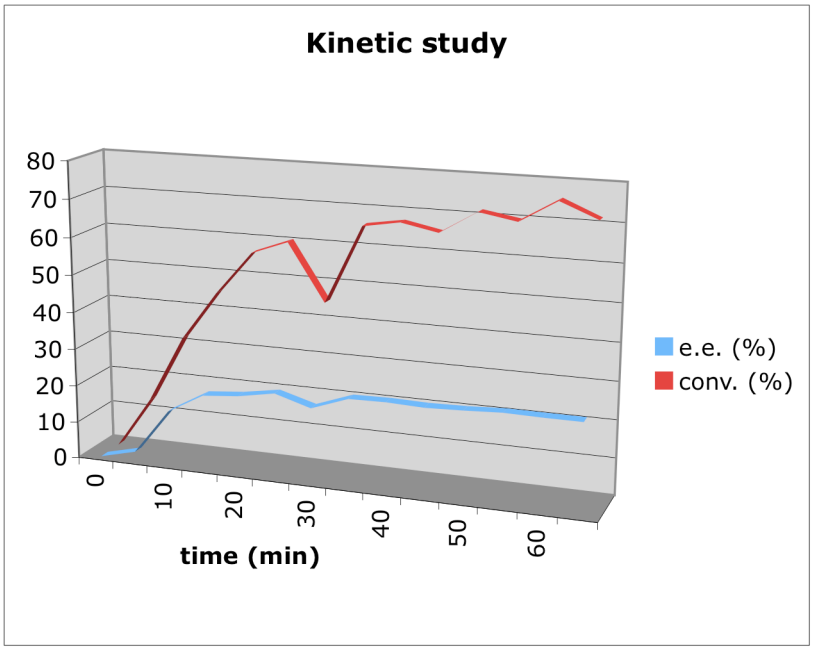

3.7.7. Formation of the salen cobalt complex *in situ*

Compared to *in situ* generation of the salen cobalt complex, isolation of the complex required an additional synthetic step. Therefore, it was interesting to determine whether both methods presented the same reaction outcome or not in order to check if a larger screening of ligands was possible. For this purpose, the salen ligand was deprotonated to form the corresponding lithium phenolate at 0°C and the temperature was allowed to reach room temperature (**Scheme 93**). As the reaction was carried out in toluene, a soluble and easy to handle source of cobalt (II) was required. The cobalt (II) 2-ethylhexanoate (65% wt, solution in mineral spirits) was therefore chosen. After 15 minutes, the cobalt precursor (purple solution) was added to the yellow solution of the dilithium salt of the ligand. The solution then turned orange and was stirred for 30 minutes. Thereafter, the usual addition of TBAT followed by acetophenone and PMHS after 15 minutes was performed. Unfortunately, the results were not as good as with the isolated complexes. There were only 80% conversion and 13% enantiomeric excess. As consequence, all salen cobalt complexes must be isolated prior to their evaluation.

It seems, as other catalytic experiments have also pointed out, that the presence of salts in the catalytic medium had a detrimental effect on both the reactivity and enantioselectivity.

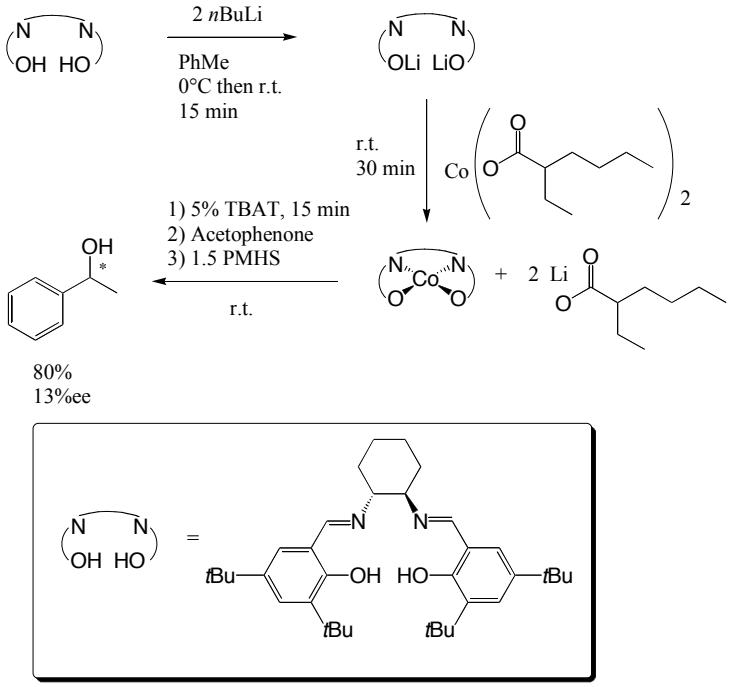

Scheme 93: Acetophenone hydrosilylation with *in situ* formation of the salen cobalt complex.

3.7.8. Variations of the salen ligand

Salen cobalt complexes with different substitution pattern were evaluated in the benchwork reaction (**Table 12**). No general trend emerged from this study. Even if conversions were unchanged, no improvement in enantioselectivity could be noticed. Changing the diimine backbone from cyclohexyldiamine to diphenylethylene diimine led to 98% conversion and

14% enantiomeric excess and with binaphthyldiimine only 74% conversion was observed without enantioselectivity. In the latter case, formation of a complex with a *cis*-ß configuration may explain the lack of selectivity.

Table 12: Salen variations.

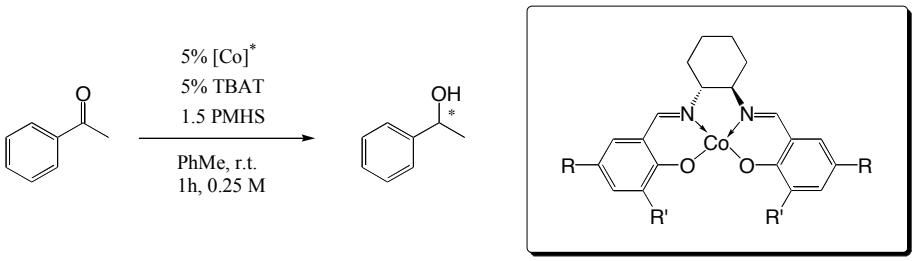

Complex	R	R'	Conv (%) [(a)]	e.e. (%) [(a)]
106	*t*Bu	*t*Bu	100	36
123	NO_2	*t*Bu	97	20
124	Cl	Cl	98	18
125	Br	H	96	16
126	H	Ph	99	0
127[(b)]	*t*Bu	*t*Bu	98	14
128[(c)]	*t*Bu	*t*Bu	74	0

(a) conversions and enantiomeric excesses determined by chiral GC. (b) with a diphenylethylene diimine moiety. (c) with a binaphthyl diimine moiety.

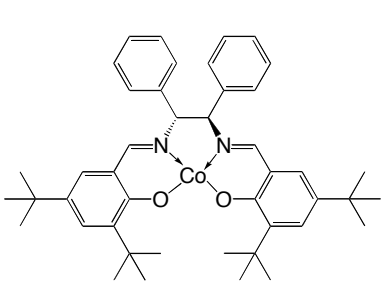

127

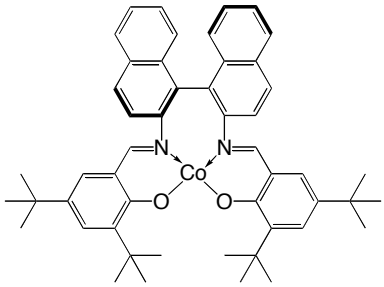

128

3.7.9. Influence of the counterion

Investigation of the reaction with a chiral counterion for the activating agent was also undertaken (**Table 13**). With 5% of this chiral activator **129** (generously provided by Doctor Raphaël Dumeunier and Professor Markó (UCL)) without cobalt complex, the substrate was reduced with 39% conversion under its racemic form. In presence of the chiral cobalt complex **106**, a lower conversion was noticed (23%) but this time with 20% enantiomeric excess.

Table 13: Influence of the counterion

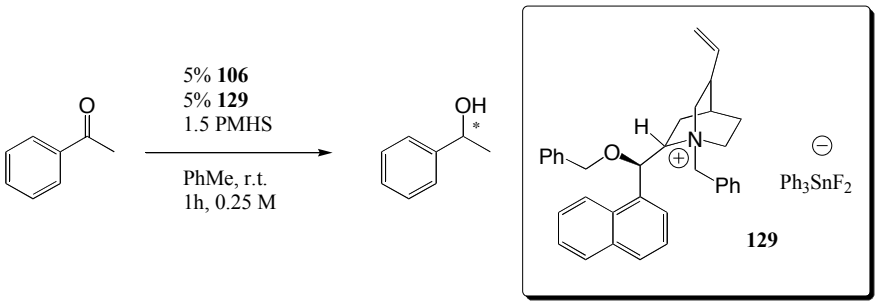

System	Conv (%) [(a)]	e.e. (%) [(a)]
129	39	0
106 + **129**	23	20

(a) conversions and enantiomeric excesses determined by chiral GC.

3.8. Synthesis of a bifunctional precatalyst and evaluation

Our attention focused on a described bifunctional catalyst allowing activation of both the electrophile and nucleophile. The precatalyst **130**, developed by Kozlowsky, was applied in the addition of diethylzinc to aldehydes,[128] α-ketoesters,[129,130] and α-aldiminoesters[131] with high enantioselectivities (**Scheme 94**). In this case, the salen ligand coordinates the metallic center, which acts as Lewis acid, activating thus the electrophile.

The side arms present the heteroatoms that activate the diethyl zinc by coordination (**Figure 22**).

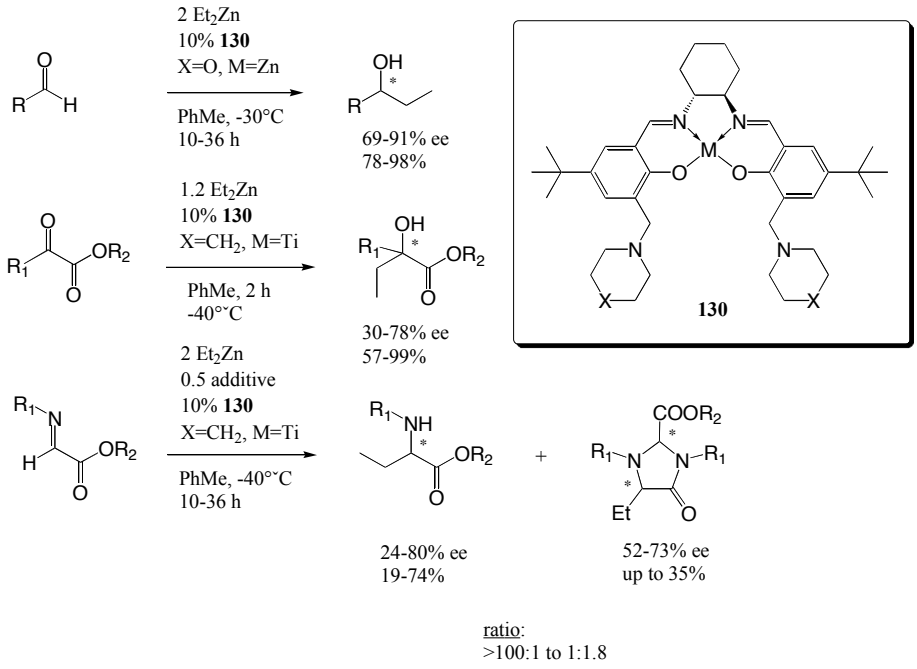

Scheme 94: Diethylzinc addition to aldehydes, α-ketoesters and α-aldiminoesters catalysed by a bifunctional catalyst.

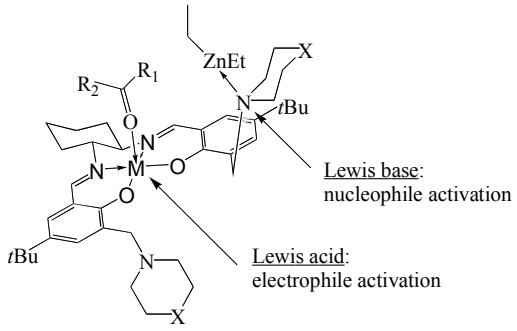

Figure 22: Bifunctional catalyst developed by Kozlowsky.

The same ligand was intended to be used with the catalytic system using a cobalt (II) complex activated by TBAT. Compared to the Kozlowsky system, the locations of the Lewis base and acid are reversed. The metallic center, coordinated by the salen ligand, would be a nucleophilic anionic cobalt ate hydride and the nitrogen bearing arms coordinated a Lewis base, which activates the electrophile.

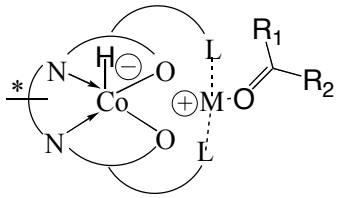

Figure 23: Schematic representation of the bifunctional catalyst for the asymmetric carbonyl reduction.

The synthesis of the aldehydic precursor was carried out according to a described procedure involving a Mannich reaction. *N*-Methylpiperazine and paraformaldehyde form an iminium ion, which is attacked by the aromatic phenol **131** (**Scheme 95**). Product purification was performed by recrystallisation of the bromhydrate salt **132**. The aldehyde **133** was liberated by neutralisation with a mild base in 82% global yield (Lit: 50%[132]).

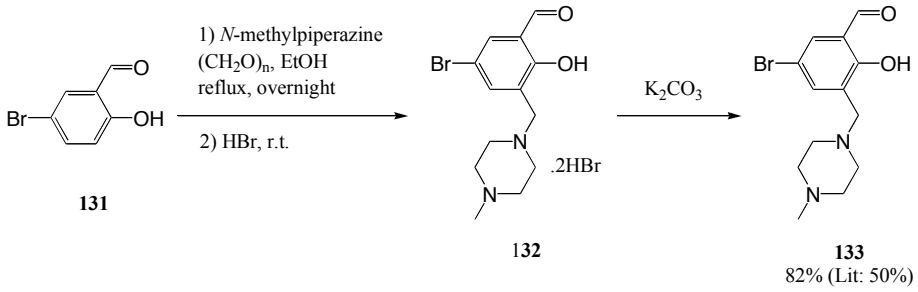

131 **132** **133**
82% (Lit: 50%)

Scheme 95: Synthesis of the aldehydic precursor of the bifunctional precatalyst.

The precatalyst **134** was synthesised by condensation of **133** with cyclohexyldiamine in refluxing methanol followed by addition of cobalt acetate (**Scheme 96**). The cobalt complex was isolated in 63% yield.

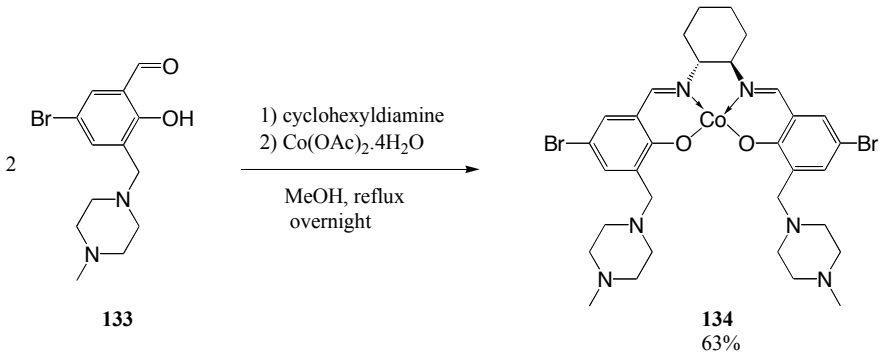

133 **134** 63%

Scheme 96: Synthesis of the bifunctional salen cobalt complex **134**.

Bifunctional catalysis was investigated with the salen cobalt complex **134** (**Table 14**). Alkaline cations with a non-coordinating counter-ion were used to act as Lewis-acids and activate the carbonyl substrate. Results showed that the presence or absence of a Lewis acid in the reaction media did influence neither the conversion nor the enantioselectivity, excepted with $LiN(Tf)_2$. In this case, the enantiomeric excess was only 5%. The detrimental effect of salts on this catalytic reaction was already noticed as quoted earlier. It might be possible that a slight increase in the ionic strength of the reaction medium has an influence on the stability of the postulated cobalt hydride intermediate. However, the enantioselectivities with the complex itself remained very low and the effects of salts on the catalytic reaction should be confirmed with a more efficient cobalt catalyst.

Table 14: Bifunctional catalysis

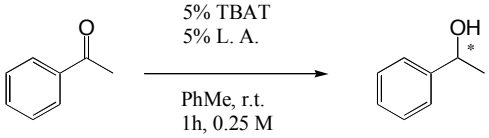

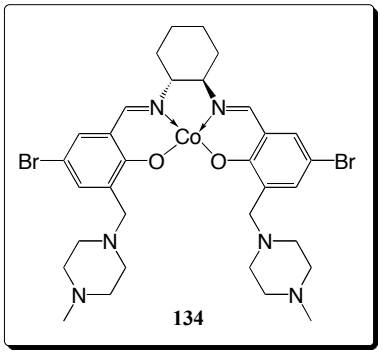

System	Conv (%) [(a)]	e.e. (%) [(a)]
134	96	16
134 + $LiBF_4$	94	16
134 + $LiN(Tf)_2$	98	5
134 + $NaN(Tf)_2$	97	17

(a) conversions and enantiomeric excesses determined by chiral GC.

3.9. Synthesis of chiral diimine-bissulfonamide cobalt complexes and evaluation

3.9.1. Synthesis of chiral diimine-bissulfonamide cobalt complexes

At this point, other salen cobalt complexes were not synthesised since there was no breakthrough by changing the substitution motif of the aromatics and the diimine backbone. Therefore, attention was paid to chiral ligands with a different structural pattern, such as salen derivatives incorporating a sulfonamide group (**Figure 24**). The following complexes **135** and **136** were evaluated in the acetophenone reduction under the usual condition, *i.e.* with TBAT activation in toluene at room temperature. A real breakthrough came with the cylohexyldiimine-bisulfonamide cobalt complex **135**. An enantiomeric excess of 51% could be reached with 94% conversion. However, its diphenylethylene analogue was inactive.

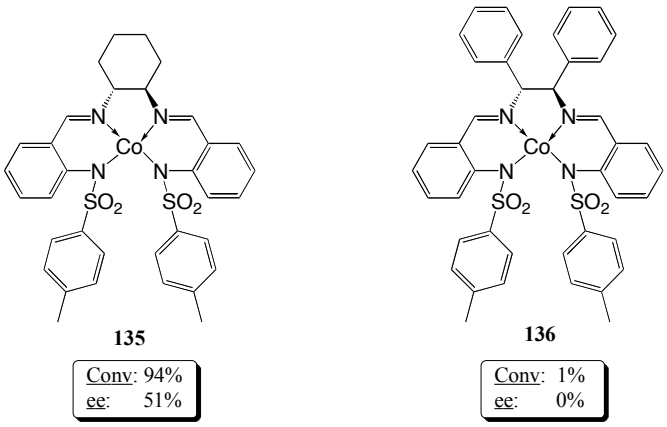

Figure 24: Diimine-bis-sulfonamide cobalt complexes and their evaluation in the hydrosilylation of acetophenone.

The synthesis of diimine-bis-sulfonamide ligands was described by different groups. The method of Bermejo implies the synthesis of 2-aminobenzaldehyde, which polymerises at room temperature (**Scheme 97**).[133] Reaction with tosylchloride in presence of a base affords 2-tosylaminobenzaldehyde, which is condensed with diaminocyclohexane. Another method described by Lemaire also used a convergent synthesis.[134,135] It starts with the condensation of a chiral diamine and 2-nitrobenzaldehyde. Reduction of the nitro groups was catalysed by Pd / C under an atmospheric pressure of hydrogen at 0°C for 4h. The reaction with tosylchloride and a base afforded the tetradentate ligand.

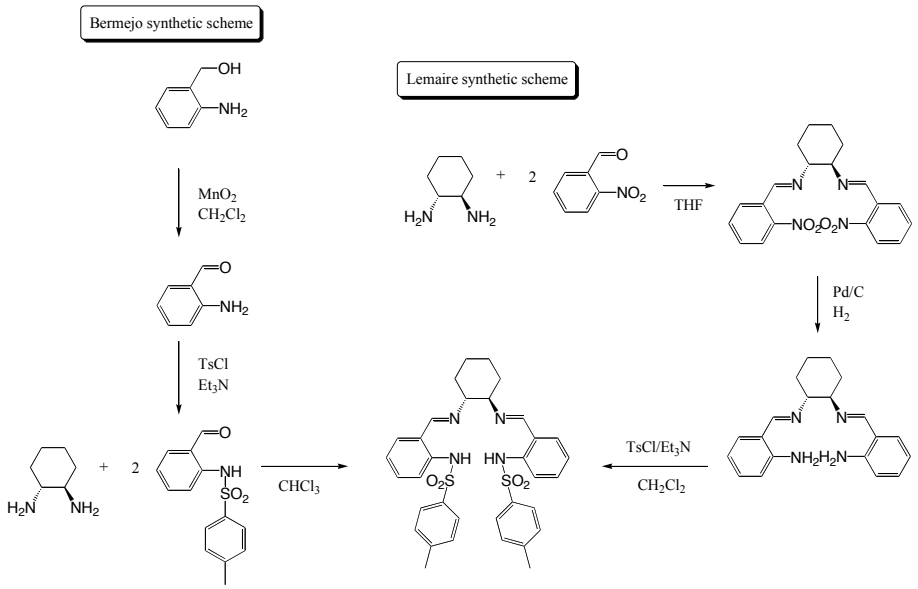

Scheme 97: Synthetic schemes of Bermejo and Lemaire.

The synthetic scheme developed by Lemaire was the most interesting. However, the reduction of the nitro functions, under the reaction conditions described previously, did not work in hour hands. Therefore, we turned our attention to a method described by Koenig, which will be described in the next section.[136] It should be noticed that this approach was first reported for achiral Schiff bases by Katsuki.[137]

3.9.1.1. Syntheses of aromatic aldehydes

Aromatic aldehydes **137**-**145** with a sulfonamide in *ortho*-position were synthesised in a very practical procedure in two steps first established by Prof. Riant. It consists in a modification of the Koenig procedure, which did not require isolation of the benzylic alcohol (**Table 15**). First, the coupling was carried out between 2-amino benzyl alcohol and a sulfonyl chloride in dichloromethane in the presence of pyridine. After stirring the reaction mixture overnight, an acidic work-up was performed. Following this, the crude alcohol was oxidised with pyridinium chlorochromate in dichloromethane for 3 h at room temperature. Decantation of the solution from the chromium salts and filtration over a plug of silica gel and celite generally furnished the desired product in high yields. Further purification could be achieved by crystallisation of the crude adehyde in ethanol. The yield for the two steps were usually good to excellent and could be scaled up to give an easy access to multigrams of various substituted aldehydes, except when pentafluorosulfonyl chloride was used. In the latter case, a side reaction involving a nucleophilic aromatic substitution took place, explaining why the product did not form.

Table 15: Syntheses of 2-sulfonamide benzaldehydes.

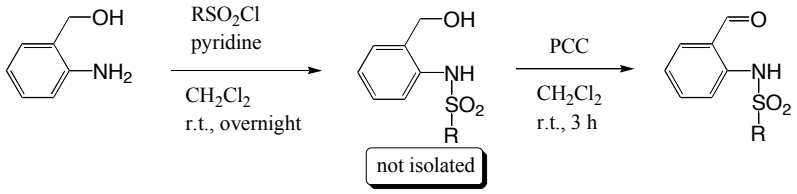

Aldehyde	**R**	**Yield (%)**
137	4-Me-Ph	93
138	4-*t*Bu-Ph	83
139	2,4,6-tri-Me-Ph	83
140	2,4,6-tri-*i*Pr-Ph	68
141	Me	34
142	4-F-Ph	85
143	4-CF_3-Ph	100
144	3,5-di-CF_3-Ph	89
145	4-MeO-Ph	77
146	F_5C_6	/

3.9.1.2. Syntheses of the corresponding diimines

Condensations were performed either in refluxing methanol in presence of a catalytic amount of acetic acid or in dichloromethane with magnesium sulfate as a drying agent (**Table 16**). Generally, the last method was used because of the better solubility of the reactants in this solvent. All products were obtained quantitatively after a simple filtration of the reaction mixture and evaporation of the solvent.

Table 16: Syntheses of chiral cyclohexyl diimine-bissulfonamide ligands

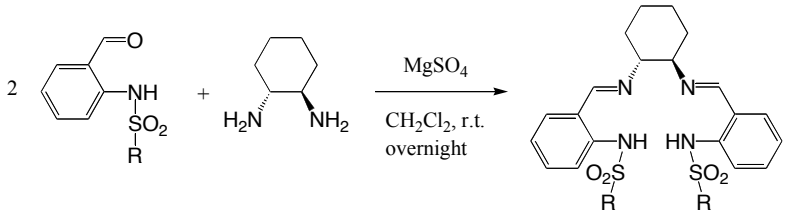

Ligand	**R**	**Yield (%)**
147	4-Me-Ph	quantitative
148	4-*t*Bu-Ph	quantitative
149	2,4,6-tri-Me-Ph	quantitative
150	2,4,6-tri-*i*Pr-Ph	quantitative
151	Me	quantitative
152	4-F-Ph	quantitative
153	4-CF_3-Ph	quantitative
154	3,5-di-CF_3-Ph	quantitative
155	4-MeO-Ph	quantitative

Other chiral diamines such as binaphthyldiamine and / or diphenylethylenediamine were also used with the 4-F-Ph and 4-Me-Ph substituted sulfonamides. Yields were also quantitative (**Figure 25**).

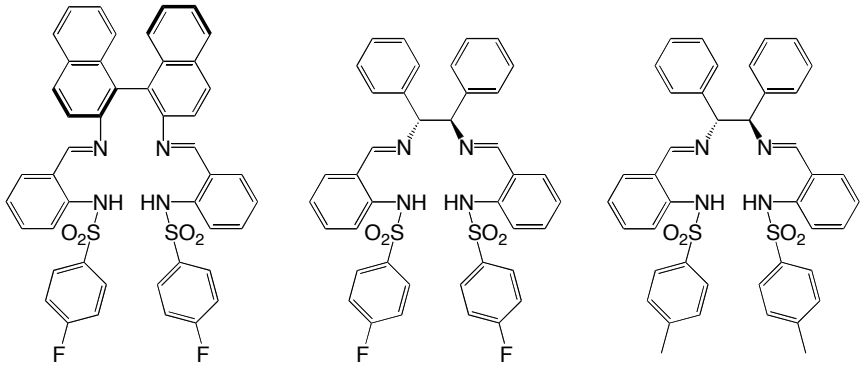

156
quantitative

157
quantitative

158
quantitative

Figure 25: Variations of the diimine bridge.

3.9.1.3. Syntheses of the corresponding cobalt complexes

Contrary to salen cobalt complexes, which precipitated when synthesised in refluxing methanol with cobalt (II) acetate as a metallic precursor, no precipitation could be observed in most cases when the sulfonamide based ligands were used in this method. Therefore another synthetic method had to be devised starting from cobalt (II) chloride. Its low solubility in organic solvents led first to use a derivative complexed by

tetrahydrofuran, expecting an increase in solubility. The synthesis of this metallic precursor involves treatment of cobalt (II) chloride with tetrahydrofuran in a Soxhlet-apparatus.[138] Solvent removal furnished a blue solid. Drying the solid on a vacuum pump did not give a mass for the product consistent with the described ratio between cobalt (II) chloride and THF (1:1.5). Indeed, the mass of product always decreased when the complex was put under vacuum. Thus, this pathway was not further pursued.

Since sulfonamides present a more acidic proton compared to salen ligands (pK_a(phenol)=9,95 versus pK_a (PhNHTs)=8.46[139]), the use of a non-nucleophilic anionic base such as an alkoxide was considered. For this purpose, cobalt (II) chloride and two equivalents of potassium *tert*-butoxide were mixed in THF in a Schlenk tube connected to the vacuum line. After 10 to 30 minutes, the blue solution turned deep purple as ligand exchange is supposed to occur to give the cobalt (II) *tert*-butoxide. As very few examples have been reported for the preparation of cobalt (II) alkoxides, and as they are supposed to be highly sensitive to oxidation, an *in situ* method was considered as more convenient for our purpose. At this point, the ligand was added and the reaction mixture was stirred overnight. The color solution generally changed to red, indicating the coordination to the ligand. In order to eliminate the salt formed, the solvent was removed under reduced pressure and degassed dichloromethane was added. The resulting suspension was filtered over a Millipore filter fitted to a syringe and transferred into a Schlenk tube kept under argon. The filtrate was then half-evaporated with a vacuum pump and degassed *n*-hexane was added to precipitate the complex.

Yields were good to high. Generally, analysis by mass spectrometry of the complexes showed only traces of free ligand, when it could be detected.

Table 17: Synthesis of chiral cyclohexyl diimine-bissulfonamide cobalt complexes.

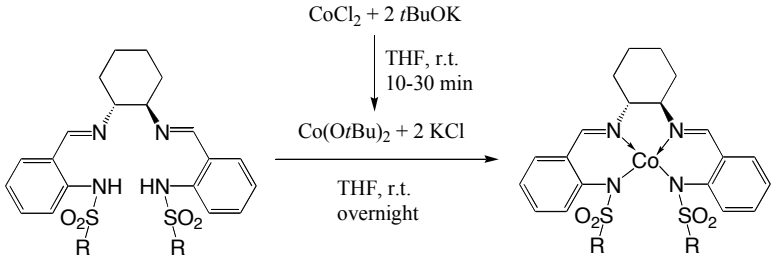

Complex	R	Yield (%)
159	4-Me-Ph	82
160	4-*t*Bu-Ph	75
161	2,4,6-tri-Me-Ph	48
162	2,4,6-tri-*i*Pr-Ph	84
163	Me	83
164	4-F-Ph	57
165	4-CF_3-Ph	49
166	3,5-di-CF_3-Ph	53
167	4-MeO-Ph	71

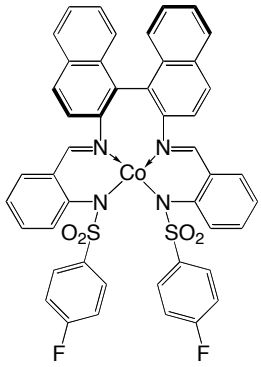

168
64%

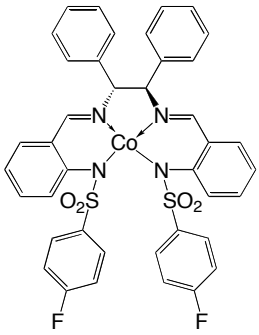

169
52%

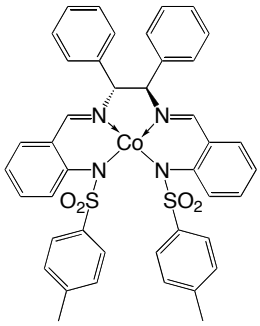

170
39%

3.9.2. Evaluation of diimine-bis-sulfonamide cobalt complexes

The variation in the sulfonamide group substitution was then studied (**Table 18**). With a methyl group (**163**), a drop in enantioselectivity was observed without affecting the conversion. With an aromatic group on the sulfonamide, effects of its substituent(s) are difficult to rationalise. With alkyl substituents (**159-162**), enantioselectivities varied between 40-52% with an almost complete conversion. Interestingly, a fluorine in *para* position (**164**) increased then enantiomeric excess to 66%. However, with a trifluoromethyl group in *para* position (**165**) the conversion decreased to 5%. With two trifluoromethyl groups in the *meta* positions (**166**), a high conversion of 95% and an enantiomeric excess of 44% were observed. A methoxy group in *para* position (**167**) gave a drop in enantioselectivity and conversion to 26 and 27%, respectively. The substitution on the diamine moiety could not be rationalised either, as there was no logical correlation with both conversion and / or enantioselectivity.

Table 18: Hydrosilylation of acetophenone with diimine-bis-sulfonamide cobalt complexes.

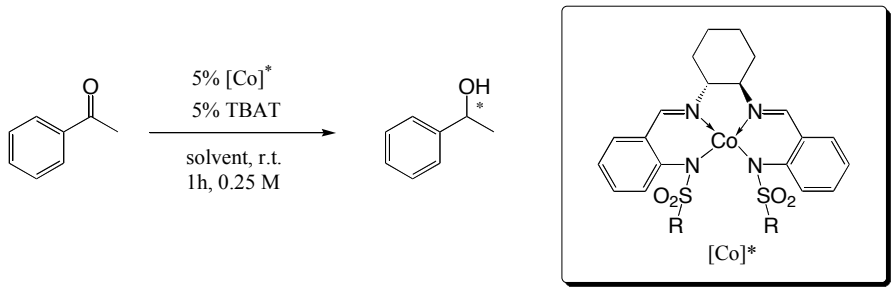

Complex	R	Conv (%) [(a)]	e.e. (%) [(a)]
159	4-Me-Ph	94	51
160	4-*t*Bu-Ph	96	43
161	2,4,6-tri-Me-Ph	97	52
162	2,4,6-tri-*i*Pr-Ph	98	40
163	Me	98	11
164	4-F-Ph	96	66
165	4-CF_3-Ph	<5	n.d.
166	3,5-di-CF_3-Ph	95	44
167	4-MeO-Ph	27	26
168	4-Me-Ph[(a)]	1	n.d.

169	4-F-Ph[(b)]	88	2
170	4-F-Ph[(c)]	5	n.d.

(a) conversions and enantiomeric excesses determined by chiral GC. (b) with a diphenyl ethylene diimine moiety. (c) with a binaphthyl diimine moiety.

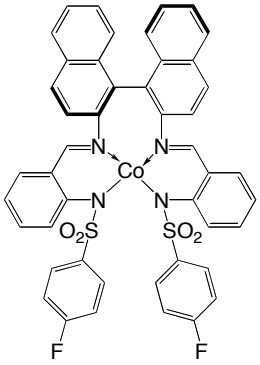

168

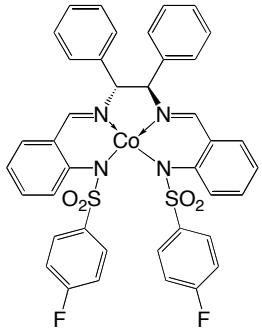

169

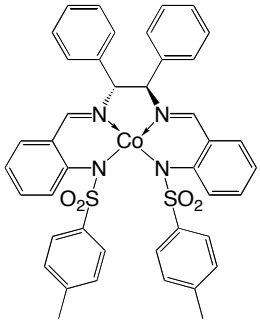

170

3.9.3. Substrates study

In a preliminary trial, other substrates than acetophenone were reduced with our new catalytic system. For example, α-tetralone was reduced with high conversion and yield in the system developed by Yamada and Mukaiyama, using sodium borohydride in presence of a chiral cobalt (II) complex **26b** (see part 2.3). With **159**, α-tetralone could be reduced with 84% enantioselectivity, under unoptimised conditions, compared to 90% for the system developed by Yamada and Mukaiyama (**Table 19**).[56] The reaction conditions (temperature, molarity, time) made our system more

advantageous for large-scale synthesis. But most interestingly, the TOF reaches 18.4 (h^{-1}). This is an important feature in asymmetric catalysis since it is difficult to reach high activity with high enantioselectivity together. It should be noticed that even if the cobalt complex **159** is not the most enantioselective, it was used here for the substrate study due to its larger availability.

Table 19: Comparison between the system of Yamada/Mukaiyama and our new catalytic system.

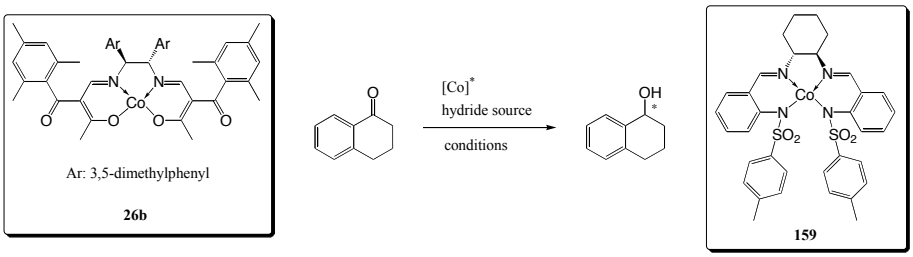

Conditions	26b [(b)]	159
Molarity (mol/L)	0.05	0.25
Temperature (°C)	-20	r.t.
Time (h)	12	1
Catalytic loading (%)	1	5
Conversion (%)	100	92[(a)]
e.e. (%)	90	84[(a)]
TOF (h^{-1})	8.3	18.4

(a) conversions and enantiomeric excesses determined by chiral GC. (b) data from the literature.[56]

This result incited to study the reduction of α-tetralone with different cobalt complexes at different catalytic loadings. Since the conversion was not quantitative, the concentration of the reaction media was increased from 0.25 to 1M. The results showed that the commercially available cobalt complexes **26** and **106**, catalysed the reaction with low and moderate conversions, respectively and low enantioselectivity in both cases. Increasing the concentration to 1M led to a decrease in enantioselectivity from 84 to 79% with 5% of **159**. Decreasing the catalytic loading to 1% gave a decrease to 75% of enantioselectivity. However, under the same condition, the cobalt complex **164** presented a better selectivity (82% ee) together with a high conversion (95%). It should be outlined that a TOF of 95 [h^{-1}] was reached with a one molar reaction media.

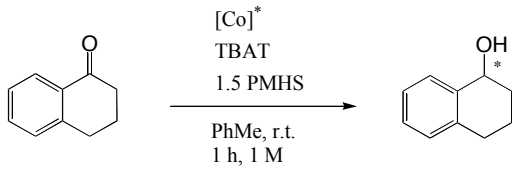

Catalyst	Cat. load. (%)	Conv. (%) [(a)]	e.e. (%) [(a)]
26a	5	11	5
106	1	60	8
159	5	92	79
	1	97	75
164	1	95	82

(a) conversions and enantiomeric excesses determined by chiral GC

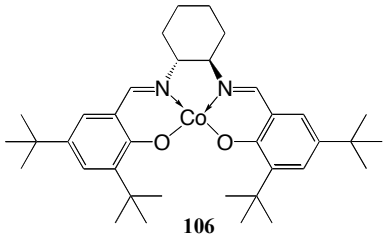

106

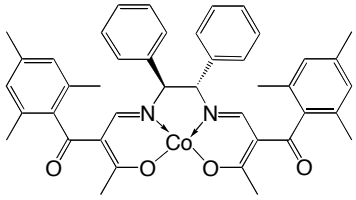

26a

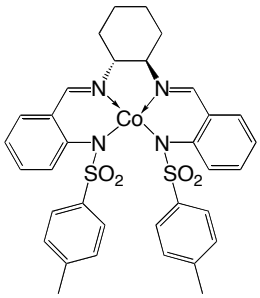

159

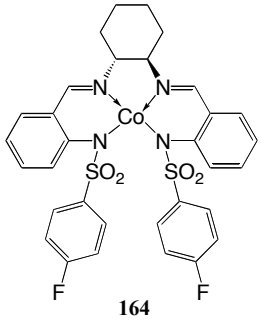

164

The chemoselectivity study of our catalytic system was performed with α,β-unsatured cyclohexenone and (*E*)-4-phenylbut-3-en-2-one. The precatalyst **159** with a tosyl group was used because of its larger availability as noticed earlier. The cyclic α,β-unsatured cyclohexenone was cleanly reduced to form the alcohol with low conversion and enantioselectivity. This clearly showed that a 1,2-reduction took place. Concerning the (*E*)-4-phenylbut-3-en-2-one, the GC analysis of the crude reaction mixture showed many peaks. However, analysis by ^{13}C NMR of the crude product after a reaction time of one night showed that no more carbonyl function was present. This supports a 1,2 reduction as in the case of the cyclohexenone.

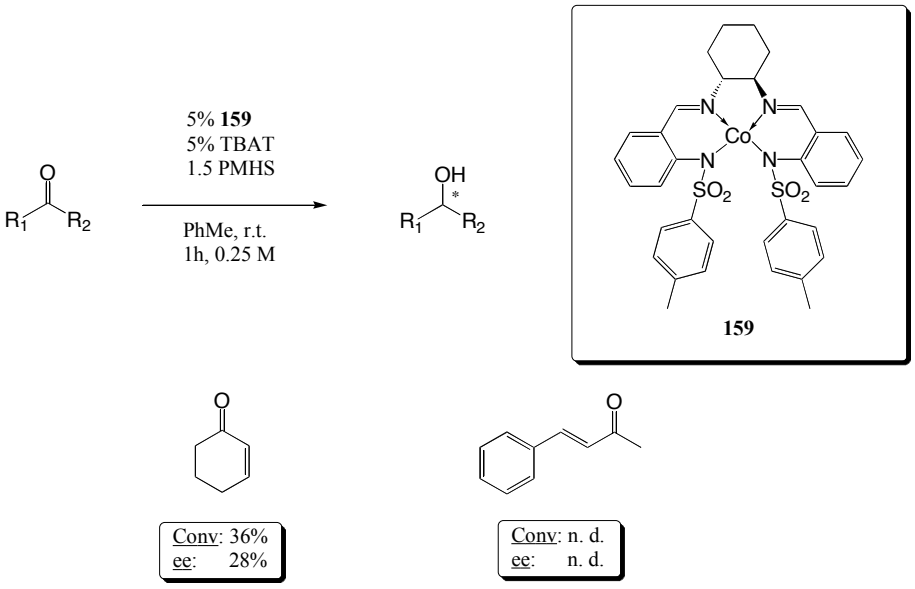

Scheme 98: Substrate study with our new catalytic system.

3.9.4. Influence of the silylating agent

Variation of the silylating agent was performed to get some mechanistic insights. Indeed, if an anionic cobalt hydride is formed as in our hypothesis, no variation of the enantioselectivity should be observed (**Scheme 99**). When ethoxydimethylsilane and diethoxymethylsilane were used in the catalytic test, acetophenone was reduced respectively with 36 and 55% of enantiomeric excess. Other silanes should be studied in order to support or refute the participation of the reducing agent in the enantiodiscriminating step.

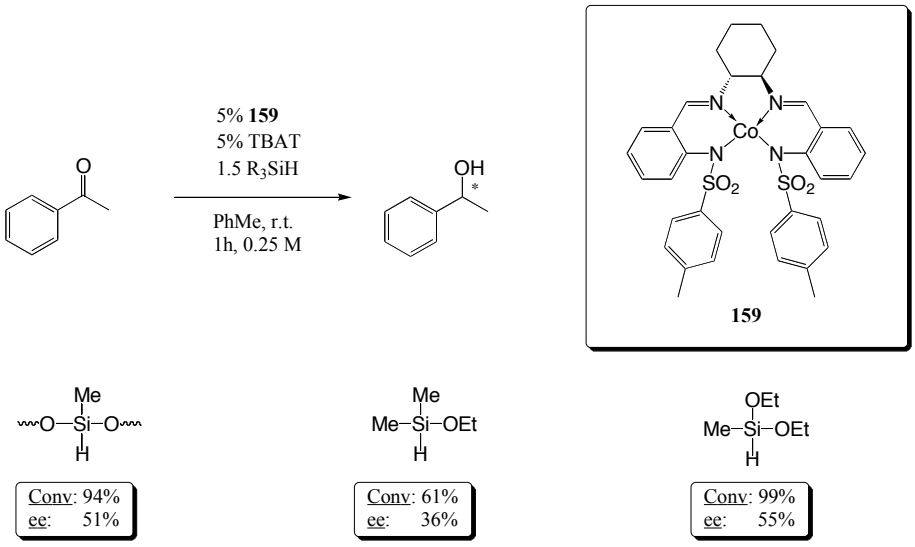

Scheme 99: Influence of the silylating agent.

3.10. Synthesis of camphor derived cobalt complexes

In the previously studied precatalysts, the chiral information was always carried in the bridge between the two nitrogen atoms. With the camphor derived cobalt complexes that we intended to develop, chirality is located in the part between the nitrogen and oxygen atoms (**Figure 26**). This kind of precatalysts has not been described in the literature but should be accessible in few steps.

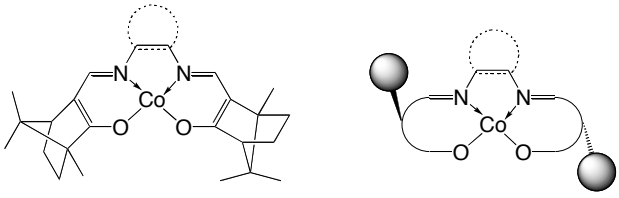

Figure 26: Camphor-based cobalt complexes

At first, formylation of camphor **171** was carried out. The procedure described by von Zelewsky[140] implied first treatment of camphor with sodium amide in refluxing benzene overnight. After cooling and addition of *iso*pentyl formate, the reaction mixture was stirred for four hours before acidic work-up to give the desired product **172** with 70% yield as a pale yellow solid. Changing the reaction conditions to toluene as solvent and ethyl formate as electrophile gave formyl camphor in 10% yield (**Table**

20).[141] This could be explained by the use of ethyl formate rather than *iso*pentyl formate. This led to a reaction mixture with high viscosity. The isolated product was also a pale yellow solid. However, its degradation was noticed, when stored under atmospheric conditions. Another experiment with longer reaction time and an additional purification by recrystallisation in *n*-hexane afforded the desired product in 16% as a white solid. When a solution of ethyl formate in THF rather than toluene was used, the reaction mixture was still as viscous as before.

At this stage, another protocol for the preparation of the enolate was considered.[142] Lithiation with *tert*-BuLi at -78°C followed by ethyl formate addition furnished an orange oil. An attempt of recrystallisation did not allow the isolation of any solid. However, the same procedure with addition of 4 equivalents of ethyl formate furnished the desired formyl camphor **172** as a white solid in 68% yield.

Table 20: Synthesis of formyl camphor **172**.

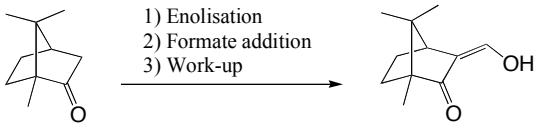

171 **172**

Enolisation	Ethyl formate addition	Yield (%)	Remarks
$NaNH_2$, PhMe Reflux, overnight	EtOCHO, PhMe 0°C to r.t. then 4h	10	pale yellow solid
	EtOCHO, PhMe 0°C to r.t. then 24h	16	white solid (recrystallisation)
	EtOCHO, THF 0°C to r.t. then 24h	n.d.	
tert-BuLi, THF, -78°C	EtOCHO, THF, -78°C then r.t. overnight	/	orange oil
	4 EtOCHO, THF, -78°C then r.t. overnight	68	white solid

With this synthetic procedure forming formyl camphor **172** in good yield and high purity, condensations with ethylenediamine and 1,2-phenylenediamine were carried out and furnished the corresponding diimines **173** and **174** in quantitative yields (**Scheme 100**). Unfortunately, the corresponding cobalt complexes could not be isolated. Refluxing a solution of the ligands in methanol under argon in the presence of cobalt (II) acetate led to a brown solution in each case, indicating that the cobalt complexes **175** and **176** might be formed. As no precipitation of the products could be observed, the methanol was removed under reduced pressure until the solution became viscous and then degassed *n*-hexane was added but no precipitate formed, even at low temperature.

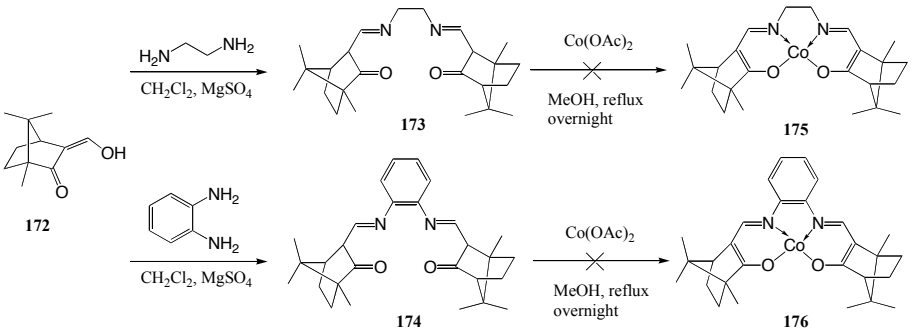

Scheme 100: Reaction of formyl camphor with achiral diamines and attempt of formation of the corresponding cobalt complexes.

The ligands could not be characterised by ^{1}H NMR at room temperature since too many isomers were detected. According to the literature,[143,144] **173** presents mainly the tautomeric forms T2, stabilised by an

intermolecular hydrogen bonding, and T3 in apolar and in hydrogen-bonding solvents respectively (**Figure 27**). However, in the presence of an acid, the rate of interconversion can be accelerated. Concerning the rotational conformation around the N-CH_2-CH_2-N, the *gauche* and *anti* rotamers, R_1 and R_2, are present in equal population in solution at room temperature. No information is given concerning the ratio between R_1 and R_2 at high temperatures. Based on these informations, the synthesis of the corresponding complex was therefore performed in refluxing methanol as exposed previously.

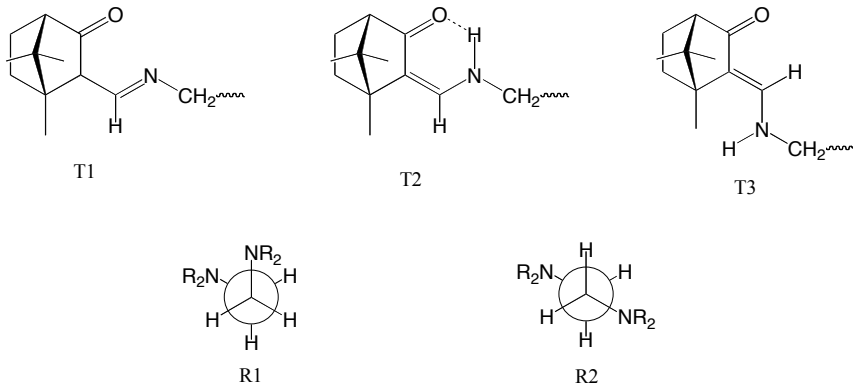

Figure 27: Tautomers and rotamers of the ligand **173**.

For the ligand **173**, three sets of signals corresponding to the methyl groups could be noticed at room temperature as well as at 90°C. The change in temperature had almost no influence on the ratio between the tautomers T1 and T2 by comparison between the =CHN areas (T1/T2: 1:1 at r.t. and 1.5:1 at 90°C). Concerning the ligand **174**, three sets of signals for the

methyl groups could also be observed although, at high temperature, a set of signals was dominant. They could be assigned to the tautomeric form T2 since there was no signal corresponding to a free NH. Unfortunately no single isomer could be obtained so as to allow the products characterisation.

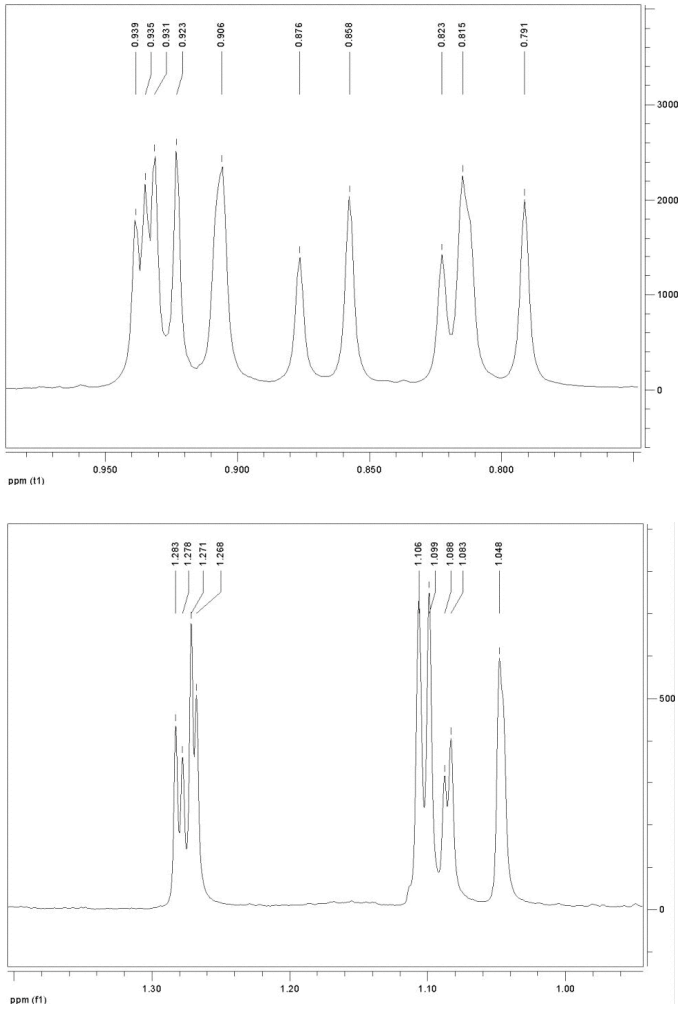

Spectrum 3: Spectrum of ligand **173** at room temperature (top) and at 90°C (bottom) in toluene-d_8.

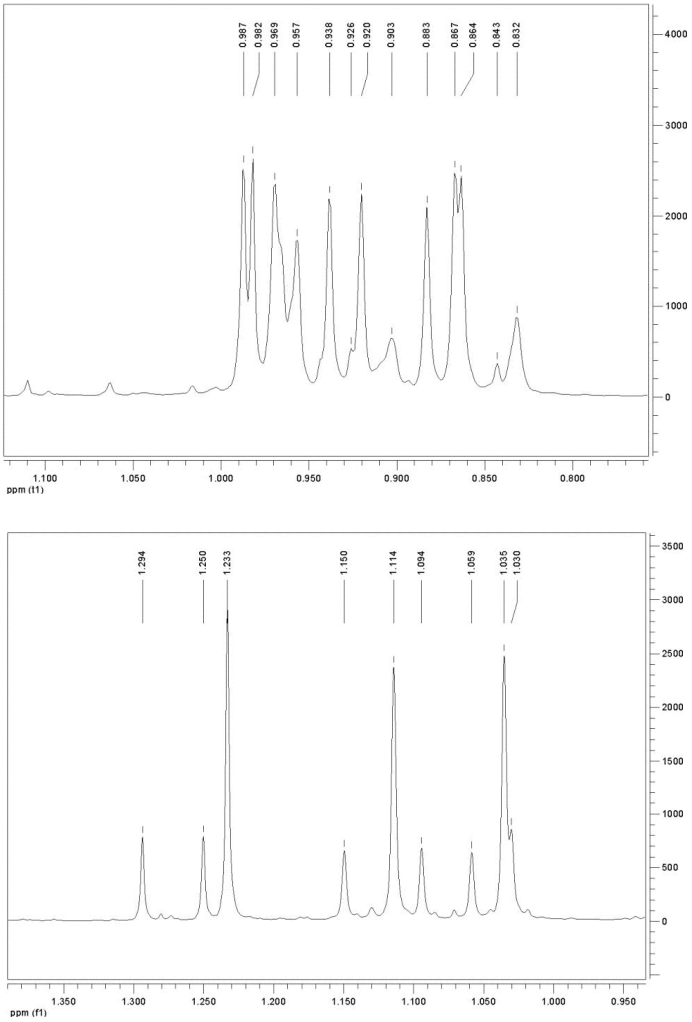

Spectrum 4: Spectrum of ligand **174** at room temperature (top) and at 90°C (bottom) in toluene-d_8.

3.11. Synthesis of diamine-bis-sulfonamide based complexes

Investigation of the diamine based complexes is of interest for two reasons. Firstly, it is supposed that the imine functions might be reduced during the reaction, so if no selectivity difference is observed between the diimine and diamine based catalysts; this would be an element supporting the reduction. Secondly, a tertiary amine next to the asymmetric carbon would allow the transmission of the chirality nearer to the metal concomitant to an increase in the steric hindrance, enhancing perhaps the enantioselectivity of the studied catalytic reaction (**Figure 28**).

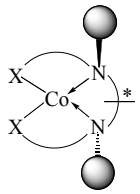

Figure 28: Tertiary chiral amines allow a better transmission of the chiral information and increase the steric hindrance at the metallic center.

The cobalt complex **178** formed from the reaction between the reduced Jacobsen ligand **177** (obtained by reduction of the commercially available salen ligand by sodium cyanoborohydride in acetic acid according to a published procedure[145]) was obtained by reaction with cobalt chloride

and two equivalents of potassium tert-butoxide. Its evaluation in the reduction of acetophenone showed an enantioselectivity of 28%, compared to 37% ee for the unreduced precatalyst **106**.

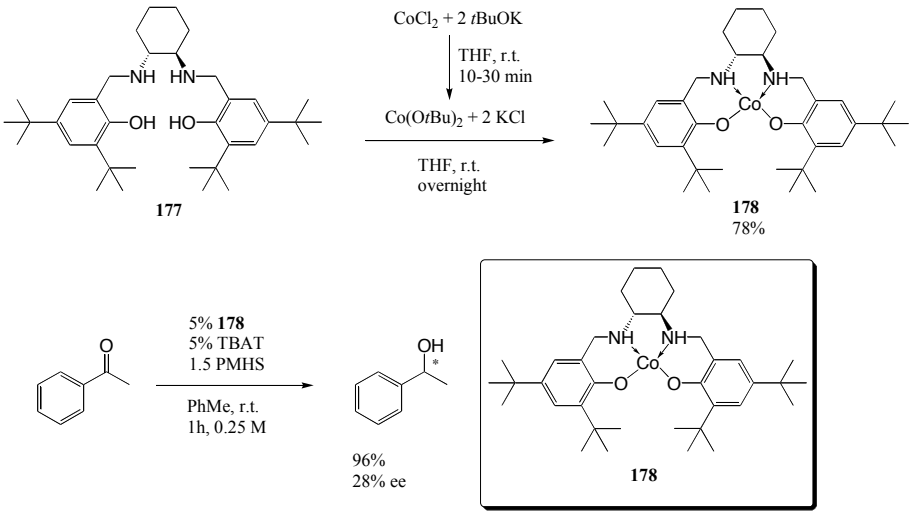

Scheme 101: Synthesis and evaluation of a reduced salenol based precatalyst.

We also decided to prepare the corresponding complexes on the new sulfonamide based ligands. For this purpose, the reduction of the diimine **147** was carried out with $NaBH_3CN$ in glacial acetic acid. With the reduced product **179**, the corresponding complex **180** could not be synthesised (**Scheme 102**). Indeed, in this case, the addition of the ligand to the cobalt (II) *tert*-butoxide solution led to a grey solution whereas the cobalt (II) complexes presented a characteristic red color. The standard work-up gave a

blue powder, which proved to contain the free ligand according to an analysis by mass spectrometry.

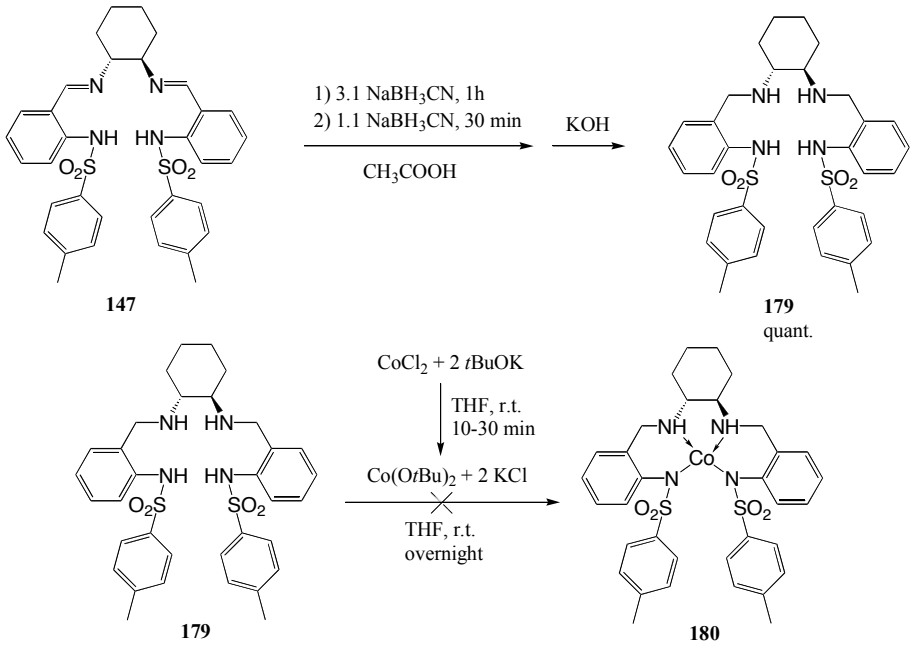

Scheme 102: Reduction of the diimine into the corresponding diamine and attempt of synthesis of the corresponding cobalt complex.

We decided next to introduce some alkyl groups on the reduced amine ligand **177**. Starting from the diamine **179**, a reductive amination affords the tertiary diamine **181** in a 75% yield. Formation of the desired complex **182** under the usual condition, *i.e.* with two equivalents of potassium *tert*-butoxide relative to cobalt chloride, did not meet the expected

success, unfortunately. The steric hindrance generated by the tertiary amines may account for the lack of reactivity.

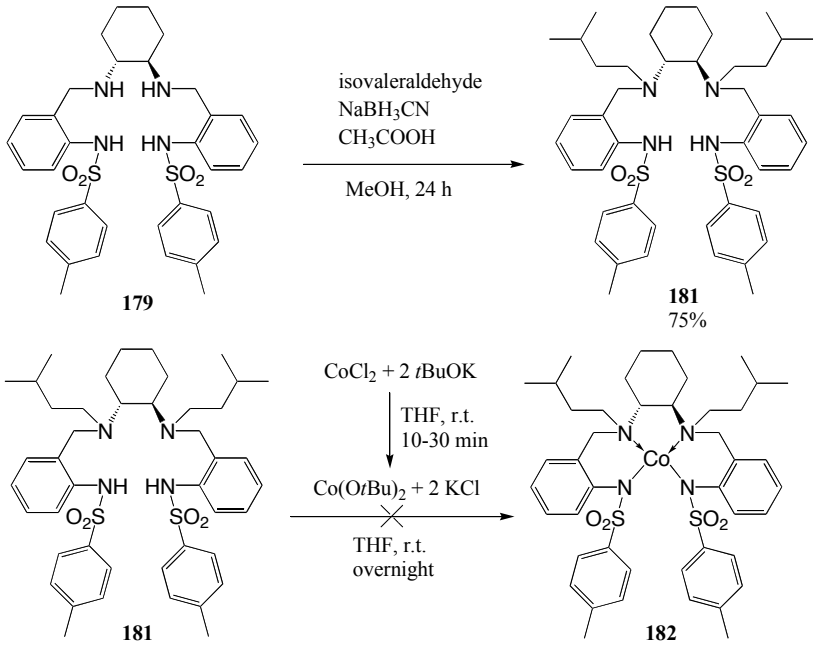

Scheme 103: Formation of a tertiary diamine-bis-sulfonamide and attempt of synthesis of the cobalt complex.

The characterisation of the ligand **181** by ^{13}C NMR in $CDCl_3$ at room temperature was not possible, because some aliphatic signals were missing (**Spectrum 5**). The rotamers number of the alkyl chain lead to multiple signals that were too weak to be detected. However, the product could be characterised at 90°C in d_8-toluene. Concerning ^{1}H NMR, broad signals were obtained, even at high temperatures.

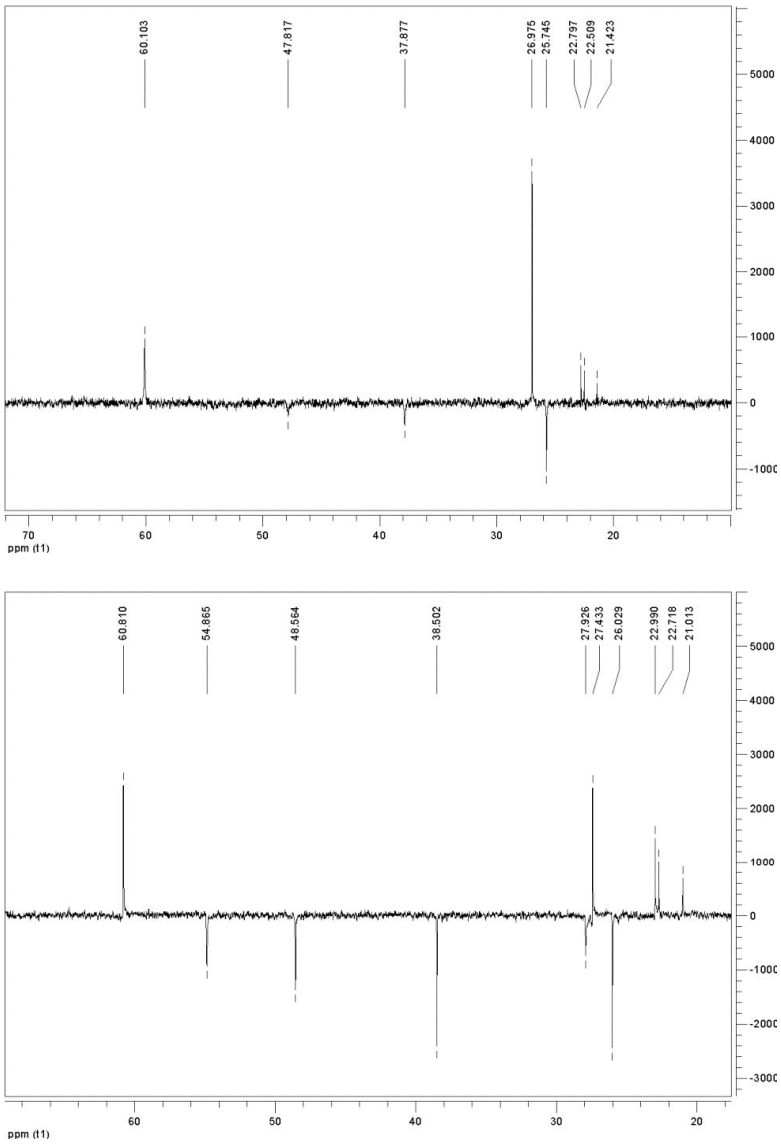

Spectrum 5: Spectra of **181** at room temperature in $CDCl_3$ (top) and at 90°C in d_8-toluene (bottom).

The search for better conditions to form the complex was also performed with Zn acetate as metallic precursor since the desired product is diamagnetic. This allows to check reaction completion by ^{1}H NMR. For this purpose, the reaction mixture was heated for 2 h but the reactant could be still detected by NMR. Attempts of recrystallisation of the complex were performed. The same difficulty was encountered by Professor Riant with the following model ligand **183**, when trying to form the corresponding zinc and cobalt complexes, **184** and **185** (**Scheme 104**).

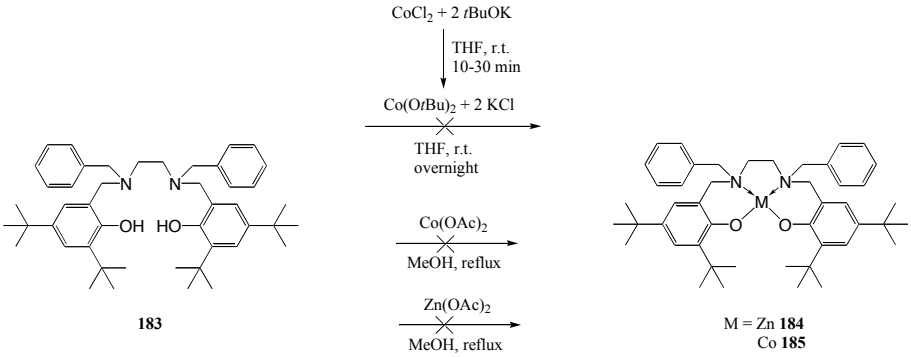

Scheme 104: Attempt of synthesis of a cobalt complex with tertiary amines.

3.12. Mechanistic considerations

From the performed experiments some trends might be interesting for the proposition of a catalytic cycle and a transition state. From the preliminary results, a cobalt ate hydride species was proposed to be formed by reaction between the cobalt complex, the silicate TBAT and PMHS. The activator study supports this hypothesis because a fluoride source such as TBAF did not allow to form the proposed intermediate and catalysed the ketone reduction without enantioselectivity.

In the literature, it was shown that the chiral ammonium salts such as **186** (derived from cinchona alkaloids) and PMHS allowed for example the reduction of acetophenone with 28% of enantiomeric excess and 98% of conversion in less than 1 min at room temperature (**Scheme 105**).[146] This high reaction rate was attributed to a "zipper" mechanism where a nucleophile, such as a fluoride or an alkoxide, reacted with PMHS to form a silicate (**Figure 29**). After reduction of substrate, the nucleophile is then transferred to another silicium atom from the PMHS. This process of nucleophile transfer did not take place with monomeric silane because the nucleophile transfer is intramolecular.

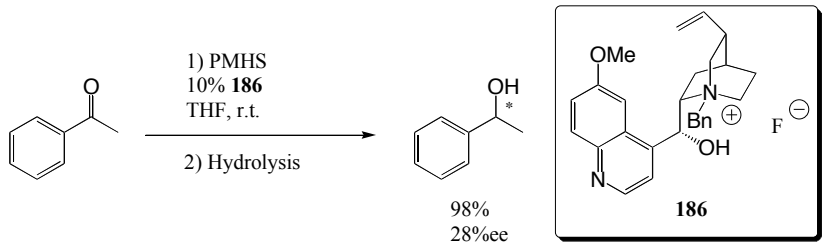

Scheme 105: Hydrosilylation of acetophenone catalysed by a chiral ammonium fluoride.

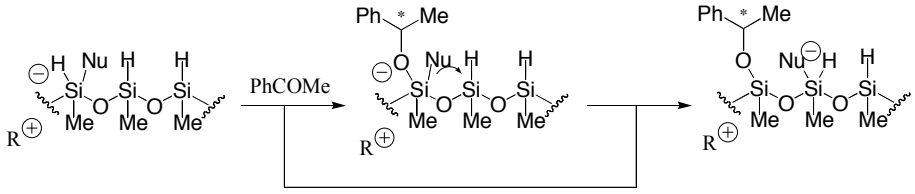

Figure 29: Proposed "zipper" mechanism.

In our case such a zipper mechanism did not occur because the acetophenone is reduced with 99% conversion with $(EtO)_2MeSiH$ as reducing agent. However, the difference in reactivity with $EtOMe_2SiH$ could not be explained and studies with an IR probe might be useful for this purpose as it could allow the kinetics to be measured with accuracy.

For the reasons exposed previously, a catalytic cycle can be proposed with a cobalt ate hydride as the nucleophilic active species (**Scheme 106**). It can be formed first by reaction between TBAT and PMHS to generate a pentavalent silicate with an activated Si-H bond, which then

reacts with cobalt complex and give thus rise to the cobalt ate hydride. After a nucleophilic attack to a carbonyl compound, the initial cobalt complex is formed together with a tetrabutyl ammonium alcoholate. The latter, as TBAT, activates the Si-H bond of PMHS. This allows to transfer the alcoholate onto the silylating agent, regenerates the cobalt ate hydride species and closes thus the catalytic cycle.

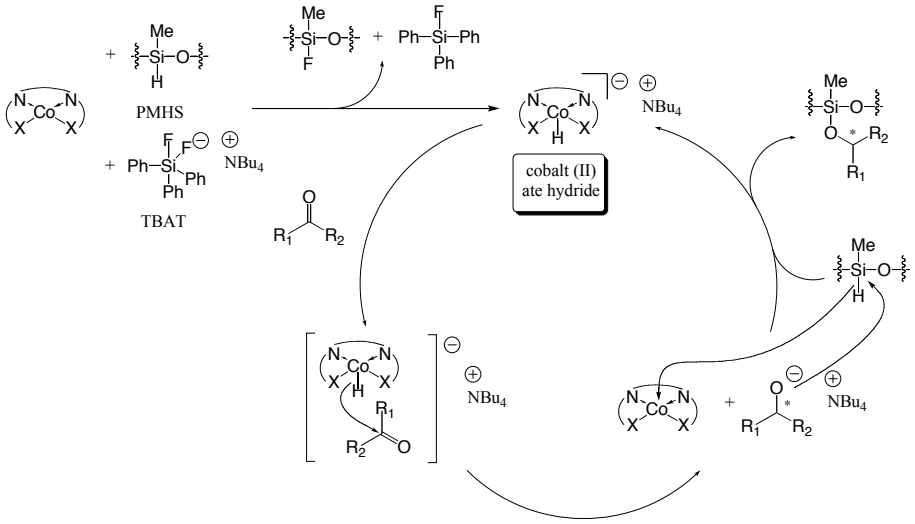

Scheme 106: Proposed catalytic cycle for the cobalt catalysed hydrosilylation of ketones.

From the variations of the sulfonamide group in the precatalysts, it was shown that the electronic effect seems more important than the steric one. It suggests that this group points out of the metallic cobalt center in the enantiodetermining step. Therefore, a possible geometry of the metal in the

transition state is supposed to involve a bipyramidal trigonal cobalt ate complex (**Figure 30**). Concerning the electronic effect, no trend could be formulated.

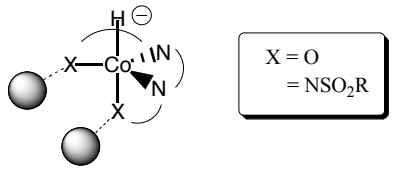

Figure 30: Proposed transition state for the anionic cobalt ate hydride.

3.13. Conclusions

A new efficient catalytic system was developed. To reach this result, the researches started from the encouraging activity and selectivity with the Jacobsen salen cobalt complex **106** activated with TBAT for the hydrosilylation of acetophenone with PMHS. A screening of various precatalysts (salenol and derivatives, oxazoline phenolate) with different transition metals (copper, aluminum, chromium, zinc and nickel) did not lead to better results. Further studies with the Jacobsen salen cobalt complex **106** investigated the activating agents, solvents, additives, temperature effects, catalytic loading, concentration, *in situ* formation and counter ion effect. The use of a bifunctional system pointed the detrimental effect of salts towards our catalytic system. A breakthrough came with cobalt based precatalyst having a diimine-bis-sulfonamide ligand. After establishment of

an efficient procedure to synthesise various cobalt complexes with this ligand type, they were prepared and evaluated with different substrates. Best results were obtained for the reduction of tetralone with 1% of the cobalt complex **164** activated with an equimolar amount of TBAT. A conversion of 95%, an enantiomeric excess of 82% and a TON of 95 were obtained at room temperature. A chemoselectivity study showed that 1,2 reduction is favored over a 1,4-one. Mechanistic investigation suggested that an anionic cobalt ate complex may be the catalytic active species. Another class of camphor based tetradentate ligand was synthesised but the formed corresponding complexes could not be isolated.

Summary of results and perspectives

Summary of results

The objective of the researches was to get an efficient access to enantioenriched alcohols. For this purpose, *N*, *S* precatalysts as well as a new catalytic system were developed. Their catalytic properties will be pointed out:

1. At first, new *N*, *S* ligands and zinc complexes were prepared by diastereoselective ortholithiation of the ferrocenyl oxazoline **54** with a *tert*-butyl group followed by reaction of sulfur to get the corresponding lithium ferrocenyl thiolate. From this intermediate, addition of zinc chloride or iodine yielded the corresponding zinc complex **58** and disulfide **55**, respectively. The reaction of this disulfide with diethylzinc lead to the thioether **56**. In case of the ferrocenyl oxazoline **53** with an *iso*-propyl group, the corresponding *N*, *S* zinc complex **61** was obtained in low yield because of a possible side reaction between sulfur and TMEDA. In addition to this, a new ferrocenyl thiolate **81** was synthesised starting from the ferrocenyl diaryl carbinol **79** by sequential addition of tetrafluoroboric acid and thioacetic acid.

2. The precatalysts **55**, **56** and **58** were evaluated in the diethylzinc addition to benzaldehyde, a reaction used only as model. Compared to other catalysts from the literature, our results are rather modest. With the disulfide as precatalyst **55**, the thioether **56** is generated *in situ* and was catalytically active with low enantioinduction. Therefore, the next studies were only oriented towards the use of *N*, *S* zinc complexes. Application to the vinylzinc addition to aldehydes was not explored because of encountered purification problems of the product when following the Oppolzer procedure modified by Dahmen and Bräse.

3. Access to secondary alcohols by ketones reduction was then studied. The addition of an equimolar amount of diethylzinc to the zinc complex **58** followed by thermal ß-elimination formed a chiral zinc hydride that catalysed the hydrosilylation of acetophenone. Following optimisation of the reaction conditions (solvents, concentration, catalytic loading, temperature Et_2Zn / **58** ratio), different substrates were reduced with the developed procedure. Generally, conversions were quantitative within hours (2-5 h) and enantioselectivities were poor to modest (9-55% ee). The most interesting point is that a dialkyl ketone could be reduced with a high conversion and a modest enantioselectivity (44% ee) because this kind of substrates generally gave low conversions as well as enantioselectivities in hydrosilylation. Besides these results obtained with the complex **58**, the other new precatalysts (**59**, **60**, **61** and **81**) gave only very low enantioselectivities.

3. The search for a more active catalyst, with salen and salenol (derivatives) as ligands lead to a new catalytic system. Its development started by determining a procedure leading to the formation of a metal hydride. This

was first achieved by mixing the Jacobsen salen cobalt complex with TBAT and PMHS. Then various complexes with different transition metal and ligand type were prepared and evaluated in the model reaction of acetophenone reduction. The Jacobsen salen cobalt complex presented the best results (97% and 37% ee). No improvement came from the variation of the reaction conditions but the catalytic loading could be decreased to 0.2% with the same enantioselectivity and a TON of 580 [h^{-1}].

4. As this catalytic system presented an impressive reactivity, the enantioselectivity was though to be improved using the Kozlowsky bifunctional ligand. It presents the salen structure with two side arms that could coordinate a Lewis base, such as an alkaline, which would orientate the electrophile approach. This did not improve at all the selectivity.

5. The impressive activity of the Jacobsen salen cobalt complex as precatalyst incited further modifications of the ligand. The breakthrough came with diimine bis-sulfonamide cobalt complexes. Various precatalysts were prepared after establishment of an efficient synthetic access. Their evaluation in catalytic hydrosilylation showed that the complex **164** was the most efficient for the reduction of tetralone (TOF: 95 [h^{-1}], 82% ee).

6. An attempt to synthesise cobalt complexes derived from camphor was carried out. The chiral information is no more located in the diimine bridge but between the nitrogen and oxygen atoms. For this, formylcamphor was prepared and condensed with diamines. No cobalt complexes could be isolated from the diimines.

Reduction of the diamine and reductive amination of **147** with isovaleraldehyde furnished the corresponding secondary diamine **180** and tertiary diamine **181**. No cobalt complex was formed from these ligands.

7. Mechanistic investigation of the cobalt catalytic system involved the use of different silanes to determine whether the hydride was delivered from the other tested reducing agents or from the hypothetical cobalt ate hydride. No obvious trend could be withdrawn and other silanes should therefore be investigated.

Perspectives

Concerning the zinc based system, a more modular catalyst type could involve a flexible and pro-atropoisomeric zinc dithiolate with a chiral diamine. Alternatively, a chiral dithiolate with an achiral diamine could also be used (**Figure 31**). This type of association has been studied with chiral diamines and achiral diols, but long reaction times are required (generally one or two days). Addition of an activator as a borate or silicate, that can potentially form a more reactive zinc ate hydride complex, may improve the activity. This catalytic system presents two possible modulations for the ligands and eventually a third one if an activating agent is added. In this way, various catalysts can be generated by mixing the different components rather than going to the bench. The use of dithiols rather than diols may lead to better enantioselectivities than those observed by Mikami since the transfer to the ligand to the silylating agent should not take place. This may

lead to the rapid identification of an efficient catalyst by high throughput screening.

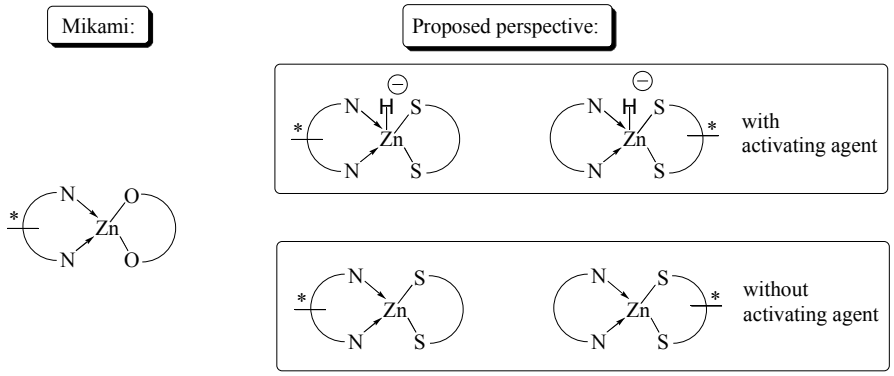

Figure 31: Proposed catalyst type for the zinc catalysed hydrosilylation of prochiral ketones

For our new efficient catalytic system involving a chiral cobalt complex activated by TBAT, further mechanistic studies by mass spectrometry may be useful to show the formation of the cobalt ate hydride and deuteride (**Figure 32**). In addition to this, an eventual reduction of the ligand may be shown with an IR probe. Lastly, other nucleophiles than hydride, such as vinyl, allyl or cyanide, can be studied.

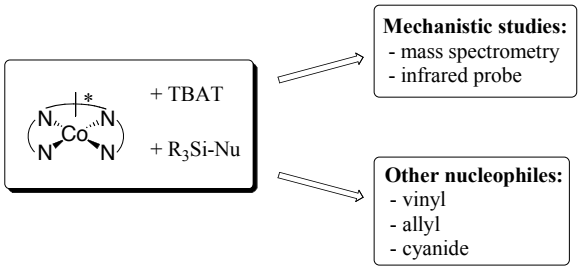

Figure 32: Proposed perspectives for our new catalytic system.

Experimental part

Generalities

Reactions employing air or water sensitive compounds were carried out under argon. Their transfer was performed with argon degassed syringes or cannula. The glassware was dried prior to use in a drying oven at 140°C and flushed three times with vacuum-argon cycle.

Concentration under reduced pressure implied first solvent removal with a rotary evaporator and / or with high vacuum pump until constant weight.

Solvents for reactions were of analytical grade. For reactions requiring anhydrous conditions, the solvents were purified by distillation: dichloromethane over calcium hydride, diethylether and tetrahydrofuran over sodium / benzophenone ketyl radical, toluene over sodium. For reactions with only air sensitive compounds, solvents were degassed with argon for one hour.

Benzaldehyde and acetophenone were distilled with a Kugelrohr oven and stored under argon atmosphere.

^{1}H and broadband decoupled ^{13}C NMR spectra were recorded on a Varian Gemini 200 BB (200 and 50 MHz), Varian Gemini 300 (300 and 75

MHz), Bruker 300 Avance II (300 and 75 MHz) or Bruker 500 Avance (500 and 125 MHz). Chemical shifts are given in ppm relative to the internal reference. Unless specified, spectra were recorded at room temperature. ^{19}F spectra were recorded on a Bruker 300 Avance II (282 MHz) with trichlorofluoromethane as reference.

Mass spectra were recorded on a Finnigan-Mat TSQ-7000 or a Finnigan-Mat LCQ apparatus in the laboratory of Professor Habib Jiwan (Université Catholique de Louvain). Values are reported in atomic mass unit per elemental charge m/z. The intensities are given in % relative to the molecular peak of the major isotope.

Chiral GC analyses were performed on a CE instrument HRGC 5300 with a Merck-Hitachi D-2500 Chromato Integrator on a Chirasil Dex (25 m x 0.25 mm – 0.25 μm) column.

IR-Spectra were recorded on a Biorad FTS-135 or a Shimadzu FTIR 8400S as KBr pellets or neat and strong absorption bands are given (in cm^{-1}).

Elemental analyses were performed in the laboratory of Dr. Stone at University College, London. The indicated values are given in percentages.

Optical rotation values were measured on a AA-10 Automatic Polarimeter. Optical path length: d=10 cm, concentration in g/100 mL. Measures were taken at room temperature with a 589 nm wavelength light (D line of a Na-lamp).

Thin layer chromatographic analyses were performed on Merck 60 F_{254} silica gel plates (coated on aluminum) and spots were visualised using

UV light. Flash chromatography separations were performed using Merck 60 40-63 μm silica.

Catalytic tests

Diethylzinc addition to benzaldehyde

In a Schlenk tube under argon, the precatalyst was dissolved in 4 mL of toluene. At 0°C, Et_2Zn (0.155 mL, 1.5 mmol, 1.5 eq) was added dropwise. After 10 min of stirring, benzaldehyde (0.110 mL, 1 mmol, 1 eq) and dodecane (0.114 mL, 0.5 mmol, 0.5 eq) were added and the reaction mixture stirred for 15 h. A sample was then hydrolysed (1M HCl), filtered over silica gel and analysed by chiral GC (90°C, 5 min; 90 to 125°C, 4°C/min, 125°C).

Zinc catalysed hydrosilylation of acetophenone

In a Schlenk tube under argon, diethylzinc (0.05 mmol, 1 mL of a 0.05 M solution, 0.05 eq) was added in a equimolar quantity to the zinc complex (0.05 mmol, 0.05 eq) in 3 mL of solvent, then PMHS (0.065 mL, 1.1 mmol) was added. The Schlenk tube was placed in a heated oil bath (60°C) for 10 min to form the zinc hydride. After this, acetophenone (0.120 mL, 1 mmol) was added at the desired temperature. Conversion and ee were followed by chiral GC (isotherm at 120°C).

Cobalt catalysed hydrosilylation of ketones

At room temperature under argon, TBAT (28 mg, 0.05 mmol, 0.05 eq) and a chiral cobalt complex (0.05 mmol, 0.05 eq) were dissolved in freshly distilled toluene (4 mL). After stirring for 15 min, the substrate (1 mmol) and PMHS (0.1 mL, 1.5 mmol, 1.5 eq) were added. After one hour of reaction, a sample was hydrolysed in a KOH solution in methanol, filtrated over a small plug of silica gel and analysed by chiral GC.

α-Tetralone (120 to 200°C, 1°C/min) R_t: 36 and 37 min; cyclohexenone (isotherm at 105°C) R_t: 7 and 6 min.

Synthesis of the precatalysts

Synthesis of ferrocene carboxylic acid 46

a) From ferrocene carboxaldehyde **45**:

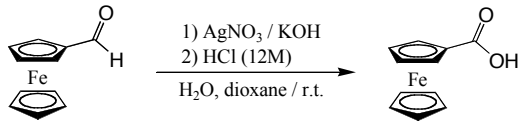

90%

In a round bottom flask fitted with a dropping funnel, silver nitrate (27.2 g, 160 mmol, 2 eq) was dissolved in 160 mL water. Potassium hydroxide (18.0 g, 320 mmol, 4 eq), dissolved in 160 mL water, was added dropwise.

Ferrocene carboxaldehyde (17.5 g 80 mmol, 1 eq), dissolved in 160 mL dioxane, was added and the reaction mixture was stirred for 19 h.

The reaction was followed by TLC (cyclohexane / ethyl acetate 1:1): R_f=0,4.2 (ferrocene carboxylic acid) and R_f=0.83 (ferrocene carboxaldehyde). The reaction mixture was filtered over celite and rinsed with dioxane. The filtrate was acidified with hydrochloric acid (32 mL, 12 M) and the precipitated orange product was washed with water until the filtrate pH was neutral. The product was dried in a dessicator.

Yield: 16.6 g, 90%

MP: 192 °C (dec.)

IR (KBr): 1654 (C=O), 1475, 1283, 1159, 834.

^{1}H NMR (300 MHz): 4.26 (5H, s, C_5H_5), 4.47 (2H, s, CH-ß), 4.87 (2H, s, CH-α).

^{13}C NMR (50 MHz): 70.3 (C-COOH), 70.8 (C_5H_5), 71.2 (CH), 72.6 (CH), 178,2 (C=O).

MS (CI): 231 (100, $[M+1]^+$), 213 (58, $[M+1-H_2O]^+$.

RN: 1271-42-7

Ref. operating procedure[77]

spectral data[77]

b) From ferrocene **47**:

In a Schlenk tube under argon, ferrocene (3.0 g, 16.1 mmol, 1 eq) and potassium *tert*-butoxide (0.23 g, 2.0 mmol, 0.13 eq) were dissolved in THF (70 mL). At -78°C, *tert*-BuLi (10.75 mL, 1.5M, 16.1 mmol) was added dropwise. After 10 to 15 min of stirring at this temperature, carbon dioxide was bubbled in the reaction mixture until a yellow precipitate formed. When the mixture reached room temperature, the ferrocene carboxylic acid was formed quantitatively by addition of HCl. The product was purified by filtration over silica gel (dichloromethane) if necessary.

Ref. operating procedure for the lithiation[78]

Synthesis of (L)-*tert*-leucinol 49:

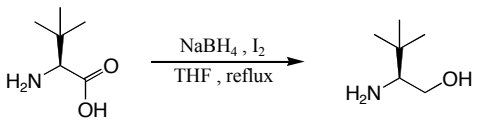

81%

In a 500 mL three-neck flask equipped with a dropping funnel and a reflux condenser, sodium borohydride (7.0 g, 182 mmol, 2.4 eq) was dissolved in 200 mL THF. (L)-*tert*-leucinol (10 g, 75.5 mmol, 1 eq) was then added in one portion. The flask was cooled down in an ice bath. The dropping funnel was charged with iodine (19.2g, 75.5 mmol, 1 eq) in 25 mL THF and the solution was added dropwise over 2 h. Gas evolution took place and the obtained milky solution was refluxed for 39 h. The dropping funnel was

charged with methanol (18.6 mL), which was added dropwise and gas evolution was observed. When the white solid dissolved, the solution was evaporated under reduced pressure giving a white gum that was dissolved in 150 mL KOH (20%) and stirred overnight. The white solution was extracted with dichloromethane (3x180 mL, 1x80 mL). The combined organic phases were dried over Na_2SO_4, filtered over a frit and concentrated under vacuum. The resulting brownish liquid was purified by Kugelrohr distillation to get a colorless liquid solidifying at room temperature.

Yield: 7.2 g, 81%

MP: 110 °C at 3 mbar

^{1}H NMR (200 MHz): 0.90 (9H, s, $C(CH_3)_3$), 1.72 (3H, NH_2 and OH), 2.51 (dd, 1H, J=3.9 Hz, J=10.3 Hz, C<u>H</u>-NH_2), 3.20 (1H, t, J=10.1 Hz, C<u>H_2</u>-OH), 3.71 (1H, dd, J=4 Hz, J=9.6 Hz, C<u>H_2</u>-OH).

RN: 112245-13-3

Ref. operating procedure[79]

Synthesis of the amide 52:

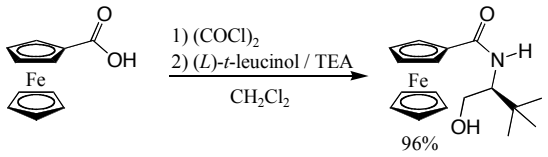

To a suspension of ferrocene carboxylic acid (1.0 g, 4.5 mmol, 1 eq) in dichloromethane (15 mL) under argon was added oxalyl chloride (0.8 mL, 9 mmol, 2 eq) at room temperature. Gas evolution was observed with dissolution of the acid to give a deep red solution after 5 min. The reaction mixture was stirred for 20 minutes. Evaporation to dryness afforded the acid chloride as a solid, which was dissolved in dichloromethane (10 mL) under argon. A solution of (*S*)-(+)-*t*-leucinol (629 mg, 5.4 mmol, 1.2 eq) and triethylamine (1.3 mL, 9 mmol) in dichloromethane (7 mL) was added at room temperature. After stirring overnight, the reaction mixture was washed with water. The organic phase was dried over Na_2SO_4, filtered and evaporated under reduced pressure. The crude amide, obtained as a yellow solid, was pure enough to be used further without purification.

Yield: 1.4 g, 96%

MP: 173 °C

IR (KBr): 3239 (OH), 2968, 1614 (C=O), 1554, 1309, 1056.

^{1}H NMR (500 MHz): 1.03 (9H, s, $C(CH_3)_3$), 3.61 (dd, 1H, *J*=8Hz, *J*=11Hz, $C\underline{H}_2$-OH), 3.91 (dd, 1H, *J*=3.5Hz, *J*=11.5Hz, $C\underline{H}_2$-OH), 3.98 (ddd, 1H,

J=3.5Hz, *J*=8Hz, *J*=11.5Hz, C<u>H</u>-NH_2), 4.22 (s, 5H, C_5H_5), 4.33-4.36 (m, 2H, C=CH of Cp in β), 4.66-4.67, 4.70-4.71 (m, 2H, C=CH of Cp in α), 5.95 (d, 1H, *J*=4Hz, NH).

^{13}C NMR (125 MHz): 27.1 (CH_3), 33.6 (<u>C</u>$(CH_3)_3$, 59.4 (<u>C</u>H-NH_2), 63.2 (<u>C</u>H_2-OH), 67.8 and 68.4 (C=<u>C</u>H of Cp in α), 69.7 (C_5H_5), 70.4 et 70.5 (C=<u>C</u>H of Cp in β), 75.9 (<u>C</u>-CO), 171.8 (CO).

MS (APCI): 330 (100, $[M+H]^+$), 312 (74, $[M+1-H_2O]^+$), 299 (16, $[M+1-CH_2OH]^+$), 282 (66).

RN: 174741-44-7

Ref. operating procedure[71]

spectral data[72]

Synthesis of the amide with iPr 51

Procedure as described above.

Yield: 4.21 g, 96%

MP: 110 °C

IR (neat): 3335, 2961, 1626, 1529, 820.

^{1}H NMR (500 MHz): 1.03 (d, *J*=3.5 Hz, 3H, CH(C<u>H</u>$_3$)$_2$), 1.04 (d, *J*=3.5 Hz, 3H, CH(C<u>H</u>$_3$)$_2$), 1.97-2.04 (m, 1H, C<u>H</u>$(CH_3)_2$), 3.48 (s, 1H, CH_2-O<u>H</u>), 3.72-3.80 (m, 2H, C<u>H</u>$_2$-OH), 3.86-3.87 (m, 1H, C<u>H</u>-NH), 4.22 (s, 5H, C_5H_5), 4.35

(s, 2H, C=CH of Cp in β), 4.69 (s, 1H, C=CH of Cp in α), 4.73 (s, 1H, C=CH of Cp in α), 6.12 (d, 1H, *J*=7.5Hz, NH).

^{13}C NMR (125 MHz): 19.0 (CH_3), 19.7 (CH_3), 29.0 ($\underline{C}H(CH_3)_2$, 57.0 ($\underline{C}H$-NH), 63.9 ($\underline{C}H_2$-OH), 67.9 and 68.4 (C=$\underline{C}$H of Cp in α), 69.7 (C_5H_5), 70.5 (C=$\underline{C}$H of Cp in β), 75.9 ($\underline{C}$-CO), 171.3 (CO).

RN: 174741-43-6

Ref. spectral data[72]

Synthesis of the oxazoline with *tert*-Bu 54

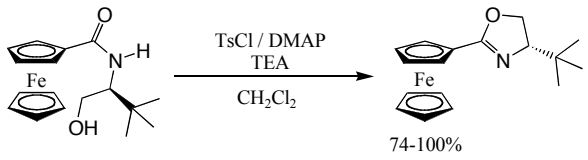

74-100%

In a round bottom flask, the amide (3.82 g, 11.6 mmol, 1 eq) was dissolved in dichloromethane (40mL) and DMAP (142 mg, 1.2 mmol, 0.1 eq) followed by tosyl chloride (2.7g, 14 mmol, 1.2 eq) were added. Triethylamine (4.9 mL, 34.9 mmol, 3 eq) was then introduced. The orange solution became dark brown after one night. Analysis of the reaction mixture by TLC (cyclohexane / ethyl acetate 1:1) showed complete consumption of the reagent: amide R_f=0.25 and oxazoline R_f=0.75.

After washing with brine and water, the organic layer was dried over Na_2SO_4 and the solvent removed under reduced atmosphere. The crude product was purified by flash chromatography (cyclohexane / ethyl acetate 9:1).

Yield: 2.7 g, 74-100%

MP: 142 °C

IR (KBr): 2957, 1664 (C=N), 1117, 970.

^{1}H NMR (500 MHz): 0.96 (s, 9H, $C(CH_3)_3$), 3.90 (dd, 1H, *J*=7.5Hz, *J*=9.5Hz,C<u>H</u>-CH_2), 4.16 (pseudo t, 1H, *J*=8.0 Hz, CH-C<u>H</u>$_2$), 4.20 (s, 5H, Cp), 4.23-4.27 (pseudo t, 1H, CH-C<u>H</u>$_2$), 4.33 (b s, 2H, Cp substituted), 4.72 (b s, 1H, Cp substituted), 4.79 (b s, 1H, Cp substituted).

^{13}C NMR (125 MHz): 25.9 ($C(\underline{C}H_3)_3$), 33.6 (($\underline{C}(CH_3)_3$), 68.4 (CH-<u>C</u>H_2), 60.0 (Cp substituted), 69.5 (Cp), 70.1 (Cp substituted), 76.0 (<u>C</u>H-CH_2).

MS (APCI): 312 (100, $[M+1]^+$), 279 (10).

RN: 162157-02-0

Ref. operating procedure[72]

spectral data[72]

Synthesis of the oxazoline with *iso*-Pr 53

Same procedure as described above.

Yield: 4.12g, 88%

MP: 72 °C

IR (neat): 1655 (CN), 1261, 1107, 752.

^{1}H NMR (500 MHz): 0.93 (d, 3H, $CH(C\underline{H}_3)_2$), 1.00 (d, 3H, $CH(C\underline{H}_3)_2$), 0.93 (d, 3H, $CH(C\underline{H}_3)_2$), 1.86 (oct, 1H, *J*=7Hz, <u>C</u>$H(CH_3)_2$), 3.96-4.01 (m, 1H,

C<u>H</u>-CH_2), 4.06 (t, 1H, CH-C<u>H_2</u>), 4.19 (s, 5H, Cp), 4.27-4.30 (m, 2H, CH-C<u>H_2</u>), 4.32-4.33 (m, 1H, Cp substituted), 4.73-4-73 (m, 1H, Cp substituted), 4.76-4-76 (m, 1H, Cp substituted).

^{13}C NMR (125 MHz): 17.8 (CH(<u>C</u>H_3)$_2$), 18.9 (CH(<u>C</u>H_3)$_2$), 32.3 ((<u>C</u>H(CH_3)$_2$), 68.9 (Cp substituted), 69.3 (CH-<u>C</u>H_2), 69.5 (Cp), 70.1 (Cp substituted), 70.5 (<u>C</u>-CNO), 72.2 (<u>C</u>H-CH_2), 165.6 (CN).

MS (APCI):

RN: 162157-03-1

Ref. spectral data[72]

Synthesis of the disulfide 55:

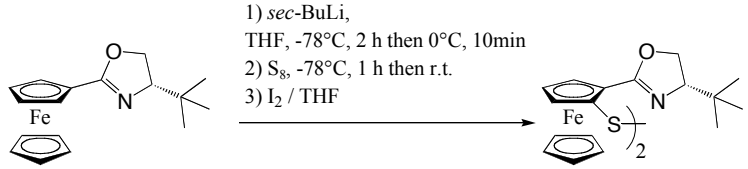

In a Schlenk tube under argon, the ferrocenyloxazoline (310 mg, 1 mmol, 1 eq) was dissolved in THF (17 mL). At -78°C, *sec*-butyl lithium (0.92 mL of a 1.3 M solution, 1.22 mmol, 1.2 eq) was added dropwise. After 1 h stirring at -78°C, the Schlenk tube was place in an ice bath for 5 min. The reaction was hydrolyzed with an aqueous solution of $KHCO_3$ (5%, 10 mL) and an iodine solution (130 mg, 0.5 mmol) in THF was added. After ether addition, the organic layer is separated from the aqueous one, washed with brine and water and dried over $MgSO_4$. A TLC (ethyl acetate / cyclohexane 9:1) of the crude product revealed mainly the disulfide (R_f=0.69) and some traces of

unreacted starting material (R_f=0.77). The crude product was purified by flash chromatography (ethyl acetate / cyclohexane 9:1).

Yield: 0.19 g, 57%

MP: 182 °C

IR (KBr): 2956, 1659 (C=O), 1145, 981.

^{1}H NMR (300 MHz): 1.02 (s, 9H, $C(CH_3)_3$), 3.94-3.99 and 4.11-4.31 (m, 4H, C<u>H</u>-CH_2 and Cp substituted), 4.17 (s, 5H, Cp substituted), 4.56-4.58 (m, 1H, Cp substituted), 4.72-4.73 (m, 1H, Cp substituted).

^{13}C NMR (125 MHz): 26.4 (CH_3), 34.2 (<u>C</u>$(CH_3)_3$), 68.7 (CH-<u>C</u>H_2), 69.8 (Cp substituted), 71.5 (<u>C</u>H-CH_2), 71.6 (Cp), 73.1 (<u>C</u>-CNO), 74.7 (Cp substituted), 76.8 (Cp substituted), 86.0 (C-S), 164.3 (CNO).

MS (APCI): 685 (100, $[M+H]^+$), 279 (86).

EA: Calculated: C, 59.66; H, 5.89; N, 4.09

Found: C, 59.21; H, 5.89; N, 3.94.

Ref. operating procedure for the oxidation[80]

Synthesis of the tioether 56:

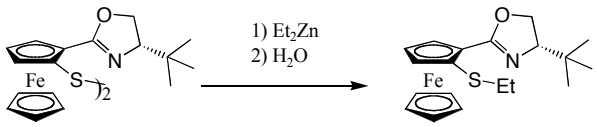

40%

In a Schlenk tube under argon, diethylzinc (4 mL of a 1M solution, 4 mmol, 4 eq) was added to the disulfide (685 mg, 1 mmol, 1 eq.) in toluene (10 mL). The reaction mixture was hydrolysed with 10 mL of water after 3 h of stirring. The organic phase was separated form the aqueous one and the solvent was removed under reduced pressure. The crude product was purified by flash chromatography (ethyl acetate / cyclohexane 9:1).

Yield: 150 mg, 40%.

^{1}H NMR (200 MHz): 0.99 (s, 9H, $(CH_3)_3$), 1.24 (t, 3H, *J*=7.4Hz, CH_2-$C\underline{H}_3$), 2.67-2.95 (m, 2H, $C\underline{H}_2$-CH_3), 3.87-3.97 (m, 1H, $C\underline{H}$-CH_2), 4.20 (s, 5H, Cp), 4.16-4.22 (m, 1H, CH-$C\underline{H}_2$), 4.25-4.31 (m, 2H, CH-$C\underline{H}_2$ et Cp substituted), 4.42-4.44 (m, 1H, Cp substituted), 4.70-4.72 (m, 1H, Cp substituted).

Synthesis of *N*, *S* zinc complex with *t*-Bu 58:

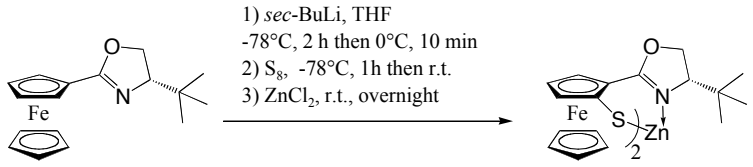

81%

In a Schlenk tube under argon, the ferrocenyloxazoline (310 mg, 1 mmol, 1 eq) was dissolved in THF (17 mL). At -78°C, *sec*-butyllithium (0.92 mL of a 1.3 M solution, 1.22 mmol, 1.2 eq) was added dropwise. After 1 h stirring at -78°C, the Schlenk tube was placed in an ice bath for 5 min. At -78°C, elemental sulfur (38 mg, 1.2 mmol, 1.2 eq) was added and the reaction mixture was stirred for at least 1 h before it was allowed to warm up to room temperature. A suspension of anhydrous zinc chloride (68 mg, 0.5 mmol, 0.5 eq) in THF (2 mL) was added at room temperature by cannula.

After one night of stirring, the solvent was evaporated and the product dissolved in dichloromethane. After washing with brine and water, the solvent was removed under reduced pressure. The crude product was purified by flash chromatography (1% methanol in dichloromethane: R_f=0.29).

Yield: 0.29 g, 81%

IR (KBr): 2956, 1606 (C=N), 1446, 1245.

^{1}H NMR (500 MHz): 0.99 (s, 9H, $C(CH_3)_3$), 3.25 (dd, 1H, *J*=5.8Hz, *J*=9.3Hz,C<u>H</u>-CH_2), 4.03 (pseudo t, 1H, *J*=9.3Hz, CH-C<u>H</u>$_2$), 4.16 (s, 5H, Cp); 4.27-4.31(m, 2H, CH-C<u>H</u>$_2$ and Cp substituted), 4.53 (m, 1H, Cp substituted), 4.69-4-70 (m, 1H, Cp substituted).

^{13}C NMR (125 MHz): 26.0 ($C(\underline{C}H_3)_3$), 33.6 (($\underline{C}(CH_3)_3$), 64.7 (<u>C</u>-CNO), 67.4 (Cp substituted), 68.6 (CH-<u>C</u>H_2), 71.5 (Cp), 74.3 (<u>C</u>H-CH_2), 75.0 (Cp substituted), 96.5 (C-S), 175.2 (CN).

MS (APCI): 845 (100, $[M+1]^+$).

$[\alpha]^{20}_D$= -317° (c = 0.7, CH_2Cl_2).

EA: Calculated: C, 54.46; H, 5.38; N, 3.74

Found: C, 52.67; H, 5.24; N, 3.42.

Synthesis of *N*, *Se* zinc complex 59

The *N*, *Se* zinc complex was synthesized as its *N*, *S* analog, i.e. with one equivalent of selenium. The crude product was purified by flash chromatography over silica gel (5% MeOH/CH_2Cl_2): desired product R_f=0.29 and ferrocene oxazoline R_f=0.15.

Yield: 0.23 g, 27%

^{1}H NMR (200 MHz): 0.96 (s, 9H, $C(CH_3)_3$), 2.66 (dd, 1H, *J*=3.5Hz, *J*=9.2Hz,C<u>H</u>-CH_2), 3.65 (pseudo t, 1H, *J*=9.2Hz, CH-C<u>H</u>$_2$), 4.14 (s, 5H, Cp); 4.20-4.34 (m, 2H, CH-C<u>H</u>$_2$ and Cp substituted), 4.54-4.56 (m, 1H, Cp substituted), 4.68-4.70 (m, 1H, Cp substituted).

MS (APCI): 845 (100, $[M+]^+$).

Synthesis of *N*, *Te* zinc complex 60:

The *N*, *Te* zinc complex was synthesized as its *N*, *S* analog, i.e. with one equivalent of tellurium. The crude product was purified by flash chromatography over silica gel (1% $MeOH/CH_2Cl_2$): desired product R_f=0.65 and ferrocene oxazoline R_f=0.12.

Yield: 0.14 g, 15%

^{1}H NMR (200 MHz): 1.03 (s, 9H, $C(CH_3)_3$), 2.75 (dd, 1H, *J*=2.9Hz, *J*=9.0Hz,C<u>H</u>-CH_2), 3.41 (pseudo t, 1H, *J*=8.9Hz, CH-C<u>H</u>$_2$), 4.10 (s, 5H, Cp); 4.12-4.19 (m, 1H, Cp substituted), 4.40 (pseudo t, 1H, *J*=2.5Hz, CH-C<u>H</u>$_2$), 4.62-4.64 (m, 1H, Cp substituted), 4.67-4.69 (m, 1H, Cp substituted).

MS (APCI): 943 (100, $[M+1]^+$).

Synthesis of the *N*, *S* zinc complex with an *i*-Pr 61:

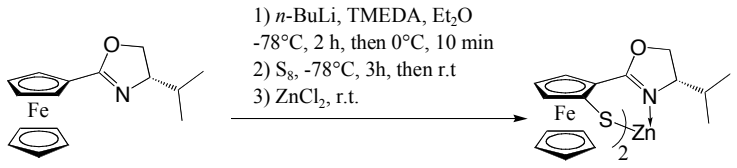

13%

Same procedure except that TMEDA (1.3 eq with respect to the ferrocene oxazoline) was added prior to the addition of *n*-BuLi.

Yield: 0.09 g, 13%

IR (neat): 2957, 1616, 1444, 986.

^{1}H NMR (500 MHz): 0.77 (d, *J*=6.5Hz, 3H, CH($C\underline{H}_3$)$_2$), 0.97(d, *J*=6.5Hz, 3H, CH($C\underline{H}_3$)$_2$), 2.29-2.41 (m, 1H, $\underline{C}$H(CH_3)$_2$), 3.89-4.01 (m, 1H, $C\underline{H}$-CH_2), 4.18 (s, 5H, Cp), 4.20-4.39 (m, 3H, CH-$C\underline{H}_2$ and Cp substituted), 4.56 (s, 1H, Cp substituted), 4.72 (s, 1H, Cp substituted)

^{13}C NMR (125 MHz): 14.5 (CH($\underline{C}H_3$)$_2$), 18.2 (CH($\underline{C}H_3$)$_2$), 28.2 (($\underline{C}$H(CH_3)$_2$),), 63.4 ($\underline{C}$-CNO), 66.8 (CH-$\underline{C}H_2$), 67.3 (Cp substituted), 68.7 (Cp), 69.7 (Cp substituted), 75.2 ($\underline{C}$H-CH_2), 96.2 (C-S), 174.3 (CN).

MS (APCI):

$[\alpha]^{20}_D$= -293° (c = 1.0, CH_2Cl_2).

EA: Calculated: C, 53.25; H, 5.03; N, 3.88

Found: C, 53.13; H, 5.04; N, 3.18.

Synthesis of (*S*)-*N*,*N*-dimethyl-1-phenethylamine 71:

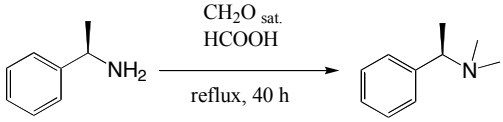

44% (Lit: 73%)

An aqueous solution of formaldehyde (37%, 28 mL, 370 mmol, 4.5 mL) and acetic acid (62 mL, 1,63 mmol, 19.7 eq) were added dropwise to (*S*)-methylbenzylamine (11 mL, 96% ee, 1 eq) at 0 °C. The solution is refluxed for 40 h, cooled with an ice bath and basified with NaOH pellets. The

product is extracted with dichloromethane. The combined organic layers were dried over Na_2SO_4. After removal of the solvent under reduced pressure, and distillation of the crude yellow oil, the product was obtained as colorless oil.

Yield: 5.45g, 44%

^{1}H NMR (200 MHz): 1.36 (d, 3H, *J*=6.7Hz, *CH-C$\underline{H}_3$), 2.19 (s, 6H, $N(CH_3)_2$), 3.23 (q, 1H, *CH, *J*=6.7 Hz), 7.22-7.31 (m, 5H, Ar).

RN: 17279-31-1

Ref. operating procedure[84]

Synthesis of the aromatic thiol 76:

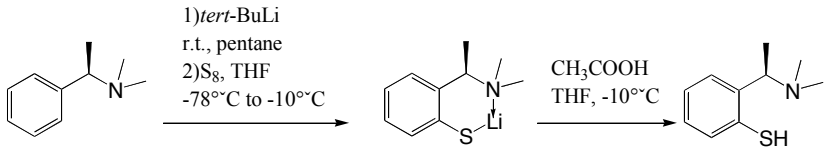

To a solution of (*S*)-*N*,*N*-dimethyl-1-phenethylamine (1.0 mL, 6 mmol, 1 eq) in hexane (12 mL) under argon was added dropwise *t*-butyllithium (4.6 mL of a 1.5 M solution, 6.9 mmol, 1.15 eq) at room temperature. After 24 h of stirring, elemental sulfur (221 mg, 6.9 mmol, 1.15 eq) was added at -78 °C and the reaction mixture stirred at this temperature before being allowed to reach room temperature. After 24 h of stirring, a solution of acetic acid (0.34

mL, 6 mmol, 1 eq) in THF (1 mL) was added at 0 °C. Evaporation of the solvent under reduced pressure afforded a yellow solid, which was purified by sublimation.

Yield: 6%

^{1}H NMR (200 MHz): 1.64 (d, 2H, CH-C<u>H</u>$_3$, J = 7.1 Hz), 2.58 (s, 6H, N(C<u>H</u>$_3$)$_2$), 4.46 (q, 1H, C<u>H</u>-CH$_3$, J = 7.0 Hz), 6.85-7.12, 7.56-7.61 (m, 4H, Ar).

RN: 357427-73-7

Ref. operating procedure[84]

Synthesis of the thioacetate 81:

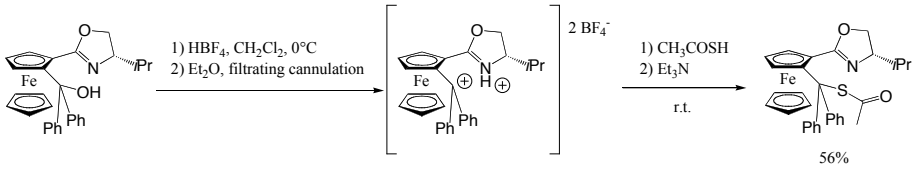

In a Schlenk tube under argon, the tertiary alcohol (1.01 g, 2.1 mmol, 1 eq) was dissolved in dichloromethane (20 mL). At 0°C, tetrafluoroboric acid in a 54% etheral solution (0.87 mL, 6.3 mmol, 3 eq) was added dropwise to the solution. Diethyl ether (3 mL) was then added. The solvents were removed by a cannula to eliminate the water. Following addition of dichloromethane (20 mL), thiolacetic acid (0.60 mL, 8.4 mmol, 4 eq) and an excess of triethylamine were successively added dropwise. After an aqueous work-up, the organic layers were dried over $MgSO_4$ and the solvents were removed

under reduced pressure. The product was purified by flash chromatography (ethyl acetate / cyclohexane 3 : 7; $R_f = 0.86$).

Yield: 0.64 g, 56%.

^{1}H NMR (250 MHz): 0.66 (d, 3H, J = 6.4 Hz, CH-C<u>H</u>$_3$), 0.81 (d, 3H, J = 6.7 Hz, CH-C<u>H</u>$_3$), 1.45 (m, 1H, C<u>H</u>-CH$_3$), 2.30 (CH_3CO), 3.48 (t, 1H, CH-C<u>H</u>$_2$), 3.62 (m, 1H, C<u>H</u>-CH$_2$), 3.76 (m, 1H, Cp substituted), 4.07 (t, 1H, CH-C<u>H</u>$_2$), 4.27 (m, 1H, Cp substituted), 4.49 (s, 5H, Cp), 4.72 (m, 1H, Cp substituted), 7.12-7.46 (m, 10H, CH Ar).

MS (APCI): 538 (1, $[M+H]^+$), 462 (100, $[M+H\text{-}SCOCH_3]^+$).

Synthesis of 108

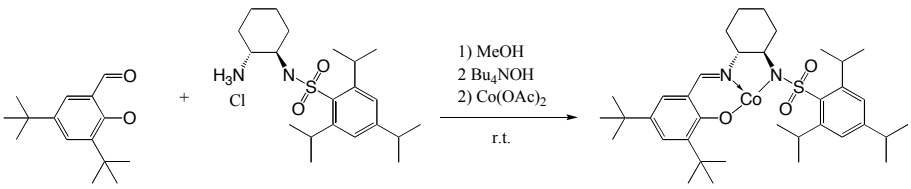

<20%

In a Schlenk tube under argon, methanol (5 mL) and tetrabutylammonium hydroxide (2.9 mmol, 3 mL of a 1 M solution in methanol, 2 eq) were successively added to the aldehyde (0.34 g, 1.45 mmol, 1 eq) and the ammonium chloride (0.30 g, 2 mmol, 1 eq). The reaction mixture was refluxed for 30 min. Then, $Co(OAc)_2$ was added and the reaction mixture was refluxed. After 1 h, the precipitate was isolated by filtration.

Yield: <0.19 g, <20%

IR (KBr): 3281, 2959, 1599, 1460, 1423, 1361, 1321, 1256, 1165, 1153, 1040, 945, 881.

Synthesis of 109:

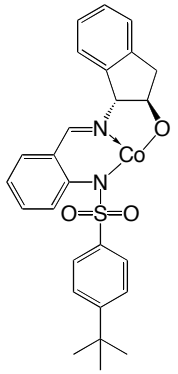

A suspension of the ligand (0.25 g, 0.36 mmol, 1 eq) and $Co(OAc)_2$ (0.13 g, 0.54 mmol, 1.5 eq) in methanol (11 mL) was refluxed for 2 h. Then, the reaction mixture was allowed to reach room temperature and the solvent was removed under reduced pressure. The residue was dissolved in ether and filtered over celite. Following solvent removal, the desired cobalt complex was isolated in form of a solid.

Yield: 0.25 g, quantitative.

IR (KBr): 2960, 1614, 1597, 1556, 1479, 1458, 1288, 1258, 1169, 1139, 1105, 1080, 945, 813, 754.

MS (ESI): 547 (100, $[M+H+CH_3CN]^+$), 506 (21, $[M+H]^+$), 471 (50), 449 (93), 242 (41).

EA: Calculated: C, 61.78; H, 5.18; N, 5.54

Found: C, 64.30; H, 5.76; N, 5.73.

Synthesis of 110:

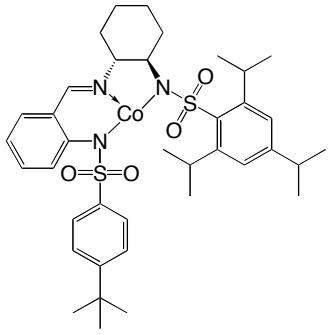

Same procedure as described before.

Yield: 0.24 g, 92%

IR (KBr): 2961, 1634, 1599, 1556, 1462, 1427, 1331, 1290, 1161, 1107, 939, 879, 754.

MS (ESI): 778 (100, $[M+H+CH_3CN]^+$), 681 (100), 381 (20).

EA: Calculated: C, 61.93; H, 6.98; N, 5.70

Found: C, 64.64; H, 7.63; N, 5.79.

Synthesis of 112:

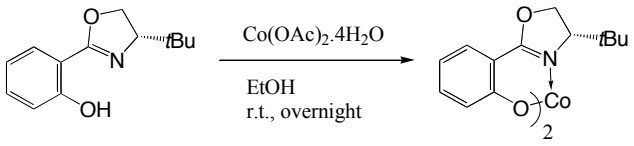

quant.

To a suspension of $Co(OAc)_2.4H_2O$ (93 mg, 0.375 mmol) in 4 mL of ethanol was added a solution of the ligand (65 mg, 0.75 mmol) in 4 mL of ethanol at room temperature. A pink precipitate formed rapidly and 3 mL of ethanol were added. After stirring the reaction mixture overnight, the precipitate was filtered and then washed with ethanol.

Yield: 0.19 g, quantitative

IR (KBr): 2966, 1609, 1585, 1539, 1483, 1439, 1387, 1337, 1238, 1082, 1063, 964, 847, 758.

EA: Calculated: C, 63.03; H, 6.51; N, 5.65

Found: C, 63.02; H, 6.55; N, 5.56.

Ref. operating procedure[127]

Synthesis of 122:

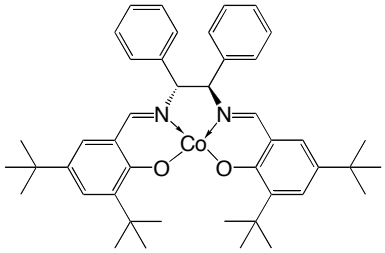

In a Schlenk tube under argon, degassed methanol (8 mL) and two drops of acetic acid were added to the diamine (0.25 g, 2.2 mmol, 1 eq) and the aldehydic substrate (0.88 g, 4.4 mmol, 2 eq). The reaction mixture was refluxed and became yellow. After 30 min, $Co(OAc)_2.H_2O$ (550 mg, 2.2 mmol, 2.2 eq) and methanol (4 mL) were added. The reaction mixture was refluxed for 2 h. The orange product, which precipitated, was isolated by filtration and rinsed with methanol.

Yield: 0.63 g, 86%

IR (KBr): 2952, 2358, 1589, 1526, 1356, 1319, 1250, 1178, 1007, 860, 780.

MS (ESI): 703 (100, $[M+H]^+$), 645 (13, $[M+H-C_4H_9]^+$).

RN: 191163-59-4

Synthesised by Professor Riant.

Synthesis of 123:

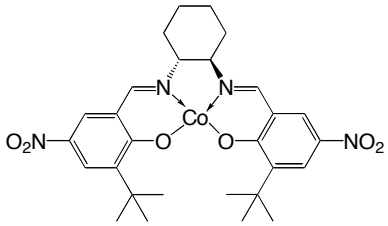

Same procedure as described before.

Yield: 0.45 g, 39%

IR (KBr): 2945, 1645, 1593, 1560, 1493, 1447, 1421, 1325, 1290, 1281, 1115, 989, 729.

MS (ESI): 695 (100, $[M+CF_3COOH]^+$).

Synthesised by Professor Riant.

Synthesis of 124:

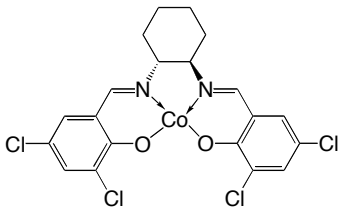

Same procedure as described before.

Yield: 0.79 g, 79%

IR (KBr): 1605, 1514, 1434, 1329, 1213, 1178, 1033, 925, 862, 752.

MS (ESI): 556 (46, $[M+K]^+$), 540 (100), 517 (70, $[M]^+$).

RN: 795307-04-9

Synthesised by Professor Riant.

Synthesis of 125:

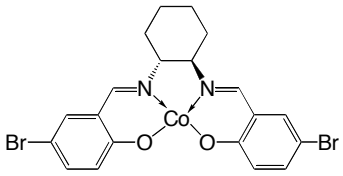

Same procedure as described before.

Yield: 1.02 g, 86%

IR (KBr): 2934, 1599, 1516, 1445, 1315, 1182, 1068, 923, 822, 721.

MS (ESI): 537 (100, $[M]^+$), 242 (42).

RN: 359015-08-0

Synthesised by Professor Riant.

Synthesis of 133:

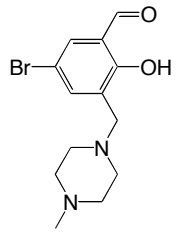

Yield: 4.3 g, 82%

MP: 83 °C

IR (neat): 2794, 1678, 1587, 1454, 1389, 1285, 1232, 1159, 1007, 961, 816.

^{1}H NMR (300 MHz): 2.26-2.64 (m, 8H, CH_2), 2.33 (s, 3H, Me), 3.73 (s, 2, $C\underline{H}_2$-Ar), 7.38 (d, *J* = 2.5 Hz, 1H, CH Ar), 7.76 (d, *J* = 2.5 Hz, 1H, CH Ar), 10.3 (s, 1H, CHO).

^{13}C NMR (75 MHz): 45.8 (CH_3), 52.5 (CH_2), 54.7 (CH_2), 59.4 (CH_2-Ar), 111.2 (C_q Ar), 123.2 (C_q Ar), 125.6 (C_q Ar), 130.5 (CH Ar), 137.3 (CH Ar), 160.5 (C_q Ar), 189.7 (CHO).

RN: 138537-72-1

Ref. operating procedure[132]

Synthesised by Professor Riant.

Synthesis of 134:

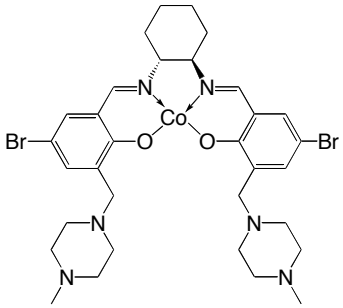

Yield: 0.84 g, 63%

IR (KBr): 2933, 2793, 2359, 1591, 1531, 1454, 1418, 1325, 1016, 860, 719.

MS (ESI): 762 (100, $[M+H]^+$).

Synthesised by Professor Riant.

Synthesis of the aldehydes 137-146:

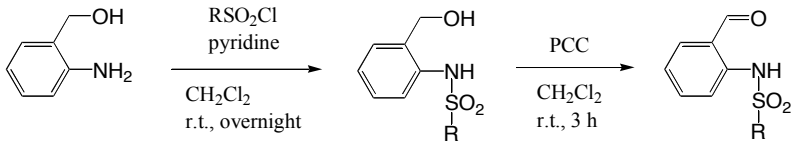

To a solution of 2-aminobenzyl alcohol (3.70 g, 30 mmol) in 90 mL of CH_2Cl_2 were added pyridine (7 mL, 90 mmol, 3 eq) and a sulfonyl chloride (30 mmol, 1 eq) in several portions. After a night of stirring, the reaction was quenched with an acidic work-up. The chlorinated phase was dried over $MgSO_4$ and added to a suspension of PCC (9.76 g, 45.3 mmol) in CH_2Cl_2

(400 mL). After 3 h of stirring at room temperature, the reaction mixture was filtered in a frit over a pad of silica gel and celite. The solvent was removed under reduced pressure to afford the sulfonamide, which was further purified by crystallisation from ethanol.

Ref. modified procedure[136]

137:

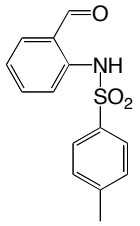

Yield: 8g, 93%

IR (neat): 3111, 1660, 1595, 1580, 1493, 1151, 1116, 1094, 1080, 1043, 837, 740.

^{1}H NMR (500 MHz): 2.36 (s, 3H, CH_3), 7.09 (pseudo t, *J*=7 Hz, 2H, Ar), 7.34 (pseudo t, *J*=7 Hz, 2H, Ar), 7.41 (d, *J*=7.5 Hz, 2H, Ar), 7.55 (d, *J*=8.5 Hz, *J*=8.5 Hz, 2H, Ar), 8.43 (s, 2H, N=CH), 12.81 (s, 2H, NH).

^{13}C NMR (125 MHz): 321.5 (CH_3), 117.6 (CH Ar), 121.8 (C_q Ar), 122.9 (CH Ar), 127.2 (CH Ar), 129.7 (CH Ar), 135.7 (CH Ar), 136.1 (CH Ar), 136.2 (C_q Ar), 139.8 (C_q Ar), 144.1 (C_q Ar), 195.0 (CN).

RN: 6590-65-4

138:

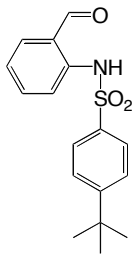

Yield: 1.24g, 83%

MP: 187 °C

IR (neat): 2964, 1666, 1580, 1398, 1342, 1200, 1169, 1155, 1112, 1084, 923, 833, 754.

^{1}H NMR (500 MHz): 1.28 (s, 9H, CH_3), 7.15-7.18 (m, 1H, Ar), 7.45-7.48 (m, 2H, Ar), 7.50-7.53 (m, 1H, Ar), 7.60-7.62 (m, 1H, Ar), 7.69-7.71 (d, *J*=8.5 Hz, 1H, Ar), 7.81-7.84 (d, 2H, Ar), 9.84 (s, 1H, HC=N), 10.85 (s, 1H, NH).

^{13}C NMR (125 MHz): 30.9 (CH_3), 35.1 ($\underline{C}CH_3$), 117.4 (CH Ar), 121.7 (C_q Ar), 122.8 (CH Ar), 126.1 (CH Ar), 126.9 (CH Ar), 135.7 (CH Ar), 136.1 (CH Ar), 136.3 (C_q Ar), 139.9 (C_q Ar), 157.0 (C=N), 195.0 (CHO).

Synthesised by Professor Riant.

139:

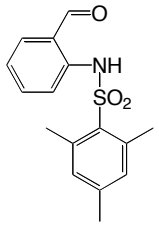

Yield: 7.64, 84%

MP: 158 °C

IR (neat): 1674, 1493, 1263, 1153, 918, 835, 748.

^{1}H NMR (500 MHz): 2.24 (s, 3H, p-methyl), 2.68 (s, 6H, o,o'-dimethyl), 6.92 (s, 2H, Ar), 7.10 (pseudo t, *J*=7.5 Hz, 1H, Ar), 7.3 (d, *J*=8.5 Hz, 1H, Ar), 7.42 (pseudo t, *J*=8.0 Hz, 1H, Ar), 7.61 (d, *J*=8.0 Hz, Ar), 9.85 (s, 1H, CHO), 10.99 (s, 1H, NH).

^{13}C NMR (125 MHz): 20.9 (p-CH_3), 22.7(CH_3 in o,o'), 116.0 (CH Ar), 120.9 (Cq Ar), 122.1 (CH Ar), 132.1 (CH Ar), 133.4 (Cq Ar), 135.7 (CH Ar), 136.1 (CH Ar), 139.2 (Cq Ar), 140.0 (Cq Ar), 142.9 (Cq Ar), 194.9 (C=O).

140:

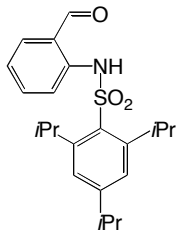

Yield: 5.27, 68%

MP: 107 °C

IR (neat): 2960, 1672, 1601, 1578, 1456, 1400, 1335, 1296, 11152, 914, 845, 751.

^{1}H NMR (500 MHz): 1.23-1.25 (m, 18H, CH_3), 2.88 (q, *J*=7 Hz, 1H, C<u>H</u>-$(CH_3)_2$) in para), 4.31 (h, *J*=6.5 Hz, 2H, C<u>H</u>-$(CH_3)_2$) in ortho and ortho'), 7.10-7.13 (m, 1H, Ar), 7.16 (s, 2H, Ar), 7.41-7.47 (m, 2H, Ar), 7.61-7.63 (m, 1H, Ar), 9.88 (s, 1H, CHO), 11.02 (s, 1H, NH).

^{13}C NMR (125 MHz): 23.4 (CH-(C<u>H</u>$_3)_2$in para), 24.7 (CH-(C<u>H</u>$_3)_2$in ortho and ortho'), 29.7(C<u>H</u>-$(CH_3)_2$in ortho and ortho'), 34.1 (C<u>H</u>-$(CH_3)_2$in para), 116.4 (CH Ar), 121.0 (Cq Ar), 122.0 (CH Ar), 124.1 (CH Ar), 132.3 (Cq Ar), 135.7 (CH Ar), 136.1 (CH Ar), 140.6 (Cq Ar), 150.7 (Cq Ar), 153.5 (Cq Ar), 194.9 (C=O).

141:

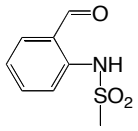

Yield: 1.36, 74%

IR (neat): 1674, 1493, 1402, 1340, 1265, 1151, 966, 843, 743.

^{1}H NMR (500 MHz): 3.12 (s, 3H, CH_3), 7.26-7.29 (m, 1H, Ar), 7.62-7.65 (m, 1H, Ar), 7.73-7.75 (m, 2H, Ar), 9.93 (s, 1H, CHO), 10.61 (s, 1H, NH).

^{13}C NMR (125 MHz): 40.3 (CH_3), 116.8 (CH Ar), 121.5 (C_q Ar), 123.0 (CH Ar), 136.1 (CH Ar), 136.4 (CH Ar), 140.0 (C_q Ar), 195 (CO).

RN: 94532-99-7

142:

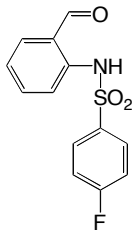

Yield: 4.8 g, 85%

MP: 145 °C

IR (neat): 1662, 1582, 1493, 1265, 1155, 1090, 927, 841, 735.

^{1}H NMR (300 MHz): 7.10-7.93 (m, 8H, CH Ar), 9.84 (s, 1H, CHO), 10.82 (s, 1H, NH).

^{13}C NMR (75 MHz): 116.2 (CH Ar), 116.5, (CH Ar), 117.8 (CH Ar), 121.9 (C_q Ar), 123.3 (CH Ar), 129.8 (CH Ar), 129.9 (CH Ar), 135.8 (CH Ar), 136.1 (CH Ar), 139.4 (C_q Ar), 163.5 (C_q Ar), 166.9 (C_q Ar), 195.1 (CHO).

^{19}F (282MHz): -104.5.

Synthesised by Doctor Chuzel.

143:

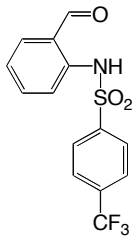

Yield: 0.64, 97%

MP: 104 °C

IR (neat): 1659, 1581, 1493, 1402, 1311, 1160, 1130, 1016, 926, 837.

^{1}H NMR (500 MHz): 7.23 (pseudo t, *J*= 7 Hz, 1H, Ar), 7.56 (pseudo t, *J*= 8.5 Hz, 1H, Ar), 7.64 (d, 1H, *J*= 7.5 Hz, Ar), 7.72 (d, *J*= 10 Hz, 3H, Ar), 8.02 (d, *J*= 8.5 Hz 2H, Ar), 9.84 (s, 1H, HC=N), 10.91 (s, 1H, NH).

^{13}C NMR (125 MHz): 117.9 (CH Ar), 122.1 (C_q Ar), 123.7 (CH Ar), 126.3 (CH Ar), 127.7 (CH Ar), 136.0 (CH Ar), 136.3 (CH Ar), 139.2 (C_q Ar), 142.9 (C_q Ar), 195.1 (CHO).

^{19}F (282MHz): -63.8.

144:

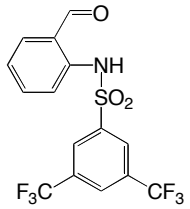

Yield: 1.32, 89%

MP: 117 °C

IR (neat): 1663, 1583, 1495, 1404, 1358, 1277, 1267, 1119, 932, 905, 845, 756.

^{1}H NMR (500 MHz): 7.27-7.31 (m, 1H, Ar), 7.62 (pseudo t, *J*= 8.5 Hz, 1H, Ar), 7.67 (d, 1H, *J*= 8.5 Hz, Ar), 7.33 (d, *J*= 8.5 Hz, 1H, Ar), 8.03 (s, 1H, Ar), 8.31 (s, 2H, Ar), 9.84 (s, 1H, HC=N), 10.94 (s, 1H, NH).

^{13}C NMR (125 MHz): 118.3 (CH Ar), 122.4 (C_q Ar), 124.3 (CH Ar), 126.7 (CH Ar), 127.4 (CH Ar), 136.1 (CH Ar), 136.4 (CH Ar), 138.6 (C_q Ar), 142.1 (C_q Ar), 195.2 (CHO).

^{19}F (282MHz): -63.6.

145:

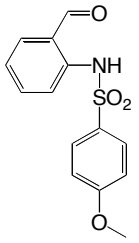

Yield: 2.44, 77%

IR (neat): 1651, 1593, 1578, 1493, 1402, 1263, 1080, 920, 833, 756.

^{1}H NMR (500 MHz): 3.81 (s, 3H, CH_3), 6.90 (d, *J*=9 Hz, 2H, Ar), 7.16 (pseudo t, *J*=7.5 Hz, 1H, Ar), 7.51 (pseudo t, *J*=7.0 Hz, 1H, Ar), 7.59 (d, *J*=6.0 Hz, 1H, Ar), 7.67 (d, *J*=8.5 Hz, 2H, Ar), 7.82 (d, *J*=9 Hz, 2H, Ar), 8.82 (s, 2H, HC=N), 10.76 (s 1H, NH).

^{13}C NMR (125 MHz): 55.6 (OCH_3), 114.2 (CH Ar), 117.7 (CH Ar), 121.8 (C_q Ar), 122.8 (CH Ar), 129.4 (CH Ar), 130.8 (C_q Ar), 135.8 (CH Ar), 136.1 (CH Ar), 139.9 (C_q Ar), 163.2 (C_q Ar), 163.9 (C=N), 195.0 (CHO).

RN: 147611-21-0

Synthesis of chiral diimine-bissulfonamide 147-155:

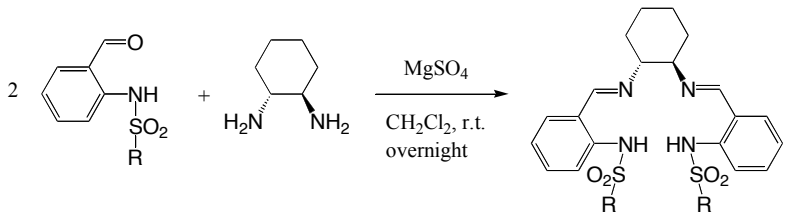

To a solution of aldehyde (3 mmol, 2 eq) in dichloromethane (25 mL) was added a chiral diamine (1.5 mmol, 1 eq) and $MgSO_4$. After stirring overnight, filtration and solvent removal under reduced pressure, the product was obtained in form of a solid.

147:

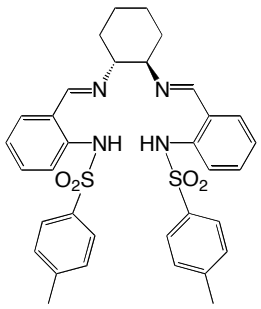

Yield: 5.69 g, quantitative.

MP: 273 °C

IR (neat): 1630, 1578, 1497, 1335, 1286, 1153, 1088, 928, 862, 756.

^{1}H NMR (500 MHz): 1.52-1.92 (m, 8H, CH_2), 2.05 (s, 6H, CH_3), 3.55-3.57 (d, 2H, C<u>H</u>-CH_2), 6.60 (d, *J*=8 Hz, 4H, Ar), 6.90 (pseudo t, *J*=7.5 Hz, 2H, Ar), 7.20 (pseudo t, *J*=8.5 Hz, 2H, Ar), 7.25 (d, *J*=8 Hz, 2H, Ar), 7.41 (d, *J*=8.5 Hz 4H, Ar), 7.48 (d, *J*=8.5 Hz 2H, Ar).

^{13}C NMR (125 MHz): 21.1 (CH_3), 24.2 (<u>C</u>H_2-CH_2-CH), 33.5 (CH_2-<u>C</u>H_2-CH), 73.3(CH_2-<u>C</u>H), 116.8 (CH Ar), 120.20 (C_q Ar), 122.2 (CH Ar), 126.9 (CH Ar), 129.1 (CH Ar), 131.2 (CH Ar), 133.6 (CH Ar), 136.30 (C_q Ar), 139.20 (C_q Ar), 143.00 (C_q Ar), 164.0 (CN).

$[\alpha]^{20}_{D}$= -122° (c = 1.0, CH_2Cl_2).

Ref. operating procedure[136]

spectral data[136]

148:

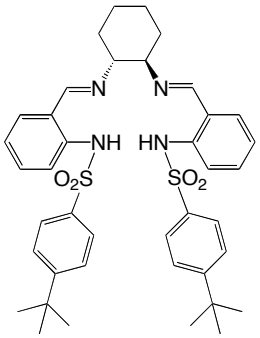

Yield: 3.44 g, quantitative.

MP: 187 °C

IR (neat): 1630, 1580, 1499, 1335, 1157, 1111, 1086, 930, 837.

^{1}H NMR (500 MHz): 1.07 (s, 18H, CH_3), 1.54-1.94 (m, 8H, CH_2), 3.58-3.60 (m, 2H, C<u>H</u>-CH_2), 6.87-6.91 (m, 6H, Ar), 7.17-7.20 (m, 2H, Ar), 7.26-7.28 (m, 2H, Ar), 7.46-7.49 (m, 6H, Ar), 7.41 (d, *J*=8.5 Hz 4H, Ar), 7.48 (s, 2H, HC=N), 13.39 (s, 1H, NH).

^{13}C NMR (125 MHz): 24.2 (<u>C</u>H_2-CH_2-CH), 30.8 (CH_3), 33.5 (CH_2-<u>C</u>H_2-CH), 73.2(CH_2-<u>C</u>H), 116.7 (CH Ar), 120.1 (C_q Ar), 122.1 (CH Ar), 125.7 (CH Ar), 126.7 (CH Ar), 131.4 (CH Ar), 133.6 (CH Ar), 136.4 (C_q Ar), 139.4 (C_q Ar), 156.0 (C_q Ar), 164.1 (CN).

HRMS: calculated for $C_{40}H_{49}N_4O_4S_2$: 713.3195 found: 713.3224.

$[\alpha]^{20}_D$= - 65° (c = 1.0, CH_2Cl_2).

Synthesised by Professor Riant.

149:

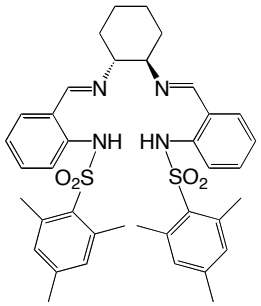

Yield: 1.16 g, quantitative.

MP: 113 °C

IR (neat): 1630, 1578, 1499, 1331, 1288, 1151, 1055, 926, 851, 753.

^{1}H NMR (500 MHz): 1.50-1.93 (m, 8H, CH_2), 2.24 (s, 6H, CH_3), 2.68 (s, 12H, CH_3), 3.42-3.43 (m, 2H, C<u>H</u>-CH_2), 6.89 (s, 4H, Ar), 6.91 (pseudo t, *J*=7.5 Hz, 2H, Ar), 7.03 (d, *J*=8 Hz, 2H, Ar), 7.13 (pseudo t, *J*=7 Hz 2H, Ar), 7.33 (d, *J*=7.5 Hz, 2H, Ar), 8.37 (s, 2H, HC=N).

^{13}C NMR (125 MHz): 20.9 (CH_3), 22.8 (CH_3), 24.1 (<u>C</u>H_2-CH_2-CH), 33.0 (CH_2-<u>C</u>H_2-CH), 73.4(CH_2-<u>C</u>H), 114.9 (CH Ar), 119.2 (C_q Ar), 121.3 (CH Ar), 131.2 (CH Ar), 132.0 (CH Ar), 133.6 (CH Ar), 134.1 (C_q Ar), 139.1 (C_q Ar), 139.3 (C_q Ar), 142.3 (C_q Ar), 164.0 (CN).

HRMS: calculated for $C_{38}H_{45}N_4O_4S_2$: 685.2882 found: 685.2861.

150:

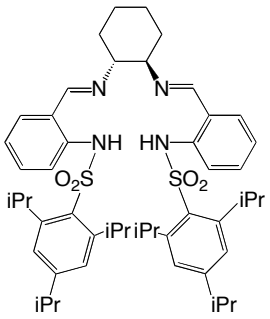

Yield: 1.35 g, quantitative.

MP: 110 °C

IR (neat): 1630, 1499, 1329, 1294, 1150, 926, 866, 750.

^{1}H NMR (500 MHz): 1.17 (d, *J*=6.5 Hz, 6H, CH_3), 1.24 (d, *J*=7 Hz, 6H, CH_3), 1.31 (d, *J*=7 Hz, 6H, CH_3), 1.21-2.01 (m, 8H, CH_2), 2.85-2.91 (m, 2H, C<u>H</u>$(CH_3)_2$), 3.36-3.38 (m, 2H, CH-CH_2), 4.38-4.34 (m, 4H, C<u>H</u>$(CH_3)_2$), 6.88 (pseudo t, *J*=7 Hz, 2H, Ar), 7.02 (d, *J*=8 Hz, 2H, Ar), 7.10 (pseudo t, *J*=7 Hz, 2H, Ar), 7.15 (s, 4H, Ar), 7.31 (d, *J*=6.5 Hz, 2H, Ar), 8.36 (s, 2H, N=CH), 13.46 (s, 2H, NH).

^{13}C NMR (125 MHz): 23.5 (CH_3), 23.5 (CH-CH_2-<u>C</u>H_2), 24.5 (CH_3), 25.1 (CH_3), 32.5 (CH-<u>C</u>H_2-CH_2), 34.1 (<u>C</u>H$(CH_3)_2$), 73.0 (<u>C</u>H-CH_2), 115.1 (CH Ar), 119.1 (C_q Ar), 121.2 (CH Ar), 123.9 (CH Ar), 131.1 (CH Ar), 133.0 (C_q Ar), 133.6 (CH Ar), 150.3 (C_q Ar), 152.9 (C_q Ar), 164.4 (CN).

HRMS: calculated for $C_{50}H_{69}N_4O_4S_2$: 853.4760 found: 853.4764.

151:

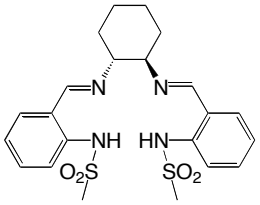

Yield: 0.78g, quantitative.

IR (neat): 1632, 1580, 1580, 1325, 1286, 1130, 926, 927, 864, 756.

^{1}H NMR (500 MHz): 1.48-1.89 (m, 8H, CH_2), 2.82 (s, 6H, CH_3), 3.44-3.46 (m, 2H, CH), 7.09 (pseudo t, *J*=7 Hz, 2H, Ar), 7.34 (pseudo t, *J*=7 Hz, 2H, Ar), 7.41 (d, *J*=7.5 Hz, 2H, Ar), 7.55 (d, *J*=8.5 Hz, 2H, Ar), 8.43 (s, 2H, N=CH), 12.81 (s, 2H, NH).

^{13}C NMR (125 MHz): 24.1 (CH-CH_2-$\underline{C}H_2$), 33.1 (CH-$\underline{C}H_2$-CH_2), 39.8 (CH_3), 73.4 ($\underline{C}$H-CH_2), 117.0 (CH Ar), 120.6 (C_q Ar), 122.7 (CH Ar), 131.7 (CH Ar), 133.7 (CH Ar), 139.4 (C_q Ar), 163.8 (CN).

HRMS: calculated for $C_{22}H_{29}N_4O_4S_2$: 477. 1630 found: 477.1610.

$[\alpha]^{20}_D$=-295° (c = 0.8, CH_2Cl_2).

152:

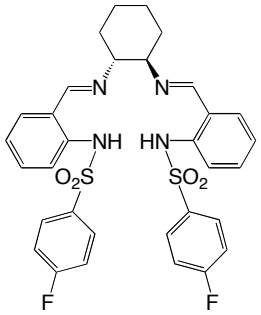

Yield: 0.63 g, quantitative.

MP: 95 °C

IR (neat): 1630, 1493, 1339, 1153, 1088, 930, 837, 756.

^{1}H NMR (500 MHz): 1.53-2.09 (m, 8H, CH_2), 3.55-3.57 (m, 2H, CH), 6.55-6.59 (m, 4H, Ar), 6.96-6.99 (m, 2 H, Ar), 7.23-7.26 (m, 2H, Ar), 7.29-7.31 (m, 2H, Ar), 7.47 (d, *J*=8 Hz, 2H, Ar), 7.53-7.57 (m, 4H, Ar), 8.47 (s, 2H, N=CH), 13.22 (s, 2H, NH).

^{13}C NMR (125 MHz): 24.2 (CH-CH_2-$\underline{C}H_2$), 33.5 (CH-$\underline{C}H_2$-CH_2), 73.3 ($\underline{C}$H-CH_2), 115.8 (CH Ar), 115.9 (CH Ar), 116.9 (CH Ar), 120.3 (C_q Ar), 122.6 (CH Ar), 129.65 and 129.73 (CH Ar), 131.5 (CH Ar), 133.7 (CH Ar), 135.4 (C_q Ar), 139.0 (C_q Ar), 164.0 (CN).

^{19}F (282MHz): -105.5.

HRMS: calculated for $C_{32}H_{31}N_4O_4F_2S_2$: 637.1755 found: 637.1753.

$[\alpha]^{20}_{D}$= -146° (c = 1.0, CH_2Cl_2).

Synthesised by Doctor Chuzel.

153:

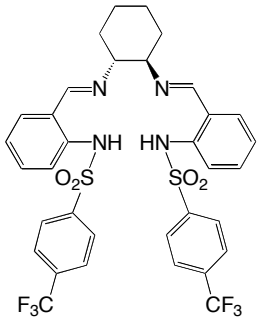

Yield: 0.81 g, quantitative.

MP: 159 °C

IR (neat): 1630, 1780, 1499, 1402, 1319, 1107, 1061, 951, 842, 758.

^{1}H NMR (500 MHz): 1.55-1.95 (m, 8H, CH_2), 3.62-3.64 (m, 2H, CH), 6.96 (pseudo t, *J*=7 Hz, 2H, Ar), 7.00 (d, *J*=8.5 Hz, 4H, Ar), 7.25 (pseudo t, *J*=7,5 Hz, 2H, Ar), 7.30 (d, *J*=7.5 Hz, 2H, Ar), 7.49 (d, *J*=8.5 Hz, 2H, Ar), 7.62 (d, *J*=8.5 Hz, 4H, Ar), 8.54 (s, 2H, N=CH), 13.59 (s, 2H, NH).

^{13}C NMR (125 MHz): 24.2 (CH-CH_2-$\underline{C}H_2$), 33.5 (CH-$\underline{C}H_2$-CH_2), 73.2 ($\underline{C}$H-CH_2), 116.6 (CH Ar), 120.1 (C_q Ar), 122.8 (CH Ar), 125.7 (CH Ar), 127.4 (CH Ar), 131.8 (CH Ar), 133.8 (CH Ar), 134.1 (C_q Ar), 138.8 (C_q Ar), 142.7(C_q Ar), 164.2 (CN).

^{19}F (282MHz): -64.0.

HRMS: calculated for $C_{34}H_{32}N_4O_4F_6S_2$: 737.1691 found: 737.1681.

$[\alpha]^{20}_D$= -98° (c = 0.5, CH_2Cl_2).

154:

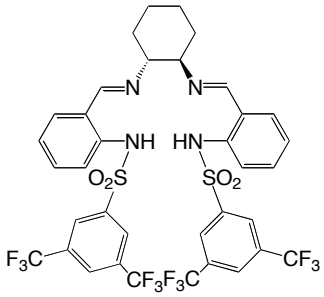

Yield: 0.89 g, quantitative.

MP: 192 °C

IR (neat): 1634, 1500, 1358, 1279, 1134, 935, 903, 844, 760.

^{1}H NMR (500 MHz): 1.26-1.96 (m, 8H, CH_2), 3.45-3.47 (m, 2H, C<u>H</u>-CH_2), 7.04 (pseudo t, *J*=7.5 Hz, 2H, Ar), 7.26-7.31 (m, 4H, Ar), 7.51 (d, *J*=8.5 Hz, 2H, Ar), 7.96 (s, 2H, Ar), 8.22 (s, 2H, Ar), 8.36 (s, 2H, Ar), 13.65 (s, 2H, HC=N).

^{13}C NMR (125 MHz): 23.9 (<u>C</u>H_2-CH_2-CH), 33.0 (CH_2-<u>C</u>H_2-CH), 72.8 (CH_2-<u>C</u>H), 117.6 (CH Ar), 120.6 (C_q Ar), 123.4 (C_q Ar), 123.6 (CH Ar), 126.2 (CH Ar), 127.2 (CH Ar), 132.0 (CH Ar), 133.8(CH Ar), 138.7 (C_q Ar), 142.9 (C_q Ar), 164.5 (CN).

^{19}F (282MHz): -63.6.

HRMS: calculated for $C_{36}H_{29}N_4O_4F_{12}S_2$: 873.1439 found: 873.1448.

$[\alpha]^{20}_D$= - 288° (c = 1.0, CH_2Cl_2).

155:

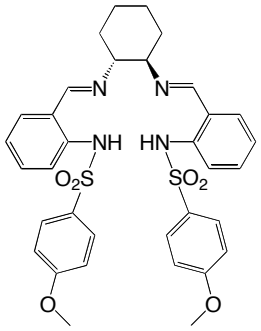

Yield: 1.30 g, quantitative.

MP: 201 °C

IR (neat): 1630, 1595, 1578, 1497, 1337, 1261, 1151, 1092, 926, 839 760.

^{1}H NMR (500 MHz): 1.52-1.92 (m, 8H, CH_2), 3.43 (s, 6H, CH_3), 3.59-3.61 (m, 2H, CH), 6.13 (d, *J*=8.5 Hz, 4H, Ar), 6.93 (pseudo t, *J*=7 Hz, 2H, Ar), 7.20 (pseudo t, *J*=7.5 Hz, 2H, Ar), 7.30 (d, *J*=7.0 Hz, 2H, Ar), 7.38 (d, *J*=9.0 Hz, 4H, Ar), 7.49 (d, *J*=8.0 Hz, 2H, Ar), 8.52 (s, 2H, N=CH), 13.20 (s, 2H, NH).

^{13}C NMR (125 MHz): 24.2 (CH-CH_2-$\underline{C}H_2$), 33.7 (CH-$\underline{C}H_2$-CH_2), 55.2 (CH_3), 73.4 ($\underline{C}$H-CH_2), 113.7 (CH Ar), 116.7 (CH Ar), 120.3 (C_q Ar), 122.2 (CH Ar), 129.2 (CH Ar), 130.5 (C_q Ar), 131.2 (CH Ar), 133.7 (CH Ar), 139.4 (C_q Ar), 162.4 (C_q Ar), 163.9 (CN).

HRMS: calculated for $C_{34}H_{37}N_4O_6S_2$: 661.2155 found: 661.2175.

$[\alpha]^{20}_D$= -45° (c = 1.0, CH_2Cl_2).

Ref. operating procedure[136]

spectral data[136]

156:

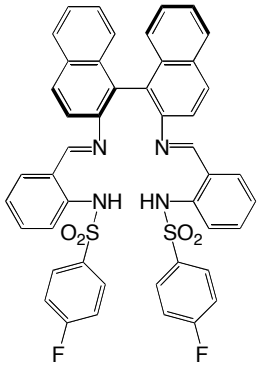

Yield: 1.13, quantitative

IR (neat): 1609, 1591, 1573, 1493, 1340, 1169, 1089, 935, 835, 748.

HRMS: calculated for $C_{46}H_{33}N_4O_4F_2S_2$: 807.1911 found: 807.1879.

Synthesised by Doctor Chuzel.

155:

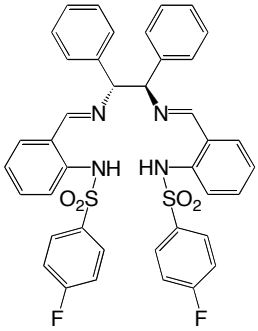

Yield: 1.40g, quantitative

IR (neat): 1628, 1591, 1493, 1339, 1292, 1236, 1167, 1090, 941, 837, 756.

HRMS: calculated for $C_{40}H_{33}N_4O_4F_2S_2$: 735.1911 found: 735.1879.

$[\alpha]^{20}_D$= -84° (c = 0.4, CH_2Cl_2).

Synthesised by Doctor Chuzel.

Synthesis of the complexes 159-167:

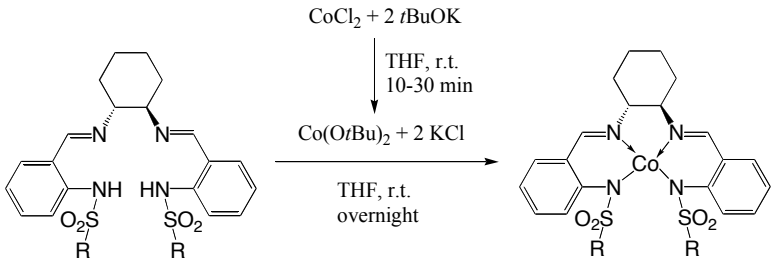

To a solution of cobalt (II) chloride (0.04 g, 1 mmol) in THF (10 mL) were added two equivalents of potassium *tert*-butoxide (0.22 g, 2 mmol) under argon. After 10 to 30 min the blue solution turned deep purple. The ligand (1 mmol, 1 eq) was then added and the reaction mixture was stirred overnight at room temperature. The color changed generally to red. To eliminate the salts, the solvent was removed under reduced pressure and degassed dichloromethane (10 mL) was added. The resulting suspension was filtered over a Millipore fitted in a syringe and transferred into a Schlenk tube under argon. The filtrate was then half-evaporated with a vacuum pump, and degassed *n*-hexane (5 mL) was added to precipitate the complex, which was isolated by filtration.

159:

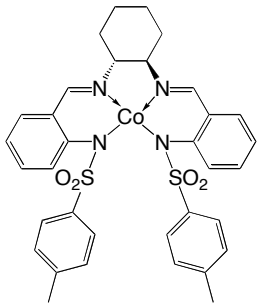

Yield: 0.52 g, 82%

IR (KBr): 1630, 1597, 14791302, 1286, 1257, 1134, 1082, 955, 876, 827.

MS (ESI): 686 (100, $[M+H]^+$), 531 (55, $[M+H]^+$-Ts)

EA: Calculated: C, 59.55; H, 5.00; N, 8.17; S, 9.35

Found: C, 59.03; H, 5.01; N, 8.07; S, 9.28.

160:

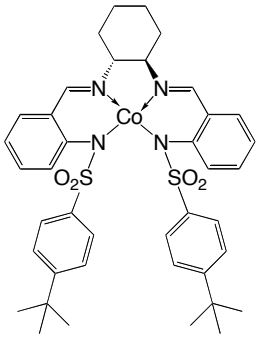

Yield: 0.58 g, 75%

IR (KBr): 2962, 2864, 1632, 1605, 1580, 1501, 1339, 1289, 1159, 1113, 1084, 932, 843, 752.

MS (APCI): 770(50, $[M+H]^+$), 713 (18), 573 (100,$[M+H]^+$-SO_2Ar).

161:

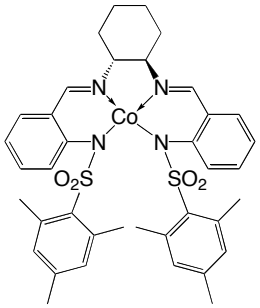

Yield: 0.18 g, 48%.

IR (KBr): 2934, 2858, 1630, 1599, 1556, 1475, 1444, 1281, 1248, 1055, 949, 820, 754.

MS (APCI): 742 (18, $[M+H]^+$), 645 (13), 559 (100,$[M+H]^+$-SO_2Ar).

EA: Calculated: C, 61.53; H, 5.71; N, 7.55

Found: C, 59.26; H, 5.63; N, 7.02.

162:

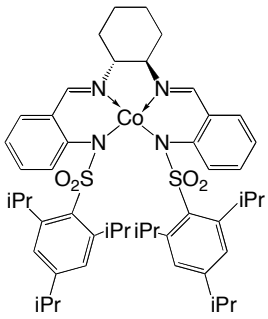

Yield: 0.76 g, 84%

IR (KBr): 2961, 2932, 1632, 1601, 1556, 1475, 1300, 1273, 1119, 957, 870, 810, 754.

MS (APCI): 910 (4, $[M+H]^+$), 849 (55), 643 (100,$[M+H]^+$-SO_2Ar), 376 (18).

EA: Calculated: C, 65.98; H, 7.31; N, 6.16

Found: C, 65.11; H, 7.36; N, 5.85.

163:

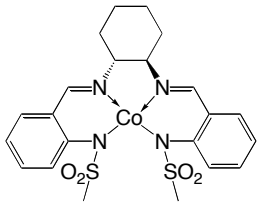

Yield: 0.23 g, 83%

IR (KBr): 2933, 2860, 1632, 1605, 1481, 1434, 1290, 1261, 1122, 931, 852, 754.

MS (ESI): 556 (100, $[M+Na]^+$), 553 (45, $[M+H]^+$).

EA: Calculated: C, 49.53; H, 4.91; N, 10.50

Found: C, 49.14; H, 4.94; N, 10.16.

164:

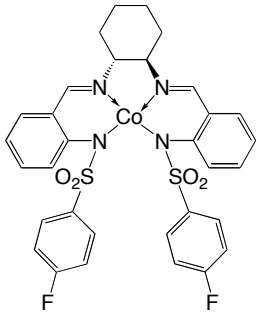

Yield: 0.39 g, 57%

IR (KBr): 2937, 1605, 1483, 1301, 1284, 1271, 1254, 1234, 1217, 1080, 959, 879, 833, 758.

MS (ESI): 1408 (17, [dimer + Na]$^+$), 807 (88), 716 (97,[M+Na]$^+$). 694 (100, [M+H]$^+$), 582 (29), 535 ([M+H]$^+$-SO_2Ar).

EA: Calculated: C, 55.41; H, 4.07; N, 8.08; S, 9.24

Found: C, 55.10; H, 4.17; N, 7.86; S, 9.46.

Synthesised by Doctor Chuzel.

165:

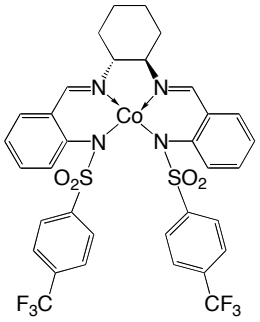

Yield: 0.26 g, 49%

IR (KBr): 2935, 2860, 1632, 1607, 1501, 1405, 1327, 1288, 1169, 1163, 1130, 1107, 1063, 957, 933, 843, 756.

MS (APCI): 794 (37, $[M+H]^+$), 737 (74), 585 (100,$[M+H]^+$-SO_2Ar).

EA: Calculated: C, 51.45; H, 3.56; N, 7.06

Found: C, 52.95; H, 3.18; N, 7.19.

166:

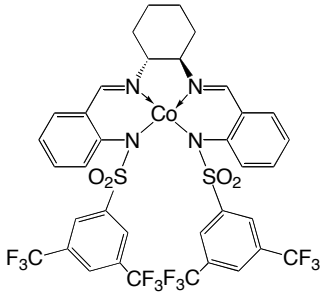

Yield: 0.09 g, 53%

IR (KBr): 2939, 2866, 1632, 1605, 1558, 1485, 1361, 1279, 1177, 1132, 955, 905.

MS (APCI): 930 100, $[M+H]^+$), 873 (6), 653 (26,$[M+H]^+$-SO_2Ar).

EA: Calculated: C, 46.51; H, 2.82; N, 6.03

Found: C, 46.66; H, 2.87; N, 5.72.

167:

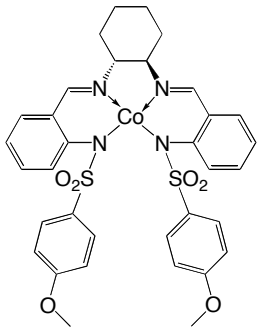

Yield: 0.25 g, 71%

IR (KBr): 2933, 2858, 1632, 1597, 1556, 1497, 1412, 1130, 1082, 1024, 933, 829, 752.

MS (APCI): 718 (21, $[M+H]^+$), 661 (100), 547 (72, $[M+H]^+$-SO_2Ar).

EA: Calculated: C, 56.90; H, 4.77; N, 7.81

Found: C, 57.86; H, 5.17; N, 7.52.

168:

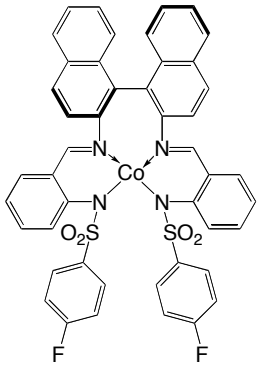

Yield: 0.30 g, 64%

IR (KBr): 1609, 1589, 1493, 1475, 1289, 1138, 1138, 949, 883, 837, 748.

MS (APCI): 886 (11, $[M+Na]^+$), 864 (100, $[M+H]^+$), 705 (6, $[M+H]^+$-SO_2Ar), 546 (30), 294 (19).

EA: Calculated: C, 63.96; H, 3.50; N, 6.49

Found: C, 63.43; H, 3.93; N, 6.07.

Synthesised by Doctor Chuzel.

169:

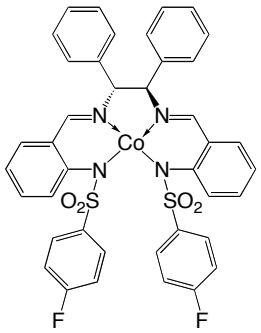

Yield: 0.26 g, 52%

IR (KBr): 1627, 1593, 1556, 1495, 1477, 1286, 1236, 1136, 1078, 957, 839, 763.

MS (ESI): 829 (23, $[M+Na+CH_4]^+$), 814 (56, $[M+Na]^+$), 792 (100, $[M+H]^+$), 633 (12, $[M+H]^+$-SO_2Ar).

EA: Calculated: C, 60.68; H, 3.82; N, 7.08

Found: C, 58.17; H, 3.65; N, 6.61.

Synthesised by Doctor Chuzel.

Synthesis of 172:

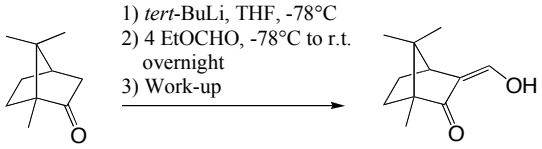

To a solution of (+)-camphor (3.04 g, 20 mmol, 1 eq) in THF (40 mL) under argon was added *tert*-BuLi (13.3 mL of a 1.5 M solution, 20 mmol, 1 eq) at -78°C over a period of 30 min. Then, a solution of ethyl formate (6.46 mL, 80 mmol, 4 eq) in THF (8 mL) was added dropwise at the same temperature and the reaction mixture was then allowed to reach room temperature. After stirring overnight, the reaction was quenched with 5 mL of isopropanol in 150 mL of water. The remaining starting material was removed by extraction (3 x 50 mL Et_2O). Following acidification to pH 1, the product was extracted (3 x 50 mL Et_2O). The combined organic layers were dried over $MgSO_4$. After solvent removal, the product was obtained as a white solid.

Yield: 2.44, 68%

MP: 74 °C

IR (neat): 2958, 1709, 1618, 1414, 1367, 1215, 1171, 1072, 1012, 947, 802.

^{1}H NMR (500 MHz): 0.84 (s, 1H, Me), 0.93 (s, 1H, Me), 0.97 (s, 1H, Me), 1.40-1.43 (m, 2H), 1.68-1.72 (m, 1H), 2.00-2.03 (m, 1H), 2.44 (s, 1H), 6.78 (s, 1H, C=CH).

^{13}C NMR (125 MHz): 8.5, 18.6, 20.3, 27.7, 30.1, 46.6, 49.8, 58.5, 119.4, 151.6, 212.7 (C=O).

$[\alpha]^{20}_D$= -156° (c = 1.0, CH_2Cl_2).

RN: 14681-31-3

Ref. lithiation procedure[142]

Synthesis of 173:

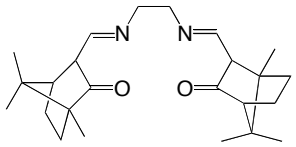

Yield: 1.71 g, quantitative.

MP: 206 °C

IR (neat): 2953, 1678, 1585, 1466, 1105, 1072, 1026, 945, 808.

HRMS: calculated for $C_{24}H_{36}N_2O_2Na$: 407.2674 found: 407.2679.

$[\alpha]^{20}_D$ = +119° (c = 1.0, CH_2Cl_2).

Synthesis of 174:

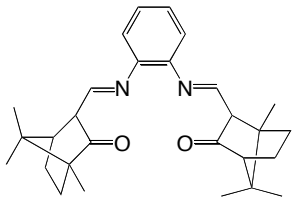

Yield: 0.86 g, quantitative.

IR (neat): 2957, 1686, 1622, 1585, 1454, 1288, 1244, 1072, 1030, 949, 743.

HRMS: calculated for $C_{28}H_{36}N_2O_2Na$: 455.2674 found: 455.2671.

Synthesis of 179:

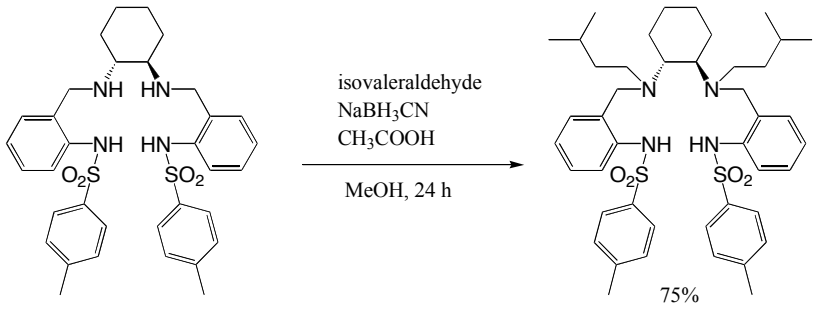

To a solution of **147** (0.63 g, 1 mmol, 1 eq) in methanol (5 mL) were added *iso*-valeraldehyde (0.45 mL, 4 mmol, 4 eq), sodium cyanoborohydride (0.25 g, 4 mmol, 4 eq) and acetic acid (0.06 mL, 1 mmol, 1 eq). The mixture was stirred for 24 h and methanol was removed under reduced pressure. The residue was dissolved in ether (5 mL) and washed with aqueous sodium hydroxide (10%, 2x5 mL), and water. The organic phase was dried over Na_2SO_4 and concentrated under reduced pressure. The crude product was purified by flash chromatography (3% MeOH/CH_2Cl_2: R_f=0.29).

Yield: 1.11 g, 75%.

MP: 87 °C

IR (neat): 2954, 1495, 1456, 1331, 1159, 1092, 923, 814, 715.

^{13}C NMR (125 MHz): inC_6D_6 at 90°C:

21.0 (Ar-$\underline{C}H_3$), 22.7 (CH-$\underline{C}H_3$), 23.0 (Ar-$\underline{C}H_3$), 26.0 ($\underline{C}H_2$-CH_2-CH), 27.4 ($\underline{C}$H-$(CH_3)_2$), 27.9 (CH_2-$\underline{C}H_2$-CH), 38.5 ($\underline{C}H_2$-CH_2N), 48.6 (Ar-$\underline{C}H_2$), 54.9

(CH_2-$\underline{C}H_2N$), 60.8 (CH_2-CH_2-$\underline{C}H$), 121.7 (CH Ar), 124.4 (CH Ar), 127.5 (CH Ar), 128.8 (CH Ar), 129.6 (CH Ar), 130.7 (CH Ar), 139.0 (C_q Ar), 139.8 (C_q Ar), 143.0 (C_q Ar).

HRMS: calculated for $C_{44}H_{61}N_4O_4S_2$: 773.4134 found: 773.4133.

$[\alpha]^{20}_D$= -20° (c = 1.0, CH_2Cl_2).

Ref. operating procedure[147]

Bibliography

1. Knowles, W. S. *Acc. Chem. Res.* **1983**, *16*, 106-112.
2. Knowles, W. S. *Angew. Chem. Int. Ed.* **2002**, *41*, 1999-2007.
3. Blaser, H. U.; Buser, H. P.; Coers, K.; Hanreich, R.; Jalett, H. P.; Jelsch, E.; Pugin, B.; Schneider, H. D.; Spindler, F.; Wegmann, A. *Chimia* **1999**, *53*, 275-280.
4. Breuer, M.; Ditrich, K.; Habicher, T.; Hauer, B.; Kesseler, M.; Sturmer, R.; Zelinski, T. *Angew. Chem. Int. Ed.* **2004**, *43*, 788-824.
5. Pamies, O.; Backvall, J. E. *Chem. Rev.* **2003**, *103*, 3247-3261.
6. Blaser, H. U.; Spindler, F.; Studer, M. *Applied Catalysis A: General* **2001**, *221*, 119-143.
7. Bürgi, T.; Baiker, A. *Acc. Chem. Res.* **2004,** *37*, 909-917.
8. Guerreiro, P.; Ratovelomanana-Vidal, V.; Genet, J. P.; Dellis, P. *Tetrahedron Lett.* **2001**, *42*, 3423-3426.
9. Brunner, H. *Angew. Chem. Int. Ed.* **1999**, *38*, 1195-1208.
10. Faller, J. W.; Grimmond, B. J.; D'Alliessi, D. G. *J. Am. Chem. Soc.* **2001**, *123*, 2525-2529.
11. Noyori, R. *Angew. Chem. Int. Ed.* **2002**, *41*, 2008-2022.
12. Knowles, W. S.; Sabacky, M. J.; Vineyard, B. D. *Chem. Commun.* **1976**, 10-11.
13. Jerphagnon, T.; Renaud, J. L.; Bruneau, C. *Tetrahedron: Asymmetry* **2004**, *15*, 2101-2111.
14. Duursma, A.; Boiteau, J. G.; Lefort, L.; Boogers, J. A. F.; de Vries, A. H. M.; de Vries, J. G.; Minnaard, A. J.; Feringa, B. L. *J. Org. Chem.* **2004**, *69*, 8045-8052.
15. Kagan, H. B.; Dang, T. P. *Chem. Commun.* **1971**, 481.
16. Sharpless, K. B. *Angew. Chem. Int. Ed.* **2002**, *41*, 2024-2032.
17. Johnson, J. S.; Evans, D. A. *Acc. Chem. Res.* **2000**, *33*, 325-335.
18. Denmark, S. E.; Stavenger, R. A. *Acc. Chem. Res.* **2000**, *33*, 432-440.
19. Denmark, S. E.; Pham, S. M.; Stavenger, R. A.; Su, X. P.; Wong, K. T.; Nishigaichi, Y. *J. Org. Chem.* **2006**, *71*, 3904-3922.
20. Kanai, M.; Nobuki, K.; Eiko, I.; Shibasaki, M. *Pure Appl. Chem.* **2006**, *77*, 2047-2052.

21. Shibasaki, M.; Matsunaga, S. *Chem. Soc. Rev.* **2006**, *35*, 269-279.
22. Trost, B. M. *Acc. Chem. Res.* **1996**, *29*, 355-364.
23. Trost, B. M.; Crawley, M. L. *Chem. Rev.* **2003**, *103*, 2921-2943.
24. Trost, B. M.; VanVranken, D. L. *Chem. Rev.* **1996**, *96*, 395-422.
25. Yorimitsu, H.; Oshima, K. *Angew. Chem. Int. Ed.* **2005**, *44*, 4435-4439.
26. Belda, O.; Moberg, C. *Acc. Chem. Res.* **2004**, *37*, 159-167.
27. Polet, D.; Alexakis, A.; Tissot-Croset, K.; Corminboeuf, C.; Ditrich, K. *Chem. Eur. J.* **2006**, *12*, 3596-3609.
28. Takeuchi, R. *Synlett* **2002**, *12*, 1954-1965.
29. Trost, B. M.; Fraisse, P. L.; Ball, Z. T. *Angew. Chem. Int. Ed.* **2002**, *41*, 1059-1061.
30. Trost, B. M.; Strege, P. E. *J. Am. Chem. Soc.* **1977**, *99*.
31. Sprinz, J.; Helmchen, G. *Tetrahedron Lett.* **1993**, *34*, 1769-1772.
32. Vonmatt, P.; Pfaltz, A. *Angew. Chem. Int. Ed.* **1993**, *32*, 566-568.
33. Coote, S. J.; Dawson, G. J.; Frost, C. G.; Williams, J. M. J. *Synlett* **1993,** 509-510.
34. Dawson, G. J.; Frost, C. G.; Williams, J. M. J. *Tetrahedron Lett.* **1993**, *34*, 3149-3150.
35. Hayashi, T.; Kanehira, K.; Hagihara, K.; Kumada, M. *J. Org. Chem.* **1988**, *53*, 113-120.
36. Trost, B. M.; McEachern, E. J.; Toste, F. D. *J. Am. Chem. Soc.* **1998**, *120*, 12702-12703.
37. Pu, L.; Yu, H. B. *Chem. Rev.* **2001**, *101*, 757-824.
38. Oguni, M.; Omi, T. *Tetrahedron Lett.* **1984**, *25*, 2823-2824.
39. Kitamura, M.; Suga, S.; Kawai, K.; Noyori, R. *J. Am. Chem. Soc.* **1986**, *108*, 6071-6072.
40. Bolm, C.; Hermanns, N.; Hildebrand, J. P.; Muniz, K. *Angew. Chem. Int. Ed.* **2000**, *39*, 3465-3467.
41. Bolm, C.; Kesselgruber, M.; Hermanns, N.; Hildebrand, J. P.; Raabe, G. *Angew. Chem. Int. Ed.* **2001**, *40*, 1488.
42. Funabashi, K.; Jachmann, M.; Kanai, M.; Shibasaki, M. *Angew. Chem. Int. Ed.* **2003**, *42*, 5489-5492.
43. Kang, J.; Kim, D. S.; Kim, J. I. *Synlett* **1994**, 842-844.
44. Gibson, C. L. *Tetrahedron: Asymmetry* **1999**, *10*, 1551-1561.
45. Masaki, Y.; Oda, H.; Kazuta, K.; Usui, A.; Itoh, A.; Xu, F. *Tetrahedron Lett.* **1992**, *33*, 5089-5092.
46. Tseng, S. L.; Yang, T. K. *Tetrahedron: Asymmetry* **2004**, *15*, 3375-3380.

47. Rijnberg, E.; Hovestad, N. J.; Kleij, A. W.; Jastrzebski, J. T. B. H.; Boersma, J.; Janssen, M. D.; Spek, A. L.; vanKoten, G. *Organometallics* **1997**, *16*, 2847-2857.
48. Wirth, T.; Kulicke, K. J.; Fragale, G. *Helv. Chim. Acta* **1996**, *79*, 1957-1966.
49. Bolm, C.; Kesselgruber, M.; Grenz, A.; Hermanns, N.; Hildebrand, J. P. *New J. Chem.* **2001**, *25*, 13-15.
50. Leutenegger, U.; Madin, A.; Pfaltz, A. *Angew. Chem. Int. Ed.* **1989**, *28*, 60-61.
51. Misun, M.; Pfaltz, A. *Helv. Chim. Acta* **1996**, *79*, 961-972.
52. Vonmatt, P.; Pfaltz, A. *Tetrahedron: Asymmetry* **1991**, *2*, 691-700.
53. Geiger, C.; Kreitmeier, P.; Reiser, O. *Adv. Synth. Catal.* **2005**, *347*, 249-254.
54. Yamada, T.; Nagata, T.; Ikeno, T.; Ohtsuka, Y.; Sagara, A.; Mukaiyama, T. *Inorg. Chim. Acta* **1999**, *296*, 86-93.
55. Paraskar, A. S.; Sudalai, A. *Tetrahedron* **2006**, *62*, 4907-4916.
56. Yamada, T.; Nagata, T.; Sugi, K. D.; Yorozu, K.; Ikeno, T.; Ohtsuka, Y.; Miyazaki, D.; Mukaiyama, T. *Chem. Eur. J.* **2003**, *9*, 4485-4509.
57. Sun, W.; Xia, C. G.; Zhao, P. Q. *Journal of Molecular Catalysis A: Chemical* **2002**, *184*, 51-55.
58. You, S. L.; Hou, X. L.; Dai, L. X.; Yu, Y. H.; Xia, W. *J. Org. Chem.* **2002**, *67*, 4684-4695.
59. Chung, K. G.; Miyake, Y.; Uemura, S. *J. Chem. Soc., Perkin Trans. 1* **2000**, 2725-2729.
60. Nishibayashi, Y.; Segawa, K.; Takada, H.; Ohe, K.; Uemura, S. *Chem. Commun*. **1996**, 847-848.
61. Nishibayashi, Y.; Uemura, S. *Synlett* **1995**, 79-81.
62. Takei, I.; Nishibayashi, Y.; Arikawa, Y.; Uemura, S.; Hidai, M. *Organometallics* **1999**, *18*, 2271-2274.
63. Nishibayashi, Y.; Takei, I.; Uemura, S.; Hidai, M. *Organometallics* **1998**, *17*, 3420-3422.
64. Nishibayashi, Y.; Takei, I.; Uemura, S.; Hidai, M. *Organometallics* **1999**, *18*, 2291-2293.
65. Sammakia, T.; Stangeland, E. L. *J. Org. Chem.* **1997**, *62*, 6104-6105.
66. Nishibayashi, Y.; Yamauchi, A.; Onodera, G.; Uemura, S. *J. Org. Chem.* **2003**, *68*, 5875-5880.
67. Bolm, C.; Muniz-Fernandez, K.; Seger, A.; Raabe, G.; Gunther, K. *J. Org. Chem.* **1998**, *63*, 7860-7867.

68. Bolm, C.; Fernandez, K. M.; Seger, A.; Raabe, G. *Synlett* **1997**, 1051-1052.
69. Bolm, C.; Hermanns, N.; Classen, A.; Muniz, K. *Bioorg. Med. Chem. Lett.* **2002**, *12*, 1795-1798.
70. Bolm, C.; Rudolphe, J. *J. Am. Chem. Soc.* **2002**, *124*, 14850-14851.
71. Richards, C. J.; Damalidis, T.; Hibbs, D. E.; Hursthouse, M. B. *Synlett* **1995**, 74-76.
72. Sammakia, T.; Latham, H. A.; Schaad, D. R. *J. Org. Chem.* **1995**, *60*, 10-11.
73. Sammakia, T.; Latham, H. A. *J. Org. Chem.* **1996**, *61*, 1629-1635.
74. Richards, C. J.; Mulvaney, A. W. *Tetrahedron: Asymmetry* **1996**, *7*, 1419-1430.
75. Sammakia, T.; Latham, H. A. *J. Org. Chem.* **1995**, *60*, 6002-6003.
76. Buscaylet, S., Université Paris-Sud, 1999.
77. Neto, A. F.; Miller, J.; de Andrade, V. F.; Fujimoto, S. Y.; Afonso, M. M. D.; Archanjo, F. C.; Darin, V. A.; Silva, M. L. A. E.; Borges, A. D. L.; Del Ponte, G. *Z. Anor. Allg. Chem.* **2002**, *628*, 209-216.
78. Sanders, R.; Mueller-Westerhoff, U.-W. *J. Organomet. Chem.* **1996**, *512*, 219-224.
79. Evans, D. A.; Peterson, G. S.; Johnson, J. S.; Barnes, D. M.; Campos, K. R.; Woerpel, K. A. *J. Org. Chem.* **1998**, *63*, 4541-4544.
80. Drabowicz, J.; Mikolajczyk, M. *Synthesis* **1980**, 32-33.
81. Chiacchio, U.; Corsaro, A.; Rescifina, A.; Testa, M.; Purello, G. *Heterocycles* **1993**, *36*, 223-229.
82. Lambin, D.; personnal communication.
83. Krasovskiy, A.; Gavryushin, A.; Knochel, P. *Synlett* **2005**, 2691-2693.
84. Sandrinelli, F.; Perrio, S.; Averbuch-Pouchot, M. T. *Org. Lett.* **2002**, *4*, 3619-3622.
85. Knotter, D. M.; Vanmaanen, H. L.; Grove, D. M.; Spek, A. L.; Vankoten, G. *Inorg. Chem.* **1991**, *30*, 3309-3317.
86. Marquarding, D.; Klusacek, H.; Gokel, G.; Hoffmann, P.; Ugi, I. *J. Am. Chem. Soc.* **1970**, *92*, 5389-5393.
87. Mugesh, G.; Singh, H. B. *Acc. Chem. Res.* **2002**, *35*, 226-236.
88. Wipf, P.; Jayasuriya, N.; Ribe, S. *Chirality* **2003**, *15*, 208-212.
89. Oppolzer, W.; Radinov, R. N. *Helv. Chim. Acta* **1992**, *75*, 170-173.
90. Fitzpatrick, K.; Hulst, R.; Kellogg, R. M. *Tetrahedron: Asymmetry* **1995**, *6*, 1861-1864.
91. Ding, K. L.; Ishii, A.; Mikami, K. *Angew. Chem. Int. Ed.* **1999**, *38*, 497-501.

92. Mikami, K.; Angelaud, R.; Ding, K. L.; Ishii, A.; Tanaka, A.; Sawada, N.; Kudo, K.; Senda, M. *Chem. Eur. J.* **2001**, *7*, 730-737.
93. Dahmen, S.; Brase, S. *Org. Lett.* **2001**, *3*, 4119-4122.
94. Mimoun, H. *J. Org. Chem.* **1999**, *64*, 2582-2589.
95. Mimoun, H.; de Saint Laumer, J. Y.; Giannini, L.; Scopelliti, R.; Floriani, C. *J. Am. Chem. Soc.* **1999**, *121*, 6158-6166.
96. Bette, V.; Mortreux, A.; Savoia, D.; Carpentier, J. F. *Adv. Synth. Catal.* **2005**, *347*, 289-302.
97. Mastranzo, V. M.; Quintero, L.; de Parrodi, C. A.; Juaristi, E.; Walsh, P. J. *Tetrahedron* **2004,** *60*, 1781-1789.
98. Braun, M. *Angew. Chem. Int. Ed.* **1996**, *35*, 519-522.
99. Cozzi, P. G. *Chem. Soc. Rev.* **2004**, *33*, 410-421.
100. Katsuki, T. *Chem. Soc. Rev.* **2004**, *33*, 437-444.
101. McGarrigle, E. M.; Gilheany, D. G. *Chem. Rev.* **2005**, *105*, 1563-1602.
102. Jacobsen, E. N.; Zhang, W.; Muci, A. R.; Ecker, J. R.; Deng, L. *J. Am. Chem. Soc.* **1991**, *113*, 7063-7064.
103. Hosoya, N.; Hatayama, A.; Irie, R.; Sasaki, H.; Katsuki, T. *Tetrahedron* **1994**, *50*, 4311-4322.
104. Sasaki, H.; Irie, R.; Hamada, T.; Suzuki, K.; Katsuki, T. *Tetrahedron* **1994**, *50*, 11827-11838.
105. Scheurer, A.; Maid, H.; Hampel, F.; Saalfrank, R. W.; Toupet, L.; Mosset, P.; Puchta, R.; Hommes, N. J. R. V. *Eur. J. Org. Chem.* **2005**, 2566-2574.
106. Zhang, W.; Jacobsen, E. N. *J. Org. Chem.* **1991**, *56*, 2296-2298.
107. Oconnor, K. J.; Wey, S. J.; Burrows, C. J. *Tetrahedron Lett.* **1992**, *33*, 1001-1004.
108. Pospisil, P. J.; Carsten, D. H.; Jacobsen, E. N. *Chem. Eur. J.* **1996**, *2*, 974-980.
109. Chang, S.; Heid, R. M.; Jacobsen, E. N. *Tetrahedron Lett.* **1994**, *35*, 669-672.
110. Samsel, K.; Srinivasan, K.; Kochi, J. K. *J. Am. Chem. Soc.* **1985**, *107*, 7606.
111. Srinivasan, K.; Michaud, P.; Kochi, J. K. *J. Am. Chem. Soc.* **1986**, *108*, 2309.
112. Jacobsen, E. N.; Zhang, W.; Guler, M. L. *J. Am. Chem. Soc.* **1991**, *113*, 6703-6704.
113. Hamada, T.; Fukuda, T.; Imanishi, H.; Katsuki, T. *Tetrahedron* **1996**, *52*, 515-530.
114. Hashihayata, T.; Ito, Y.; Katsuki, T. *Synlett* **1996**, 1079.

115. Hashihayata, T.; Ito, Y.; Katsuki, T. *Tetrahedron* **1997**, *53*, 9541-9552.
116. Miura, K.; Katsuki, T. *Synlett* **1999**, 783-785.
117. Janssen, K. B. M.; Parton, R. F.; Jacobs, P. A. *Tetrahedron: Asymmetry* **1997**, *8*, 3039-3042.
118. Palucki, M.; Pospisil, P. J.; Zhang, W.; Jacobsen, E. N. *J. Am. Chem. Soc.* **1994**, *113*, 9333-9334.
119. Jacobsen, E. N.; Deng, L.; Furukawa, Y.; Martinez, L. E. *Tetrahedron* **1994**, *50*, 4323-4334.
120. Katsuki, T. *Chem. Soc. Rev.* **2004**, *33*, 437-444.
121. Calligaris, M.; Manzini, G.; Nardin, G.; Randaccio, L. *J. Chem. Soc., Dalton Trans* **1972**, 543-547.
122. Belokon, Y. N.; Caveda-Cepas, S.; Green, B.; Ikonnikov, N. S.; Krustalev, V. N.; Larichev, V. S.; Moscalenko, M. A.; North, M.; Orizu, C.; Tararov, V. I.; Tasinazzo, M.; Timofeeva, G. I.; Yashkina, L. V. *J. Am. Chem. Soc.* **1999**, *121*, 3968-3973.
123. Belokon', Y. N.; Green, B.; Ikonnikov, N. S.; Larichev, V. S.; Lokshin, B. V.; Moscalenko, M. A.; North, M.; Orizu, C.; Peregudov, A. S.; Timofeeva, G. I. *Eur. J. Org. Chem.* **2000**, 2655-2661.
124. Che, C. M.; Huang, J. S. *Coord. Chem. Rev.* **2003**, *242*, 97-113.
125. Corden, J. P.; Errington, W.; Moore, P.; Wallbridge, M. G. H. *Chem. Commun.* **1999**, 323-324.
126. Brunner, H.; Amberger, K. *J. Organomet. Chem.* **1991**, *417*, C63-C67.
127. Mugesh, G.; Singh, H. B.; Butcher, R. J. *Eur. J. Inorg. Chem.* **2001**, 669-678.
128. DiMauro, E. F.; Kozlowski, M. C. *Org. Lett.* **2001**, *3*, 3053-3056.
129. Dimauro, E. F.; Kozlowski, M. C. *Org. Lett.* **2002**, *4*, 3781-3784.
130. Dimauro, E. F.; Kozlowski, M. C. *J. Am. Chem. Soc.* **2002**, *124*, 12668-12669.
131. Basra, S.; Fennie, M. W.; Kozlowski, M. C. *Org. Lett.* **2006**, *8*, 2659-2662.
132. Crane, J. D.; Fenton, D. E.; Latour, J. M.; Smith, A. J. *J. Chem. Soc. Dalton Trans.* **1991**, 2979-2987.
133. Vazquez, M.; Bermejo, M. R.; Sanmartin, J.; Garcia-Deibe, A. M.; Lodeiro, C.; Mahia, J. *J. Chem. Soc.,Dalton Trans.* **2002**, 870-877.
134. Karame, I.; Jahjah, M.; Messaoudi, A.; Tommasino, M. L.; Lemaire, M. *Tetrahedron: Asymmetry* **2004**, *15*, 1569-1581.

135. Karame, I.; Tommasino, M. L.; Faure, R.; Lemaire, M. *Eur. J. Org. Chem.* **2003**, 1271-1276.
136. Fonseca, M. H.; Eibler, E.; König, B. *Tetrahedron: Asymmetry* **2003**, *14*, 1989-1994.
137. Irie, R.; Ito, Y.; Katsuki, T. *Tetrahedron Lett.* **1991**, *32*, 6891-6894.
138. Fowles, G. W. A.; Rice, D. A.; Walton, R. A. *J. Inorg. Nucl. Chem.* **1969**, *31*, 3119-3131.
139. Willi, A. V. *Helv. Chim. Acta* **1956**, *39*, 46-56.
140. Gianini, M.; von Zelewsky, A. *Synthesis* **1996**, 702-706.
141. Gianini, M.; vonZelewsky, A. *Synthesis* **1996**, 702.
142. Bocknack, B. M.; Wang, L. C.; Hughes, F. W.; Krische, M. J. *Tetrahedron* **2005**, *61*, 6266-6275.
143. Jensen, H. P.; Larsen, E. *Acta. Chim. Scand.* **1975**, *A 29*, 159-162.
144. Jensen, H. P.; Larsen, E. *Gaze. Chim. Ital.* **1977**, *107*, 143-146.
145. Pratt, R. C.; Stack, T. D. P. *J. Am. Chem. Soc.* **2003**, *125*, 8716-8717.
146. Drew, M. D.; Lawrence, N. J.; Watson, W.; Bowles, S. A. *Tetrahedron Lett.* **1997**, *38*, 5857-5860.
147. Kizirian, J. C.; Caille, J. C.; Alexakis, A. *Tetrahedron Lett.* **2003**, *44*, 8893-8895.